Partitioning of sulfur between primary and secondary metabolism in *Arabidopsis thaliana*

Inaugural-Dissertation

zur

Erlangung des Doktorgrades

der Mathematisch-Naturwissenschaftlichen Fakultät

der Universität zu Köln

vorgelegt von

Süleyman Günal

aus Ürgüp,

Türkei

2025

KÖLN

Berichterstatter/in: Prof. Dr. Stanislav Kopriva

Prof. Dr. Tatjana Hildebrandt

Prüfungsvorsitzender: Prof. Dr. Günter Schwarz

In memory of my grandmother

Neriman Balcı

ABSTRACT

Sulfur is a fundemental element for all living organisms. It is essential for plant development and defense against biotic and abiotic stresses. The partitioning of sulfur between primary and secondary sulfur metabolism is controlled with delicate balance in *Arabidopsis thaliana*. An increased drought endurance of secondary sulfur metabolism mutants gave rise to a question about the importance of the distribution of sulfur metabolites under stress. Decreasing the secondary sulfur metabolism caused accumulation of primary sulfur metabolites cysteine and glutathione. The secondary sulfur mutant *apk1apk2* (*APS kinase*) possessed an enhanced primary sulfur reservoir. This observation and crosses we created in the sulfur metabolism gave us a great opportunity to investigate role of sulfur compounds under stress conditions. To understand underlying mechanism better we crossed *apk1apk2* mutant with previously well characterized Arabidopsis mutants from primary sulfur metabolism, *apr2* (*APS reductase*), *cad2* (*γ-glutamylcysteine synthetase*), and *des1* (*L-cysteine desulfhydrase*). The *apk1apk2apr2*, *apk1apk2cad2* triple mutants, as well as *cad2apr2* and *cad2des1* double mutants were analyzed for alterations in key processes of sulfur metabolism. We observed increased drought tolerance and ability to contain photosynthetic efficiency in GSH accumulating mutants and decrease of stomata density and enhanced water retention abilities in cysteine accumulating mutants. We also showed higher concentrations of cysteine alone is not sufficient for drought endurance, cysteine degradation is also needed for the resistance mechanism. The mutants with alternating sulfur metabolite profiles gave us a comparative advantage for understanding the different roles of cysteine and glutathione.

For the second part of this thesis we investigated the role of PAP in mitochondria. PAP is a phosphorylated nucleotide which is well characterized as a retrograde signaling molecule from chloroplasts to nucleus. In plants SAL1 enzyme recycles PAP. However, neither the connections between metabolic reactions producing PAP in mitochondria as a by-product nor the role of PAP as a counter-transport molecule of Coenzyme A or its inhibitory effect on mitochondrial iron transport have been investigated in plants yet. PAP is formed primarily, after consumption of PAPS for sulfation of secondary sulfur metabolites in animals and plants. Effects of in vivo PAP accumulation to mtFAS, CoA transport into the mitochondria and downstream mtFe-S assembly

are still open questions. We investigated the possible effect of PAP accumulation on lipolylation of GDC and lipolylated TCA cycle enzymes with metabolomics approach. We used loss of function mutant, *fou8,* of PAP degradation enzyme SAL1 which has PAP accumulation and as a contrasting genotype we used *apk1apk2* double mutant which has decreased concentrations of PAP. We observed, strongly and oppositely affected TCA cycle intermediates for both mutants. Our findings and reanalysis of existing expression data open the way for possible and intriguing connection of PAP and mitochondria.

TABLE OF CONTENTS

1. INTRODUCTION

The warmest year ever recorded since 1850 on earth was 2024. In fact, according to data from U.S-based National Oceanic and Atmospheric Administration (NOAA), top ten warmest ever recorded were all in the last decade. European Union's climate change service reported already this year that the month of January of 2025 was the hottest January ever recorded. The globe is warming and as a result, drought and heat stress are impacting larger areas for longer periods of time. The demand for discovery of new and better mechanisms to combat abiotic stress in plants is getting increasingly urgent. According to United Nations numbers, the world population surpassed 8 billion and food security is becoming a more delicate topic and stress on the arable lands is threatening more people every year. Moreover, increasing drought stress conditions are making the crops more susceptible to biotic stress factors and causing further yield decreases. Fluctuations in crop yield across the globe are expected to increase even more due to climate change (Cooper & Messina, 2023)

1.1. Plants Response to Drought Stress

Drought impedes photosynthesis, transpiration, growth, flowering and reproductive development in plants (Pinheiro & Chaves, 2011). To be able to survive under drought, plants have adapted various physiological, morphological and metabolomic strategies. Drought stress causes water loss and reduces the turgor tension in root cells. Plants can receive osmotic signal in three different ways. It can be perceived from the membrane tension change, local imbalance on the cell membrane or disruption of the integrity of cell wall (Gorgues et al., 2022). Once the drought sensed, plants activate their defense mechanisms, such as accumulation of osmoprotectanct amino acid proline, up-regulation of sugar transporters, chaperons, aquaporins, late embryogenesis abundant (LEA) proteins and enzymes to counter reactive oxygen species (ROS) (Urano et al., 2009; Yamaguchi-Shinozaki & Shinozaki, 2006; Yoshida & Fernie, 2023; Zhu, 2016). These include fine tuning stomata conductance, cuticle thickness, xylem conductance, shoot and root size and architecture (Ullah et al., 2017). Additionally, balance between root and shoot growth is crucial to survive under drought conditions. Stomata should be tightly controlled to provide important balance of the gas exchange. Plants should keep the water loss at minimum with transpiration via closing their stomata but also should not get overheated with closing the

stomata for too long (Skirycz and Inzé 2010; Tardieu et al., 2018) Plants endure and response to drought stress period also with other mechanisms including, osmoprotectant metabolite accumulation, by their turgor sensitive ion transporters, protective proteins and their phytohormones (Yang et al., 2021).

Among these, hormones absisic acid (ABA) has several key roles in responding drought and activation of defense mechanism against the stress (Finkelstein, 2013). For example, ABA induced phosphorylation of OPEN STOMATA1 (OST1) activates SLOW ANION CHANNEL1 (SLAC1) ion channel, causing anion efflux from guard cells and as result stomata closes (Munemasa et al., 2015) whereas KAT1, the guard cell membrane cation channel, is inhibited by OST1 (Raghavendra et al., 2010). Furthermore, Ca^{+2} ion channels sense cell wall tension and can work as osmosensor in drought conditions(Suzuki et al., 2011).

The role of sulfur containing metabolites, including sulfide, cysteine, glutathione or glucosinolate under enviromental stress conditions has garnered growing scientific attention in recent years (Laxa et al., 2019; Takahashi et al., 2023). Sulfate assimilation is one of the essential pathways in plant primary metabolism, providing great number of vital compounds, including the amino acids cysteine and methionine, as well as co-enzymes, such as iron sulfur centers, lipoic acid, thiamine, S-adenosylmethionine, coenzyme A, molybdenum coenzyme, and many others (Takahashi et al., 2011). This compounds central to response to oxidative stress conditions like drought (Chan et al., 2019). The reactive oxygen species(ROS) scavenging role of GSH and signaling functions of H_2S for stomatal closure points an important role of sulfur metabolism in drought stress (Mirza Hasanuzzaman et al., 2020; Ren et al., 2022). On the other hand secondary sulfur metabolites, especially glucosinolates, proposed to have an connection with drought stress via auxin signaling pathway (Salehin et al., 2019a). After sulfation of secondary sulfur metabolites what is left over from sulfur donor 3′-Phosphoadenosine-5′-phosphosulfate (PAPS) is by-product 3′-Phosphoadenosine 5′-phosphate (PAP). PAP accumulation in the mutants of Arabidopsis has been proven to be extremely important for drought resistance (Estavillo et al., 2011; Wilson et al., 2009).

1.2. Plant Sulfur Metabolism

Sulfur is one of the vital macronutrients for plant growth and development, and is required for the biosynthesis of essential amino acids cysteine and methionine, various co-enzymes, co-factors and numerous secondary metabolites. Sulfate is taken up to the cells via sulfate transporters localized in the plasma membrane and is distributed to vacuole for storage or plastids and cytosol for further metabolism (Gigolashvili & Kopriva, 2014). For assimilation, the inert sulfate needs to be activated by adenylation, at the expense of ATP, in a reaction catalyzed by ATP sulfurylase (Murillo & Leustek, 1995). The product, adenosine 5-phosphosulfate (APS) is a branching point to reductive and oxidative assimilation, often called primary and secondary (Kopriva et al., 2012). In the reductive branch, APS is reduced by APS reductase to sulfite, which is subsequently reduced by sulfite reductase to cysteine, the first product of primary sulfate assimilation (Figure.1). Cysteine serves as a donor of reduced sulfur for other S-containing metabolites, including methionine and the tripeptide glutathione (GSH) (Kopriva, Malagoli, & Takahashi, 2019). In the oxidative branch of sulfate assimilation APS is phosphorylated to 3-phosphoadenosine 5-phosphosulfate (PAPS), which is a donor of activated sulfate for synthesis of various secondary metabolites, or sulfated peptides (Mugford et al., 2009).

1.2.1. Primary sulfur metabolism in plants

For sulfur assimilation into organic molecules sulfate needs to be activated by ATP sulfurylase (ATPS) before the reduction or phosphorylation steps. ATPS chloroplast located 4 isoforms but as a result of alternative splicing ATPS2 can be located in the cytosol too, (Bohrer et al 2015). In plants, ATPS occurs as a homodimer, consisting of two 48 kDa monomers (Herrmann et al., 2014). Plants and algae have multiple ATPS isoforms localized in chloroplast and cytosol; the model plant Arabidopsis thaliana possess four (Rotte & Leustek, 2000). The partitioning of Arabidopsis sulfur metabolism as a primary and secondary metabolism starts from adenosine 5-phosphosulfate (APS). The reduction of APS to SO_3 (sulfite) by APS reductase is classified as reductive sulfur assimilation or primary sulfur metabolism. On the other hand, the pathway starts with phosphorylation of adenosine 5-phosphosulfate (APS) to 3´-phosphoadenosine 5'-phosphosulfate (PAPS) by APS Kinase (APK) classified as oxidative sulfur assimilation, sulfation reactions or secondary sulfur metabolism in plants. This two gate keeping enzyme is

redox regulated. During the posttranslational activation of APR enzyme by oxidative stress conditions, APK enzyme is reciprocally more active in its reduced form (Telman & Dietz, 2019).

Sulfur reduction differentiates from secondary sulfur metabolism with the reduction of APS to sulfite by APS reductase (APR). This reaction requires GSH as an electron donor (Jobe & Kopriva, 2018). APR reduces APS to sulfite and AMP. N-terminal of APR has a reductase domain and utilizes the iron-sulfur [Fe_4S_4] cluster as a cofactor. There are three isoforms of APR in Arabidopsis thaliana APR1, APR2 and APR3 all located in chloroplast which makes reduction of APS limited to only in chloroplast. *APR2* is considered as being main isoform, flux analysis with radioactively traceable isotope ^{35}S showed strongest control over flux provided by this isoform (Vauclare et al., 2002). Experiments with a knock out mutant *apr2* yielded only ca. 20% of wild type APR activity. Mapping the sulfur accumulation with using population genetics with natural ecotypes hit the *APR2* as a reason for more than six-fold difference in sulfur accumulation (Chao et al., 2014). Another experiment cross population of the natural accessions Bayreuth-0 x Shahdara again revealed *APR2* mutation as a cause for sulfate accumulation (Loudet et al., 2007).

The subsequent enzyme in the sulfur assimilation pathway is sulfite reductase (SiR). It is encoded by only single gene in Arabidopsis but expressed nearly all tissue types (Kopriva, 2006) SiR reduces sulfite to sulfide, ferrodoxin donates six electrons for this reaction (Takahashi et al., 2011). The enzyme has siroheme and 4Fe-4S iron-sulfur cluster domains as a prosthetic group for its activity(Anoman et al., 2019). *sir1-1* is a knock down mutant that has TDNA insertion in the promoter region and has only 28% of SiR enzyme activity on the leaves of the mutant compare to wild type. Its loss of function in Arabidopsis has shown to be early seedling lethal (Khan et al., 2010).

After the reduction of sulfite to sulfide, sulfide is incorporated into to backbone O -acetylserine (OAS) by O-acetylserine thiollyase (OAS-TL). OAS-TL requires pyridoxal-5'-phosphate as a cofactor for cysteine synthesis. Serine acetyltransferase and OAS-TL proteins form hetero-oligomeric structures called cysteine synthase complex (Wirtz & Hell 2006). OAS-TL-like gene family is complicated has 9 identified members in Arabidopsis but only three of them; A,B and C, considered to be main isoforms (Wirtz et al.,2004). Isoforms of OAS-TL is located in cytoplasm, mitochondria and chloroplast. Some of this isoforms have different enzymatic

ectivities like; β-cyanoalanine synthase (CAS), S-sulfocysteine synthase (SSCS) and L-cysteine desulfhydrase (DES1) which actually degrades cysteine (Romero et al., 2014).

Glutathione synthesis is a two-step process, in which both steps need ATP consumption. The first step is catalyzed by γ-glutamylcysteine synthetase (GSH1), which is located exclusively in the chloroplast. It catalyzes the rate-limiting step, incorporation of cysteine to glutamate to form γ-glutamylcysteine. The second step is catalyzed by glutathione synthetase (GSH2), where glycine is added to dipeptide to form tripeptide GSH. GSH2 is considered to be dual located in chloroplast and cytosol (Pasternak et al., 2008). GSH1 is redox sensitive; it loses most of its activity in its reduced form (Hell & Bergmann 1990). The redox regulation of GSH1 is obtained by intramolecular disulfide bridges. There are several mutants that have been created to study distinct glutathione levels in the cell (Cobbett et al., 1998; Ball et al., 2004). The knock-out mutant of GSH1 is embryo lethal and can only be developed if it is supplied with external GSH (Cairns et al., 2006). The *cad2* is a knockdown mutant, which has an impairment of GSH synthesis and has only ca. 15-30% of the wild type, while it accumulates cysteine which in turn overoxidized its cytosol (Speiser et al., 2018). This mutant was identified in the heavy metal tolerance screening because of its high sensitivity to cadmium (Cobbett et al., 1998). The *pad2* mutant has 80% lower GSH levels in all cell compartments, except for mitochondria, it causes *pad2* mutant to be sensitive to fungal pathogens (Parisy et al., 2007). The *rml1* mutant has low GSH in all cellular compartments and has an attenuated shoot and root phenotype (Zechmann & Muller 2010). GSH is also required as a sulfur donor for glucosinolates synthesis, *cad2* mutant accumulating Cys and lacking GSH, under herbivore attack have not able to increased indolic glucosinolates synthesis indicating the role of GSH rather than Cys as a sulfur donor (Sonderby et al., 2010).

DES1 is a cysteine degrading enzyme, which is located in the cytosol and responsible of desulfuration of cysteine to sulfide, pyruvate and ammonia (Álvarez et al., 2010). DES1 needs pyridoxal-5′-phosphate to function. Since SiR is located in chloroplast, cysteine-degrading enzymes, particularly DES1 is essential for sulfide generation in the cytosol for further signaling roles of H_2S (Aroca et al., 2023). A growing number of studies have been focusing on the signaling role of sulfide for plant growth and stress response (Chen et al., 2020; García-Calderón et al., 2023; Liu et al., 2021; Shen et al., 2020) Production of sulfide with DES1 in the guard

cells has been shown to be an essential component of ABA related stomatal regulation and abiotic stress response(Scuffi et al., 2014). Persulfidation of cysteine residues (Cys44 and Cys205) of DES1 regulates stomatal closure through ABA (Shen et al., 2020).

The mechanism of H_2S signaling is the persulfidation of proteins, which was shown to regulate autophagy and stomatal conductance in Arabidopsis (Aroca & Gotor, 2022; Gotor et al., 2019). In rice, H_2S regulated drought tolerance through persulfidation of aquaporins (Zhang et al., 2024) Aquaporins are large family of membrane proteins that play an important role in water transport to the cell (Maurel et al., 2015). However how the specific cysteine residues are targeted by persulfidation is not well understood and how reversible the process is and which enzymes are responsible for de-persulfidation is also not clear (Moseler et al., 2024).

The role of cysteine in persulfidation is very critical since it is a residue in the proteins as a target of persulfidation and also as a donor of sulfur after its degradation to H_2S. GSH is another sulfur metabolite which is vital for different post translational modification, S-glutathionylation. All the post translational modifications connected with sulfur metabolites still needs to be investigated further for better understanding.

In reductive sulfur assimilation, where sulfite is further reduced to sulfide (H_2S) by Sulfite Reductase (SiR), sulfide is later incorporated to *O*-acetylserine (OAS), derived from acetylation of amino acid serine. Serine is activated by serine acetyltransferase (SAT or SERAT). After OAS is created, *O*-acetylserine thiollyase (OASTL) exchanges acetyl group with sulfide to synthesize the amino acid cysteine (Takahashi et al., 2011).Cysteine is another essential amino acid for the synthesis of proteins, together with its other biosynthetic roles in cell. Cysteine is required as a sulfur moiety for the crucial co-factors, such as iron-sulfur clusters, lipoic acid and thiamine. Cysteine can be used as a precursor of another essential amino acid Methionine. Methionine is essential for synthesis of numerous active compounds in plants like; ethylene, S-adenosylmethionine (SAM), S-methylmethionine (SMM) and dimethylsulfonium propionate (DMSP) (Jobe & Kopriva, 2018). Cysteine is also required for the synthesis of ROS scavenger molecules; ferredoxin and glutathione (GSH). Glutathione is a tripeptide and synthesized in two-step reaction. First, γ-glutamylcysteine synthetase (GSH1) synthesizes dipeptide γ-glutamylcysteine using cysteine and glutamate. Second, glutathione synthetase (GSH2) adds to the third amino acid glycine to γ-glutamylcysteine to form GSH. Glutathione is one of the major

antioxidant molecules in plants, taking part in redox homeostasis, detoxification of xenobiotics (Jobe & Kopriva, 2018)

1.2.2. Secondary sulfur metabolism: Sulfation reactions

Sulfur is an essential nutrient for all life forms. It is present in a plethora of metabolites of primary and secondary metabolism, most prominently in the amino acids cysteine and methionine, and cofactors such as iron sulfur clusters, lipoic acid and coenzyme A. In the majority of these metabolites, sulfur is present in its reduced form of organic thiols, however, some compounds contain S in its oxidized form of sulfate (Beinert, 2000; Takahashi et al., 2011). Sulfate is transferred to suitable substrates onto hydroxyl or amino groups, by sulfotransferases (Coughtrie, 2016; Hirschmann et al., 2014). These biological sulfation reactions as well as desulfation catalyzed by sulfatases are often denoted as sulfation pathways (Mueller et al., 2015; Mueller & Shafqat, 2013). The activated sulfate for the sulfation pathways, 3´-phosphoadenosine 5-phosphosulfate (PAPS), is formed from sulfate by two ATP-dependent steps: adenylation, i.e. the transfer of the AMP moiety of ATP to sulfate to form adenosine 5´-phosphosulfate (APS) by ATP sulfurylase (ATPS) and phosphorylation of APS at its 3'-OH group by APS kinase (Figure.1). The two enzymes are either fused into a single enzyme PAPS synthase (PAPSS) in the animal kingdom or occur as independent proteins in the green lineage (Patron et al., 2008). The by-product of PAPS- dependent sulfation reactions, 3´-phospho-adenosine 5-phosphate (PAP) is finally dephosphorylated to AMP by 3´- nucleotidases. This reaction to remove PAP is important beyond sulfation pathways, as PAP accumulation has many additional physiological effects (Chan et al., 2013; Lee et al., 2012).

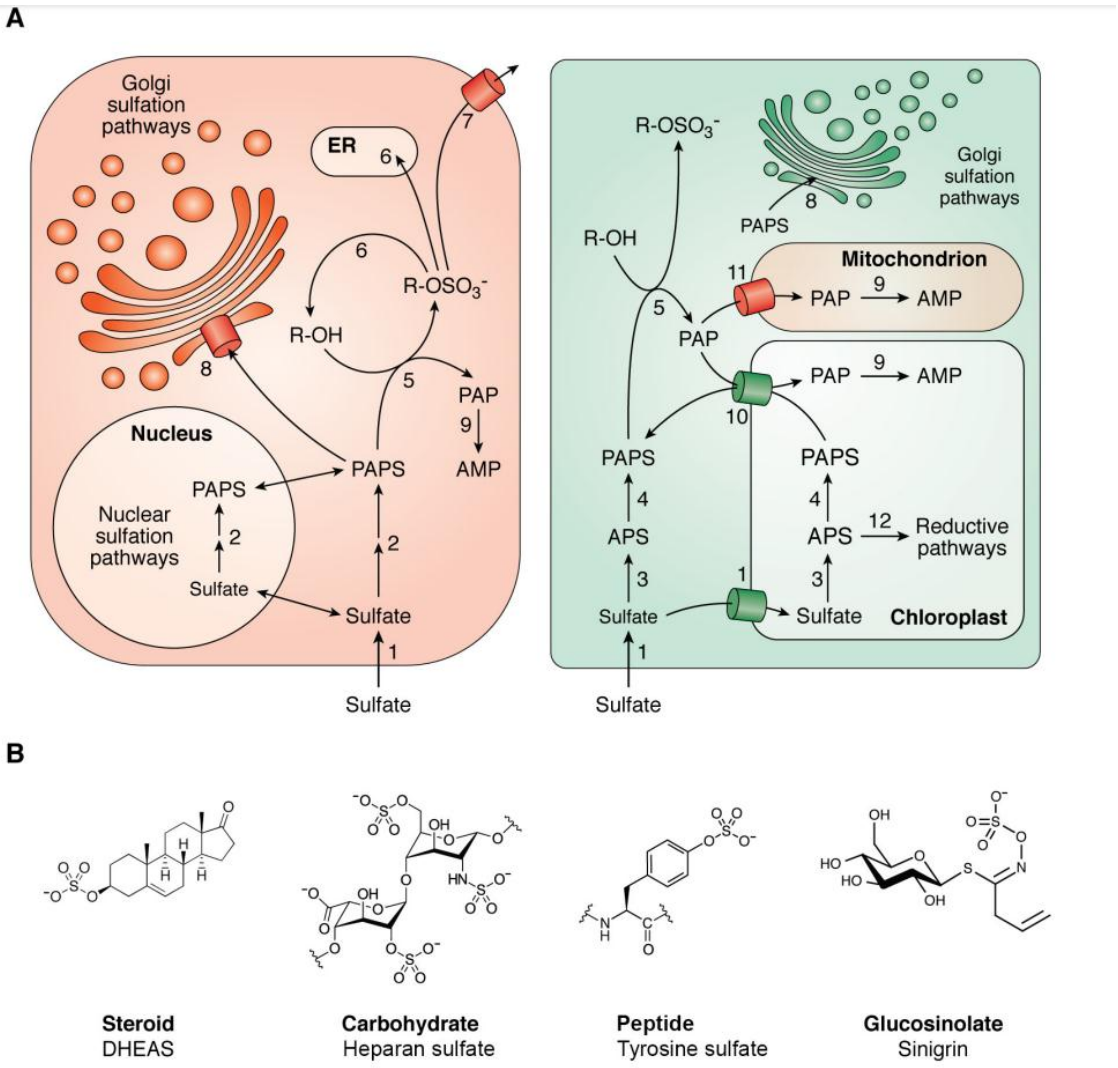

Figure.1: Red and green sulfation pathways

A, sulfate is taken up by various sulfate transporters; in plants, some of them transport sulfate into the chloroplast (1). Sulfate activation occurs via animal bifunctional PAPS synthases (2) that shuttle between cytoplasm and nucleus or plant ATP sulfurylase(3) and APS kinase (4) isoforms that are localized in cytoplasm and the chloroplast. PAPS serves as a substrate for cytoplasmic sulfation pathways (5),where PAP is produced. Sulfated compounds can then be de-sulfated by sulfatases (6), enzymes that are absent in plants, or they are secreted via OATPs (7). Two animal PAPS transporters (8) channel PAPS into the Golgi apparatus where many carbohydrate and protein sulfotransferases modify macromolecules for secretion. Although plant protein sulfotransferases are known that reside in the Golgi, an analogous transporter (8) has not yet been identified. Human PAP phosphatases (9) are in the Golgi and the cytoplasm; plant PAP phosphatases are, however, localized in the mitochondrion and the chloroplast. Dedicated PAP(S) transporter in the chloroplast (10) and the mitochondrion (11) deliver PAPS to the cytoplasm and

play an important role in the degradation of PAP. In plants, APS represents a branching point where reductive biosynthetic pathways diverge (12). B, examples of structures of sulfated metabolites.

The organification or activation of sulfate to PAPS by ATPS and APS kinase initiates sulfation pathways (Lipmann et al,., 1958). The catalytic and substrate binding sites of the ATP sulfurylases from plants and animals are highly conserved (Jez et al., 2016), however, subsequent reactions and the enzymatic blueprints vary greatly between different lineages (Patron et al., 2008). Also the localization and regulation of ATP sulfurylase and APS kinase shows lineage specific differences.

While essential and sufficient for sulfate reduction, ATPS has to be coupled with the APS kinase for sulfation pathways. This enzyme, ubiquitous in nature and highly conserved in structure and sequence, shows the same localization in plants as ATPS. Arabidopsis possesses four APS kinase genes, which encode three plastidic and one (APK3) cytosolic isoforms (Mugford et al., 2010). APS kinase phosphorylates APS produced by ATPS and competes thus with APS reductase for this substrate. The two enzymes represent entries into the two branches of sulfate assimilation: a primary reductive assimilation pathway and a secondary oxidized sulfur metabolism involving sulfation pathways (Kopriva et al., 2012). The secondary pathway has been rarely investigated, since PAPS production is not necessary for the primary sulfate reduction and synthesis of cysteine and glutathione (Kopriva et al., 2012).

However, even though APS kinase is part of the secondary sulfate assimilation pathway, it is vital for plant survival (Mugford et al., 2009; Mugford et al., 2010). Interestingly, it is the loss of two plastidic APS kinase isoforms *APK1* and *APK2* which results in strongly reduced accumulation of sulfated metabolites, such as glucosinolates, and not the disruption of the cytosolic enzyme APK3 (Mugford et al., 2010). This on one hand again challenges the significance of cytosolic APS and PAPS synthesis; on the other hand, it shows the necessity of intracellular PAPS transport. Indeed, a PAPS transporter has been identified in chloroplast envelope membranes, part of glucosinolate co-expression network, whose mutation shows a phenotype similar to *apk1apk2* mutants (Gigolashvili et al., 2012).

The *apk1apk2* double knockout turned out to be an excellent tool to dissect the importance of secondary sulfate assimilation (Bohrer et al., 2014; Mugford et al., 2010). The reduced synthesis of PAPS in *apk1apk2* results in a shift of sulfur flux from the secondary to the primary sulfur

assimilation pathway, increased accumulation of reduced sulfur compounds and highly reduced glucosinolate levels (Bohrer et al., 2014; Mugford et al., 2010). Furthermore, all components of the glucosinolate synthesis pathway were coordinately up-regulated leading to substantial accumulation of the desulfo-precursors of glucosinolates (Mugford et al., 2010).

Although glucosinolates and other sulfated secondary metabolites seem not to be essential for Arabidopsis growth, the *apk1apk2* mutants are significantly smaller than the wild type plants (Mugford et al., 2010). When additional APS kinase gene, *APK3* or *APK4*, is mutated, the semi-dwarf phenotype is even stronger (Mugford et al., 2010). The generation of multiple mutations in APS kinase genes revealed that the enzyme is essential for Arabidopsis growth (Mugford et al., 2010). Which acceptors of PAPS are essential remains to be determined, as neither glucosinolates, nor sulfated peptide hormones such as the phytosulfokines (Matsubayashi & Sakagami, 1996), root growth factors (Matsuzaki et al., 2010), or Casparian strip integrity factors (Nakayama et al., 2017) discovered so far seem to be crucial.

APS kinase is regulated on both transcriptional and post-transcriptional levels. The genes are part of the glucosinolate transcriptional network, under control by a family of six MYB transcription factors in Arabidopsis and thus co-expressed with genes providing the main substrate for PAPS (Yatusevich et al., 2010). In addition, according to the demand-driven concept, sulfate starvation represses APS kinase in order to channel the scarce sulfur to the primary sulfate assimilation. Excitingly, redox regulation of APS kinase enzyme activity through dimerization of the protein and formation of disulfide bridges has been revealed in a structural analysis (Ravilious et al., 2012). Reducing conditions leading to monomerization of the protein increase the catalytic efficiency including alleviation of enzyme inhibition by its substrate, APS (Ravilious et al., 2012). This is particularly interesting as it complements the redox regulation important for control of the reductive branch of sulfate assimilation (Takahashi et al., 2011). APS reductase is activated by oxidation, e.g., during abiotic stress, which leads to higher activity and synthesis of cysteine and GSH (Bick et al., 2001). Accordingly, recombinant APS reductase is inactivated by incubation with reductants (Kopriva & Koprivova, 2004). APS reductase and APS kinase occupy the opposite branches of sulfate assimilation from APS (Bohrer et al., 2014). Considering that APS reductase is activated by oxidation (Bick et al., 2001), the reciprocal activation of APS

kinase by reduction indicates that this redox mechanism may control the distribution of sulfur fluxes between primary and secondary sulfur metabolism (Jez et al., 2016).

Sulfotransferases are the first enzymes of the core sulfation pathways. They transfer sulfate from PAPS to the hydroxyl or amino group of a wide variety of acceptors: carbohydrates, lipids, peptides, hormone precursors, xenobiotics, and other molecules (Coughtrie, 2016; Dias et al.,

The functions of other SOTs remain to be elucidated, particularly given the large variety of so far unknown sulfur-containing metabolites in Arabidopsis (Gläser et al., 2014).Protein sulfation by TPSTs. Tyrosine sulfation is a major post-translational regulation of secreted proteins and peptides, in both animals and plants. However, this modification seems to be confined to multicellular eukaryotes, as *tyrosylprotein sulfotransferases (TPST)* have been found neither in bacteria nor yeast (Kehoe & Bertozzi, 2000). TPST enzyme catalyzes the transfer of sulfate from PAPS to the phenolic group of the amino acid tyrosine in the Golgi (Komori et al., 2009; Hartmann-Fatu & Bayer, 2016; Goettsch et al., 2006). It is estimated that one third of all secreted human proteins are tyrosine sulfated (Monigatti et al., 2002).

The importance of tyrosine sulfation in plants has been known for long, because of the number of sulfated growth-regulating peptides (Matsubayashi & Sakagami, 1996; Amano et al., 2007). Despite the importance of the tyrosine sulfation, however, the corresponding sulfotransferase remained elusive in plants, as no homologous proteins to the animal enzyme could be found. AtTPST was identified in Arabidopsis after isolation of the enzyme from microsomal fraction and proteomics analysis (Komori et al., 2009). AtTPST is a 62-kDa transmembrane protein located in the Golgi that lacks the characteristic cytosolic sulfotransferase domain (Komori et al., 2009). The importance of plant tyrosine sulfation is confirmed by the semi-dwarf phenotype of Arabidopsis *tpst1* mutant with early senescence, light green leaves and diminutive roots (Komori et al., 2009).

1.2.3 PAP accumulation and degradation

The nucleotide 3′-phosphoadenosine-5′-phosphate (PAP) is produced during PAPS-dependent sulfation pathways (Günal et al., 2019). It is also formed during coenzyme A-dependent fatty acid synthetase activation (Moolman et al., 2014), though how or whether these two pathways interconnect is currently unclear. As a reaction product, PAP strongly inhibits sulfotransferase

activity (Rens-Domiano & Roth, 1987). With its two phosphate moieties, PAP may be regarded as the shortest possible RNA strand and, consequently, PAP interferes with RNA metabolism, inhibiting the XRN RNA-degrading exoribonucleases (Gy et al., 2007). To prevent the toxic effects of PAP, dedicated PAP phosphatases are found in all kingdoms of life. Most of the enzymes from higher eukaryotes show multiple specificity towards PAP or PAPS, and also impact inositol signaling by removing phosphate from inositol bis- and tri-phosphates (Quintero et al., 1996; López-Coronado et al., 1999), all representing small and negatively charged substrates.

It has to be noted that in Arabidopsis, *SAL1* is a member of a small gene family with seven members. *SAL1* is, however, the only gene that has been found in numerous genetic screens and which, when disrupted, causes the various phenotypes. Two additional isoforms, *AHL* and *SAL2*, were confirmed to function as PAP phosphatases (Gil-Mascarell et al., 1999), but only *AHL* is expressed at levels comparable to *SAL1* (Kim & von Arnim, 2009). In contrast to SAL1, AHL protein does not seem to use inositol 1,4-bisphosphate as substrate (Gil-Mascarell et al., 1999) and its overexpression complements the loss of *SAL1* for at least some phenotypes (Kim & von Arnim, 2009). While this is clear evidence for PAP being the causal metabolite for many phenotypes, the reason why in WT Arabidopsis AHL protein does not suffice to metabolize PAP remains to be elucidated. Another unsolved question is the physiological relevance of PAPS dephosphorylation.

The alteration in glucosinolate synthesis is the first direct metabolic link of SAL1 with sulfation pathways (Lee et al., 2012). In the *fou8* allele of *sal1* mutant, glucosinolate levels were lower than in WT Col-0 (Lee et al., 2012). This was caused by reduction in sulfation rate, as the mutants also accumulated the desulfo-glucosinolate precursors (Lee et al., 2012). The phenotype thus strongly resembled that of *apk1apk2* mutants with low provision of PAPS (Mugford et al., 2010). Interestingly, combining the *fou8* mutant with *apk1apk2* resulted in alleviation of many of the phenotypic alterations connected with loss of SAL1 function, strongly suggesting that PAP was the responsible metabolite (Lee et al., 2012). This observation forms a second direct link of SAL1 and sulfation pathways: the SAL1-PAP signaling is dependent on synthesis of PAPS and sulfation reactions, i.e., secondary sulfur metabolism (Chan et al., 2019). This is particularly important for plants, which do not synthesize glucosinolates or other major class of sulfated

secondary metabolites but still possess functional PAP signaling (Manmathan et al., 2013). Which sulfotransferase isoforms provide the majority of PAP for the stress signaling is, however, still unknown.

1.3 Sulfur Metabolism and Drought

Sulfur can be found in its reduced form in primary plant metabolites like sulfide, cysteine and glutathione or in the form of organic sulfate in secondary sulfur metabolism compounds like glucosinolates or flavonoids (Ristova & Kopriva, 2022). The chemical properties of sulfur provide this element an ability to readily change its oxidation state in nature. Sulfate assimilation is tightly regulated by plant demand for reduced sulfur and by sulfate supply (Koprivova & Kopriva, 2014; Lappartient & Touraine, 1996; Takahashi et al., 1997). Thus, numerous reports described changes in transcriptome and metabolome of plants under conditions changing the demand for sulfur molecules, such as oxidative or biotic stress (Ball et al., 2004; Kruse et al., 2007; Van Hoewyk et al., 2008; Vauclare et al., 2002). The molecular mechanisms responsible for these regulatory processes are, however, still largely unknown (Ristova & Kopriva, 2022). In particular, it is not always clear which alterations in steady-state levels of transcripts and metabolites actually affect the sulfur fluxes in the plants (Calderwood, Morris, & Kopriva, 2014).

.

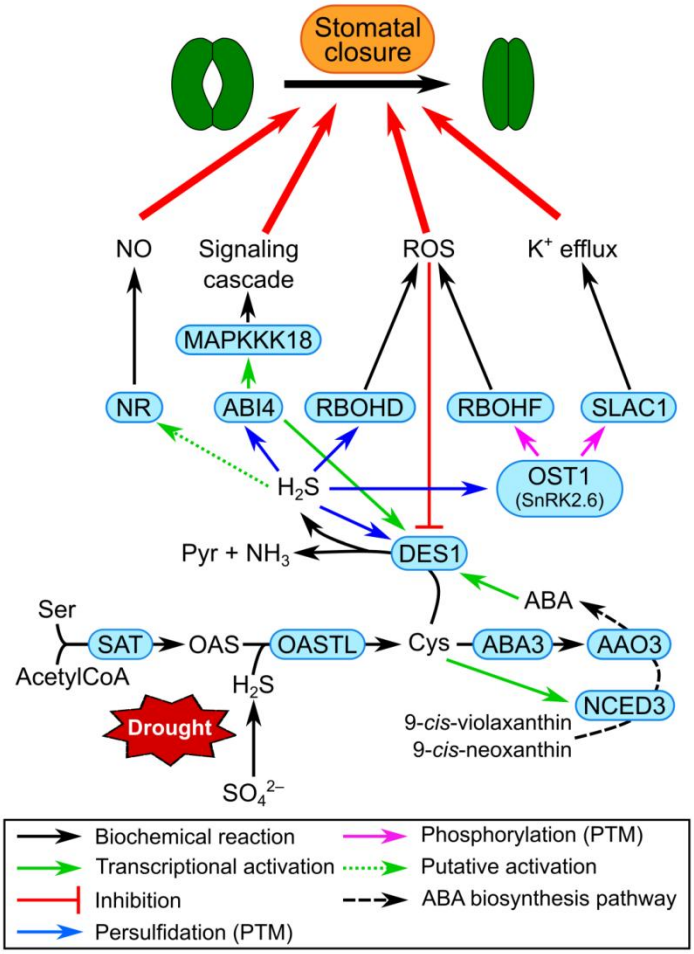

Figure.2: Cysteine biosynthesis, catabolism and signaling pathways that connects it to stomatal closure.

L-cysteine desulfhydrase1 (DES1) catalyzes cysteine degradation and the accumulation of H_2S, which is responsible for the post-translational modification (PTM), S-persulfidation of DES1, ABA insensitive4 (ABI4), respiratory burst oxidase homologue D/F (RBOHD/F) and open stomata1 (OST1) which are critical for stomata. Abscisic aldehyde oxidase3 (AAO3), mitogen-activated protein kinase kinase kinase18 (MAPKKK18), nine-cis-epoxycarotenoid dioxygenase3 (NCED3), nitrate reductase (NR), O-acetlyserine (OAS), (OAS) (thiol)lyase (OASTL), reactive oxygen species (ROS), serine acetyltransferase (SAT), slow anion channel1 (SLAC1). Published figure has taken from Ingrisano et al., (2023) article.

It has been suggested that sulfate has a critical role as a signal from root to shoot, and sulfur reduction metabolite cysteine promoting stomatal closure under drought stress (Batool et al., 2018). Cysteine is required for Moco (molybdenum cofactor). which is needed for ABA synthesis and ABA mediates stomata closure (Figure.2) (Batool et al., 2018; Ingrisano et al., 2023; Ren et al., 2022).

While the next molecule on the downstream of sulfur reduction pathway, sulfite is a necessary molecule for sulfide synthesis and sulfolipid biosynthesis, its accumulation is deleterious in the cell (Naumann et al., 2018). To control the sulfite concentration, it can either be oxidized to sulfate by sulfite oxidase (SO) or reduced to sulfide by sulfite reductase (SiR) (Takahashi et al., 2011). A recent study by Bekturova et.al(2023) made a connection between stomatal regulation and SO_3 and showed that the accumulation of SO_3 by sulfite overexpression by producing enzyme APS reductase 2 (APR2) or knock-out mutant of sulfite oxidase (SO) causes induction of stomata opening (Bekturova et al., 2021).

The primary sulfur metabolite cysteine has essential roles under abiotic stress conditions, as a precursor of indispensable redox buffer GSH and as a donor of sulfuration of cofactor Moco(molybdenum cofactor) for induction of ABA biosynthesis (Kopriva et al., 2024; Schwarz & Mendel, 2006). Redox active(R-SH) thiol group of cysteine makes this amino acid crucial for protein modifications and regulation under redox altering diverse abiotic stress conditions. Plants, which have mutations on sulfate transporter genes, exhibit decreased levels of sulfate in chloroplasts and also reduced levels of ABA. Cysteine feeding experiments with sulfate transporter mutants restored the ABA to the normal levels (Cao et al., 2014). All the studies indicated that sufficient concentration of cysteine in the cell is required for ABA directed drought response (Ingrisano et al., 2023).

Another primary sulfur metabolite, GSH is an antioxidant with a pivotal role for the elimination of ROS in the plant cells (M. Hasanuzzaman et al., 2018). Because of its role in detoxifying cells from ROS, elevated GSH concentration of crop species is linked to cold and osmotic stress resistance in crop cultivars (Kocsy et al., 2013).

Under drought stress Arabidopsis, GSH1 is activated post transcriptionally (May et al., 1998). Interestingly, expression levels of the *VrGSH1* remain the same, while VrGSH1 protein is modified posttranslationally in *Vigna radiate* (Sengupta et al., 2012). Another study expressed *Brassica rapa GSH1* orthologs *BrECS1* and *BrECS2* are expressed in rice under stress inducible Rab21 promoter that provided better germination under salt stress as well as enhanced growth and tolerance under abiotic stress for the transgenic rice (Bae et al., 2013).

Early stages of drought causes reduction of GSH concentrations in the mitochondria and in the nucleus in the young leaves of Arabidopsis plants (Koffler et al., 2014). Reduced levels of GSH in plants are associated with an increased stomatal closure. Plants treated exogenously with a chemical interfering with GSH synthesis, such as 1-chloro-2,4- dinitrobenzene, and GSH1 mutant *cad2* plants, are shown to have increased stomatal closure (Munemesa et al., 2013). Later, it was suggested that not the lower concentrations of GSH causes ABA triggered stomatal closure but the synthesis and accumulation of cysteine promotes ABA response (Batool et al., 2018). More recent studies have focused on H_2S, which is another sulfur metabolite for the stomata closure under drought stress (Chen et al., 2020; Fuentes-Lara et al., 2019; García-Calderón et al., 2023; Liu et al., 2021; Shen et al., 2020)

The endogenous synthesis of sulfide is very intertwined with cysteine synthesis and catabolism H_2S is produced either with degradation of Cys or reduction of sulfite. H_2S is a sulfur donor for Cys synthesis and degradation product of it in different compartments of cell (Gotor et al., 2015).

The gaseous signaling molecule H_2S has various important physiological functions in mammalians. In plants it is discovered having functions in autophagy, pesulfidation and stomatal aperture (Álvarez et al., 2012; Scuffi et al., 2014) (Figure.2). One of the responses to the drought stress is increasing the synthesis of ABA which consequently induces DES1 expression quickly in the guard cells (Shen et al., 2020). DES1 then degrades cysteine and creates H_2S. One of the most critical functions of sulfide is called persulfidation, which is a post-translational modification of cysteine residues, in which thiol groups are added to Cys residues with a covalent bond to form persulfides (Filipovic et al., 2018). Persulfidation alters the structure of proteins, and their activity and even subcellular localization, thus making this process a quick and flexible response to environmental stress (Corpas et al., 2021).

Glucosinolates are secondary sulfur compounds produced for chemical defense against biotic stress conditions and pathogen attacks in plants in the *Brassicales* order. Glucosinolates are normally stored in the vacuole and are not toxic to the cell. Myrosinase enzymes in plants hydrolyze and break glucosinolates during herbivore attack into isothiocyanate (mustard oil) Glucosinolates are synthesized from amino acid precursors and divided into 3 sub-group: aliphatic mainly derived from methionine but also alanine, leucine, isoleucine, valine; aromatic glucosinolates with a benzene ring derived from phenylalanine or tyrosine; and indolic derived

from bicyclic indole ring of tryptophan (Sønderby et al., 2010).The roles of secondary sulfur metabolites and glucosinolates under abiotic stress conditions have not reached a full consensus. If the secondary sulfur metabolites accumulate or not is still not very clear, since inconsistent results have been collected in different species in *Brassicaceae* under drought conditions (Abuelsoud et al., 2016)Because of the role of GSH and vital importance of the amino acid synthesis from primary sulfur metabolism it has speculated that secondary metabolism needs to be down regulated under abiotic stress (Kopriva et al., 2012). This view is supported by enzymatic activity experiments of sulfur metabolism enzymes in different redox states. APK and APR are regulated in opposite fashion, the reduced form of APK is more active on the other hand the oxidized form of APR is more active (Telman & Dietz, 2019).One study argued that drought stress causes the accumulation of aliphatic glucosinolates while indolic GSLs stayed unchanged or reduced in Arabidopsis (Mewis et al., 2012). While another study found, two weeks drought in broccoli (*Brassica oleracea L*) also caused reduction in indolic GSLs and aliphatic GSLs only slightly decreased (Abuelsoud et al., 2016).

The phytohormone auxin (IAA) and indolic glucosinolates are synthesized from a common downstream amino acid, tryptophan (Kopriva et al 2021). Auxin sensitive Aux/IAA proteins are transcriptional repressors of *AUXIN RESPONE FACTOR*(ARF). Triple knock-out mutant of *iaa5 iaa6 iaa19* interestingly had lower aliphatic glucosinolates and reduced drought tolerance. It is shown that Aux/IAA regulates the levels of aliphatic glucosinolate. *cyp79f1f2* double mutant and *myb28myb29* double mutants both has decreased aliphatic glucosinolates and they both showed decreased drought tolerance in water withholding experiment (Salehin et al., 2019a)

1.4 PAP in mitochondria

3′-phosphoadenosine-5′-phosphate (PAP) is a diphosphorylated adenosine found in all living organisms. Even though present in all kingdoms of life, PAP considered to be an unintended metabolite that needs to be rapidly removed to prevent toxicity. Plant PAP phosphatase *SAL1* belongs to the most pleiotropic plant genes. It was first identified in rice as a protein complementing an inability to grow on sulfate in cysQ mutants of E. coli and met22 yeast mutants (Peng & Verma, 1995). It was subsequently shown to catalyze conversion of PAPS to APS and PAP to AMP, and this function was speculated to regulate sulfur fluxes (Neuwald et al., 1992). A homologue from Arabidopsis was identified in a screen for genes improving salt

sensitivity and was named *SAL1* (Quintero et al., 1996). Since then, *SAL1* has been found in numerous genetic screens for a number of unrelated phenotypes, and is therefore described under many different names. A common denomination, *FIERY1* or *FRY1*, comes from a screen for mutants in abscisic acid and stress signaling, where its loss of function resulted in hyperinduction of the luciferase reporter gene driven by a stress-responsive promoter (Xiong et al., 2001).

The phenotypes observed in the various alleles of *sal1* mutants include cold and drought tolerance and signaling (Estavillo et al., 2011; Xiong et al., 2004), leaf shape and venation pattern (Robles et al., 2010), RNA silencing (Gy et al., 2007), increased jasmonate levels (Rodríguez et al., 2010), glucosinolate and sulfur accumulation (Lee et al., 2012), lateral root formation (Chen & Xiong, 2010), increased circadian period (Litthauer et al., 2018), and many others. Initially it was believed that these phenotypes were caused by defects in inositol phosphate signaling (Xiong et al., 2001), but current evidence points to PAP being the main factor (Estavillo et al., 2011; Lee et al., 2012; Kim & von Arnim, 2009; Chan et al., 2019), linking thus sulfation pathways with a number of cellular processes.

In plants it is mainly formed as a by-product of sulfation reactions after transfer of a sulfate group of 3′-phosphoadenosine-5′-phosphosulfate (PAPS) to suitable acceptors by sulfotransferases (SOTs). PAP is recycled into adenosine monophosphate (AMP) and phosphate by a 3'(2'),5'-bisphosphate nucleotidase enzyme named SAL1 (Estavillo et al., 2011). PAP accumulation and SAL1 enzyme have been intensively studied in Arabidopsis in the last decade, as the corresponding gene, AT5G63980, was found in a numerous genetic screens, and is therefore also known as *FIERY1* (*FRY1*;(Xiong et al., 2001)), *SAL1* (Quintero et al., 1996), *HIGH EXPRESSION OF OSMOTICALLY RESPONSIVE GENES2* (*HOS2*;(Xiong et al., 2004)), or *ALTERED EXPRESSION OF APX2 8* (*ALX8*;(Wilson et al., 2009)). PAP has been in the center of attention because of its role as a retrograde signal between chloroplast and nucleus. SAL1 is a redox regulated protein which is inhibited by oxidation (Chan et al., 2016). Oxidative stress, for example as a result of drought or high light, inactivates the SAL1 enzyme in the plastids which results in the accumulation of PAP in the cell (Chan et al., 2016). Accumulation of PAP inhibits 5‟-3‟ exoribonucleases (XRNs) which in turn alters RNA Polymerase II activity and up-regulates many abiotic stress response genes (Crisp et al., 2017). This result in an

increased stress tolerance of the *sal1* mutant in Arabidopsis compared to the wild type (Wilson et al., 2009).

In contrast to animal PAP phosphatases in the Golgi and the cytoplasm, the plant SAL1 enzyme in chloroplasts and mitochondria has a different localization than the sulfotransferases forming PAP (Estavillo et al., 2011). A number of the phenotypes described in *sal1* mutants resemble those of loss-of-function mutants in XRN exoribonucleases (Hirsch et al., 2011), and can be complemented by expression of SAL1 in the nucleus, implying that one mode of action of PAP is inhibition of XRNs (Estavillo et al., 2011). A model in which PAP acts as retrograde signal from chloroplast to nucleus during abiotic stress has been proposed (Estavillo et al., 2011). This in turn results in accumulation of PAP, its transport to the nucleus, and induction of expression of stress response genes (Chan et al., 2016). Accordingly, PAP accumulation due to loss of function of SAL1 leads to stress tolerance, such as drought tolerance (Estavillo et al., 2011). In addition, the SAL1-PAP regulatory module has an intermediary role connecting hormonal signaling pathways, such as germination and stomatal closure (Pornsiriwong et al., 2017).

PAP and SAL1 connect multiple compartments in the cell. SAL1 is dual located in chloroplasts and mitochondria, but sulfotransferases (SOTs) in Arabidopsis are localized in cytosol and Golgi (Estavillo et al., 2011).PAP is transported by PAPST transporters between cellular compartments. There are two PAP transporters characterized in Arabidopsis so far. PAPST1 is responsible for the export of PAPS from chloroplast to cytoplasm for sulfation reaction while transporting PAP into chloroplast for degradation by SAL1 (Gigolashvili et al., 2012). On the other hand, PAPST2 is dual-located in both mitochondria and chloroplast and its function is the import and export of PAP into both organelles (Ashykhmina et al., 2019). The complementation of *sal1* mutant in different cell compartments revealed that expressing SAL1 protein exclusively in chloroplast or cytosol is not entirely rescuing the mutant phenotype but that it can be fully rescued when expressed in mitochondria or in nucleus (Ashykhmina et al., 2022). The PAP transport into mitochondria via PAPST2 or degradation in the nucleus before inhibiting XRNs was sufficient for rescuing the phenotype of *sal1* mutants. The function of PAP as a retrograde signal molecule from plastids to nucleus explains the interplay of these compartments, but the evolutionary reason of why PAP degradation in mitochondria in plants is important remains elusive.

Interestingly, there is another enzymatic reaction which produces PAP as a by-product, the phosphopantetheinylation. 4'-phosphopantetheine is an essential prosthetic group of acyl carrier proteins (ACP), aryl carrier proteins and the peptidyl carrier proteins (PCP) (Beld et al., 2014; Lambalot et al., 1996). Acyl carrier proteins have a vital role in fatty acid synthesis (FAS). The enzyme responsible for this reaction, 4'-phosphopantetheinyl transferase (PPT), has been well characterized in yeast and in humans (Joshi et al., 2003; Stuible et al., 1998). PPT enzyme transfers phosphopantetheine moiety from CoA to apoACP to create an active holoACP, which is necessary for fatty acid synthesis. So far in plant kingdom only one PPT enzyme has been characterized, the mtPPT located in mitochondria (Guan et al., 2015). The study of enzymatic activity of PPTases in bacteria showed that PAP binds strongly to the protein at high concentrations and inhibits PPTase activity as a feedback mechanism (Foley & Burkart, 2009)(Figure.3). mtPPT in plants is a key enzyme for mtFAS as well. mtFAS is particularly needed for synthesis of lipoic acid an essential cofactor of pyruvate dehydrogenase complex (PDC), glycine decarboxylase complex (GDC), 2-oxoglutarate (2-OG) dehydrogenase complex (OGDC) and the branched-chain a-keto acid (BCKA) dehydrogenase complex (BCKDC) enzymes (Solmonson & DeBerardinis, 2018; Taylor et al., 2004). *mtPPT* knock-out mutation is lethal and knock-down RNAi lines exhibit a semi dwarf phenotype. As with other mutants of mtFAS this is caused by reduced production of lipoic acids and consequently reduction in lipoylation of H-protein of GDC, resulting in reduction of photorespiration (Guan et al., 2015). Indeed, *mtPPT* knock-down mutants accumulate glycine and the phenotype of the mutant can be rescued under non-photorespiratory conditions (Guan et al., 2015).

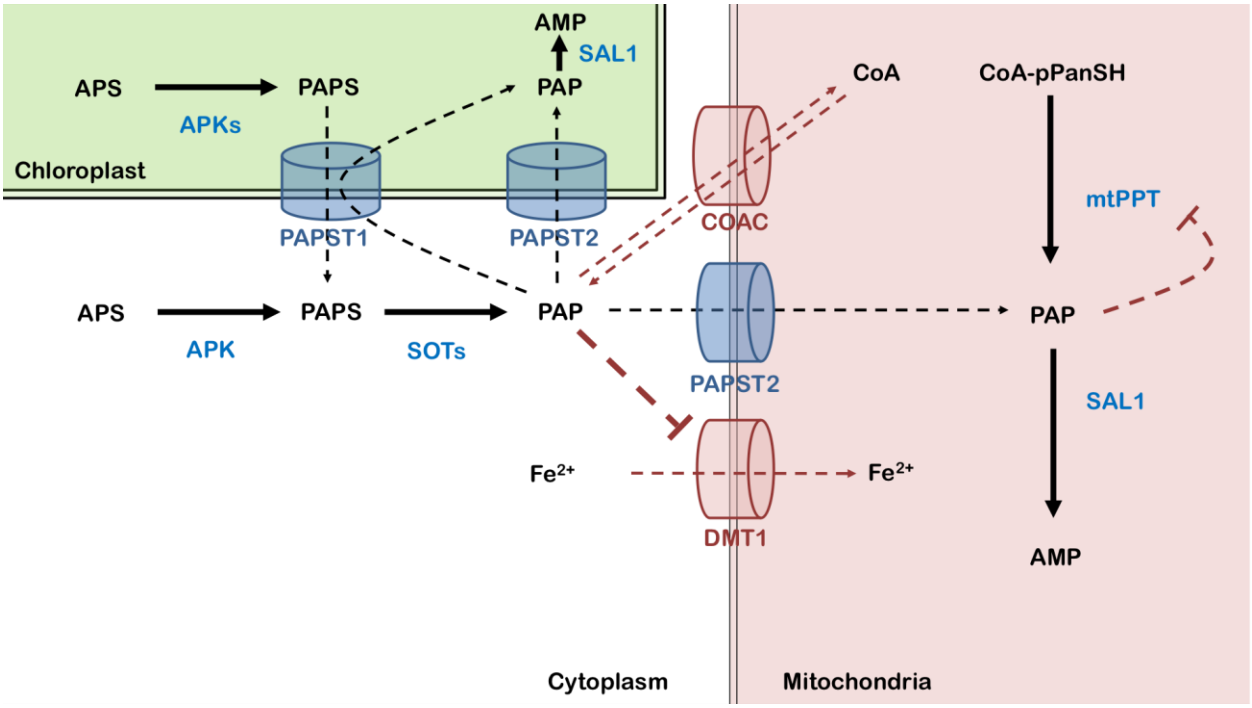

Figure.3: Compartmentalization of PAP production, degradation, transport and feedback mechanisms in cell.

Metabolites written in black(APS: Adenosine 5'-phosphosulfate, PAPS: 3′-phosphoadenosine-5′-phosphosulfate, PAP: 3′-phosphoadenosine-5′-phosphate, AMP: Adenosine monophosphate, CoA: Coenzyme A, pPanSH: phosphopantetheine), enzymes previously described in plant kingdom shown in **blue** (APK: APS Kinase, SOT: Sulfotransferase, PAPST: PAPS Transporter, SAL1: 3'(2'),5'-Bisphosphate Nucleotidase, mtPPT: mitochondrial Phosphopantetheine Transferase), transporters and enzymes which are feedback regulated by PAP mechanism described in living organism other than plants in **red**(COAC:CoA Carrier, DMT1: Divalent Metal Transporter 1).

Another interesting connection between mitochondria and PAP is mitochondrial transport of Coenzyme A. In humans, the inner mitochondrial transport protein SLC25A42 counter-exchanges CoA and PAP with high affinity (Fiermonte et al., 2009) (Figure.3). In plants, the last step of CoA synthesis is cytosolic (Webb & Smith, 2011). However, CoA is needed to be transported into mitochondria for tricarboxylic acid (TCA) cycle and mtFAS synthesis and therefore lipoic acid production (Zallot et al., 2013). Two CoA transporters located in mitochondria were characterized in Arabidopsis, COAC1 and COAC2, however, not in relation to PAP (Zallot et al., 2013).

The fact that many different forward genetic screens identified the same gene, *SAL1*, proves the importance of PAP for many cellular processes. PAP was also found as a connecting metabolite

to sulfur metabolism during an analysis of one of *sal1* alleles, *fou8*. *fou8* has been discovered through screening for changes in fatty acid oxygenation (Rodríguez et al., 2010). As all *sal1* alleles, the *fou8* mutant accumulates high concentrations of PAP and has an interesting semi dwarf phenotype with curled leaves and extensive drought tolerance (Wilson et al., 2009).

As a contrasting mutant we used Adenosine 5'-phosphosulfate (APS) kinase double mutant *apk1apk2*. APS kinase (APK) is a highly conserved enzyme located in chloroplast and cytoplasm in Arabidopsis. APK phosphorylates APS to create PAPS. APK has 4 isoforms in Arabidopsis and plastidic *apk1apk2* double knock-out mutant has semi-dwarf phenotype (Mugford et al., 2009). It has reduced synthesis of PAPS and drastically reduced glucosinolate concentrations. *apk1apk2* also shows a lower level of PAP accumulation (Lee et al., 2012).

1.5 Aim of the thesis

1.5.1 Interlink between sulfur metabolism and drought tolerance

Our observation of increased drought endurance of secondary sulfur metabolism mutants made us question the importance of the distribution of sulfur metabolites in the plant under stress. Hindering the secondary sulfur metabolism caused accumulation of primary sulfur metabolites cysteine and glutathione. The secondary sulfur restrained mutant *apk1apk2* gained increased drought tolerance. This tolerance and increased reservoir of sulfur to the primary pathway in this genotype gave us a chance to investigate the importance of different sulfur compounds under stress.

We hypothesized the increased GSH content might be the cause of drought tolerance. At the same time enhanced reducing sulfur metabolites in this mutant might be the cause of developmental problems of this mutant. To test this hypothesis we created new mutants and tested their respective drought stress performance.We crossed *apk1apk2* with *apr2* to decrease the synthesis of reducing sulfur compounds and changing the redox state of this mutant. We also crossed *apk1apk2* with *cad2* to decrease only GSH synthesis and observe the effects.To create an antagonist metabolic profile we crossed *apr2* and *cad2* mutants to achieve a mutant with very low capacity of GSH synthesis.Playing with the repository of GSH in the cell we created cysteine accumulating mutants and we wanted to test if the accumulation of only cysteine can provide protection under the drought. To test this third hypothesis we included cysteine

catabolism mutant, *des1* to render the sulfide synthesis and able to separate the impact of to metabolite from each other under stress conditions. We finally crossed *des1* with *cad2* and created a mutant with cysteine accumulation but lacking other primary sulfur metabolites.

With this set of mutants we investigated the impact of in vivo concentration of sulfur compounds on drought tolerance. We designed metabolomic and physiological experiments to test the impact of these novel sulfur compound combinations (Figure.4).

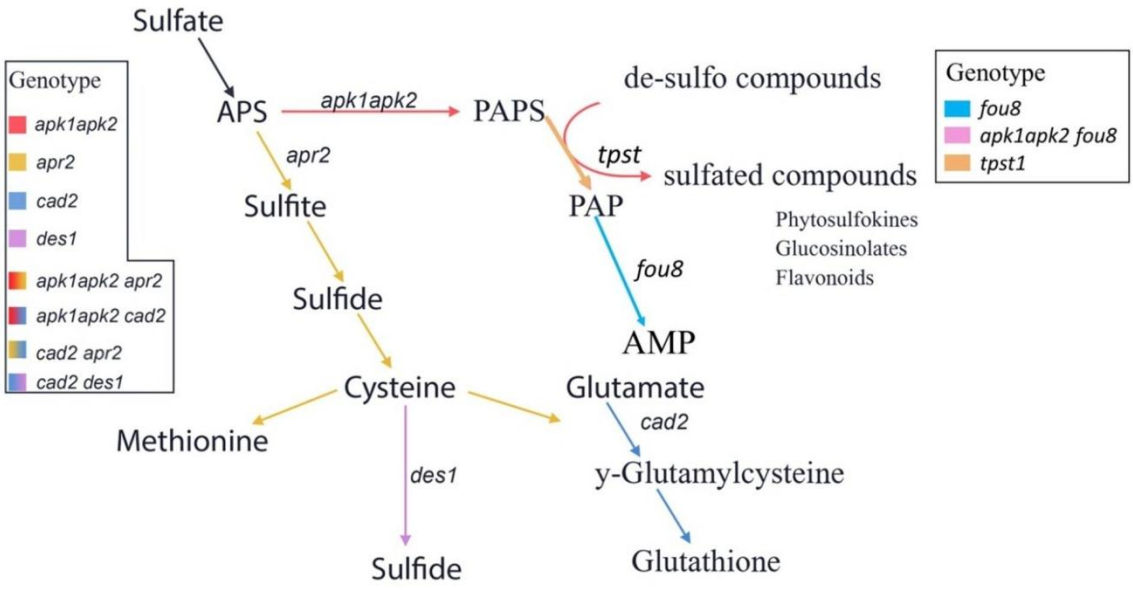

Figure.4: Sulfur metabolism mutants used for this thesis

1.5.2 The role of PAP in mitochondria

For the second part of this thesis we investigated the enigmatic question, why SAL1 is needed in the mitochondria? We hypothesized that the semi-dwarf phenotype of *fou8* may be at least partially caused by the inhibition of mtFAS, due to increased PAP concentrations in the mitochondria. mtFAS mutants characterized with their altered performance under high CO_2. We, therefore, exposed these mutants to non-photorespiratory (high CO_2) conditions and investigated the effect of PAP accumulation on primary metabolites using a gas chromatography–mass spectrometry (GC-MS) metabolomic analysis. As a contrasting mutant we used *apk1apk2* which has a lower level of PAP accumulation (Lee et al., 2012). This experiment gave us new directions for the interactions of PAP in mitochondria beyond mtFAS.

2. MATERIAL AND METHODS

2.1 Plant material

As a wild type ecotype Col-0 was used. In this study *Arabidopsis thaliana* ecotype Col-0 was used as a wild type. The single, double and triple mutants utilized for all the experiments listed in Table.1.

Table.1: List of Arabidopsis mutants used in this thesis. Locus numbers and reference articles for corresponding mutants.

Arabidopsis mutants	Locus	Reference
apr2	AT1G62180	(Loudet et al., 2007)
cad2	AT4G23100	(Cobbett et al., 1998)
des1	AT5G28030	(Álvarez et al., 2012)
tpst1	AT1G08030	(Komori et al., 2009)
fou8	AT5G63980	(Rodríguez et al., 2010)
shm1	AT4G37930	(Voll et al., 2006)
apk1apk2	AT2G14750, AT4G39940	(Mugford et al., 2009)
apk1apk2fou8	AT2G14750, AT4G39940, AT5G63980	(Lee et al., 2012)

2.2 Genotyping

Primer pairs were specifically designed for the genes and mutant lines with the T-DNA. In case of *cad2* mutant, 6 base pair deletion detected with 3-4% agarose gel electrophoresis (Cobbett et al., 1998). Seeds were grown on ½ Murashige and Skoog (MS) media (Sigma-Aldrich) containing 0.5% sucrose and numbered for genotyping. A leaf from one-week old plants was placed in a 1.5 mL tube containing 3 glass beads and 300 µL of Magic Buffer (Tris/HCl ph 7.2 50 mM; NaCl 300 mM; Sucrose 10%). Samples were then homogenized using a Bead Ruptor 24 3D (Omni International, USA). The genomic DNA (gDNA) was extracted and used for PCR reactions with the respective primer pairs for wildtype and mutant alleles. Homozygous seedlings were transferred into greenhouse and grown on soil and seeds are harvested for further experiments.

Table 2: Primers used in this thesis for PCR

apk1_F-SG	*AATCGCTATTAGGGCTTTCG*
apk1_R-SG	*GCTTAGCAACCTCTCCTAAA*
apk2_F	*TAACGTCTCTGCTCAAGC*
apk2_R	*ATGTTTTCGGTGAGGTGC*
LBb1_TDNA	*GCGTGGACCGCTTGCTGCAACTC*
apr2_F	*CTCCCTAACTGAAGCTCTTGCTTA*
apr2_R	*TCGAGAAGCAGTACGGGATT*
apr2_TDNA_R	*ATATTGACCATCATACTCATTGC*
cad2_F-SG	*GTGTAATGTGTTCTGTGCAG*
cad2_R-SG	*GCATCATATCAAGACCAAGG*
DES1_F	*GCGGTCTTTTGTCTCTTCTTC*
DES1_R	*TGTTCCAGTAACCGTTCCAC*
Des1_F-tDNA	*ACCATCAAACAGGATTTTCG*

2.3 Growth Conditions

Before every experiment seeds were sterilized 3 hours using chlorine gas under the fume hood. 2.5 mL hydrochloric acid (HCl) added in to 125 mL sodium hypochlorite (NaOCl) to fumigate the seeds for non-invasive sterilization. To break the dormancy seeds were stratified 2-3 days in dark at 4°C.

For seed sterilization by chlorine gas, put ca. 20µL Arabidopsis seeds in 0.5mL Eppendorf tube and place inside a desiccator kept in a laminar flow hood. Add 125mL of 5% NaOCl into a 250mL beaker and place inside the desiccator. Add 2.5mL concentrated HCl to the beaker and quickly close the desiccator lid. Keep in the laminar flow hood for 4h, carefully open the desiccator lid and close the tubes with sterile seeds (Günal & Kopriva, 2022). To break the dormancy seeds were stratified 2-3 days in dark at 4°C.

2.3.1 High light growth chamber: extreme drought and heat experiment

After stratification seeds were directly transferred to soil for germination. 9 cm in diameter pots used and five plants per were grown in the green house under long day conditions, 16hours light/

8hours dark at 21°C. The plants grown in the green house conditions for 3 weeks then transfered to high light chamber, 30°C 600 μmol m^{-2} s^{-1} light and 50% humidity ,for 5 days. After that full rosettes collected weighted fresh and after drying in 60°C drying oven.

2.3.2 Growth chamber: drought experiment

For the water retention experiment in growth chamber plants were also directly germinated on soil. One plant per 6 cm in diameter pot was sown. Growth conditions set to 10 hours light /14 hours dark, 22°C and 100 μmol m^{-2} s^{-1} intensity of light. Trays containing the pots were watered one time a week from the bottom.

2.3.4 Growing conditions: High CO_2 experiment

Seeds (stratification overnight at 4°C) were sown on 1/2 MS plates without addition of Sucrose and incubated at 3,000 ppm CO_2 in air (12 h light at 22 °C / 12 h dark at17 °C) for 10 days. Seedlings were transferred after 10 days onto soil (Arabidopsis substrate) and grown at 3,000 ppm CO2 in air (12 h light at 22 °C / 12 h dark at 17 °C). After 25 days, half of the plants were shifted in the evening/dark phase to 390 ppm CO_2 in air (ambient CO2) and the other half kept at 3,000 ppm CO_2 in air (12 h light at 22 °C / 12 h dark at 17 °C). After another 3 days, plants were harvested 1 h before light off. For plant growth, 100 μmol m^{-2} s^{-1} light intensity was applied

2.4 Water content calculation

For the high light chamber extereme drought experiment full rosettes were harvested and placed in previously weighted paper bags.pEach sample was immediately weighted (FW) fresh weight (FW) and placed into a drying oven at 60 °C for a week to measure dry weight (DW).

Samples from the water withdrawal experiment were collected into weighted tubes and fresh weight was measured. Open tubes were placed into -80 °C precooled blocks for lyophilization that were then placed into a laboratory freeze dryer for 48 hours running main dry mode set to 0.070 mbar (Alpha 3-4 LSCbasic, Christ).

$$\text{Water Content \%} = ((FW-DW)/FW)*100$$

Equation.1: Water content calculation. ater weight to the weight of water and remaining content. FW: fresh weight, DW: dry weight.

2.5 Isotope ratio mass spectrometry

Stable carbon isotope composition analysis is used to as an indirect indicator for water use efficiency (WUE) in plants (Ormrod et al., 1997). For each plant 1 mg of lyophilized dry adult leaf was analyzed. The method was run by CEPLAS Metabolomics Platform in Düsseldorf. Results are also represented as $\delta^{13}C$ the overall isotope carbon content of tissues in percent (Equation. 2)

$$\delta^{13}C = ((R_{sample}/R_{standard})-1)*1000$$

Equation 2: Isotope ratio δC13 calculation . R_{sample} is the carbon isotope ratio of the sample and $R_{standard}$ is the standard carbon isotope ratio (Farquhar et al., 1982)

2.6 Anion analysis

First samples were grinded for the analysis. After adding 1 mL of sterile water to each tube, samples were incubated for one hour at 4ºC and 1500 rpm. Subsequently samples were heated at 95ºC for 15 minutes and vortexed and centrifuged at maximum speed for 15 min. The resulting supernatant was collected into plastic vials and diluted with water when required. Anions were measured and separated using a Dionex ICS-1100 chromatography system with a Dionex IonPac AS22 RFIC 4x 250 mm analytic column (Thermo Scientific, Germany). External standards of nitrate, phosphate and sulfate were prepared as 0.5mM, 1 mM and 2 mM mix of KNO3, KH2PO4 and K2SO4 and 4.5 mM NaCO3/1.4 mM NaHCO3 was used as running buffer.

2.7 Counting of stomata

Stomata were counted by creating imprints of the abaxial side of adult leaves. After cutting each leave, it was immediately covered in transparent nail polish. Four biological replicates were taken from each genotype. After the nail polish dried after ca. 2 min the leaf was pulled off the hardened polish to leave imprints of the surface cells. This imprint was then explored by usual bright field microscopy (Leica DM3 XL, Leica Microsystems). Stomata density was therefore calculated using Equation 3 to show stomata number per mm^2. Five different locations from each imprint were counted.

Stomata density = stomata counts / area of counting

Equation 3: Stomata density calculation

2.8 PAM analysis

To assess changes in photosynthesis, the fluorescence of photosystem II was measured following a period of dark adaptation, allowing evaluation of the efficiency and activation dynamics of the light-harvesting system. The exact methods for using a pulse amplitude modulation (PAM) to measure kinetic fluorescence and mathematic relations are described (Genty et al., 1989). First PAM analysis was performed on 5 week old plants that were grown under control conditions. Later same analysis performed with drought treatment plants which were not watered since 2 weeks.

Following 15 min of dark adaptation the the minimum fluorescence (F_O) measured. To measure the maximum fluorescence (F_m) plants are exposed to short bursts of saturating light (0.8 sec, ~ 6000 μmol photon $m^{-2}s^{-1}$). as all reaction centers are closed due the antennas absorbing photons. The variable fluorescence (F_v) is the difference between the two extremes and originate from PSII Reaction centers. Both F_O and F_m values are essential to generate photosynthetic quenching as well as non-photochemical quenching. Photoinhibition effects are introduced by F_v in relation to maximum fluorescence Fm, see Equation 4 and Equation 5 (Genty et al.,, 1989).

F_O = minimum fluorescense of Chl-a in dark adapted plant

F_V = variable Fluorescense in light originating from PS II reaction centers

F_m= maximum variable fluorescence in a dark adapted plant

F'_m = maximum variable fluorescence in light adapted plant

F_t = variable fluorescense in light

Absorbed light is distributed into three categories. ΦPSII represents the relative yield of PSII by photochemical quenching; ΦNPQ displays regulated dissipation, non-photochemical quenching, and ΦNO equals non light induced quenching. Sum of these ΦPSII+ΦNPQ+ΦNO three values equals to 1 (Genty et al., 1989). Calculations done automatically in Imaging PAM software according to equations described in Klughammer et al., 2008.

$$\Phi PSII = (F´m - Ft)/F´m$$

Equation 4 Yield of PSII calculation (Klughammer et al., 2008)

2.9 PAP extraction and analysis

Tubes were prepared with heated extraction buffer, containing 62 mM citric acid and 76 mM K_2HPO_4 arranged to pH 4 with KOH. Samples were homogenized in a buffer and heated in a heat block at 80 °C for 5 minutes before being placed on ice for 15 minutes. Extracts were centrifuged at max speed for 10 minutes at 4 °C and 150 µl supernatant was transferred into 305 µl extraction buffer. For standards, 50µl of different concentrations were added to 405 µl of extraction buffer. 45 µl chloroacetaldehyde was added to the samples and standards. Tubes were vortexed and heated for 40 minutes at 60 °C before placing samples on ice again for 15 minutes. Samples were centrifuged at max speed for 10 minutes at 4 °C and supernatant transferred into new tubes containing 500µl sterile water. Tubes were then vortexed and the mix was transferred into plastic HPLC tubes. PAP concentrations were detected using high-performance liquid chromatography (HPLC; UltiMate 3000, Thermo Fischer Scientific Inc.) after the method from (Haink & Deussen, 2003). Running buffer A contained 5,7 mM TBAS and 30,5 mM KH_2PO_4 adjusted to pH 4 with KOH and B was 60% acetonitrile in water.

2.10 Metabolomic analysis with GC-MS

Metabolomic analysis of plants performed by Dr. Philipp Westhoff from CEPLAS Metabolomics platform. As described in Zenzen et al., 2024. 1.5 ml of 4 °C pre-cooled solvent mixture of methanol/chloroform/ water (2.5:1:1 v/v/v) containing 5 µM ribitol used for extraction from samples. Each sample was taken from 35-40 mg of frozen plant material. Samples were vortexed for 20 s and then placed in a shaker at 4°C for 6 min and centrifuged for 2 min at 4°C with 12700 rpm. The supernatant was transferred and stored -80°C for later analysis. 50 **µ**l of the extract wee dried in a speed vacuum concentrator and subjected to a two-step automatic sample derivatization. Subsequently 10 **µ**l of freshly mixed methoxyamine hydrochloride were added to pyridine 20 mg*ml-1 and shaken for 90 min at 37°C. Next 90 **µ**l N-Methyl-N-(trimethylsilyl) trifuoroacetamide (MSTFA) was added to the mixture and samples were shaken at 37°C for 30 min. Samples were then incubated at room temperature for 2 h. Then 1 µl of the derivatized compounds were analyzed by gas chromatography coupled to mass spectrometry. To identify

metabolites MassHunter Workstation Qualitative Analysis Software (version B.06.00, Agilent Technologies, Santa Clara, California, USA) was utilized. In the output metabolites were identified by comparison by comparison of spectra to the NIST14 Mass Spectral Library As a response check and retention time reference a standard mixture containing all target compounds at a concentration of 5 µM was processed in parallel. Subsequently found peaks were integrated using MassHunter Workstation Quantitative Analysis Software (version B.08.00, Agilent Technologies, Santa Clara, California, USA), and quantified relatively from the integration of metabolite peak areas normalized to the corresponding sample fresh weight used for extraction and the peak area of the internal standard (ribitol).

2.11 Gene set enrichment analysis

The gene enrichment analysis was performed with g:profiler (Raudvere et al., 2019). Differentially expressed genes (DEG) list of *sal1-8* was taken from a previous study (Crisp et al., 2017). The complete list of genes located in mitochondria (GO:0005739) and chloroplast (GO:0009507) was compared with DEG list of *sal1-8* mutant.

2.12 ^{35}S Flux analysis

Flux analysis with radioactive ^{35}S is carried out as described in Günal & Kopriva (2022). We analyzed the 2.5 weeks old total(shoot+root)seedlings grown in ½ MS media after labeling with [^{35}S] solution for 4 hours.

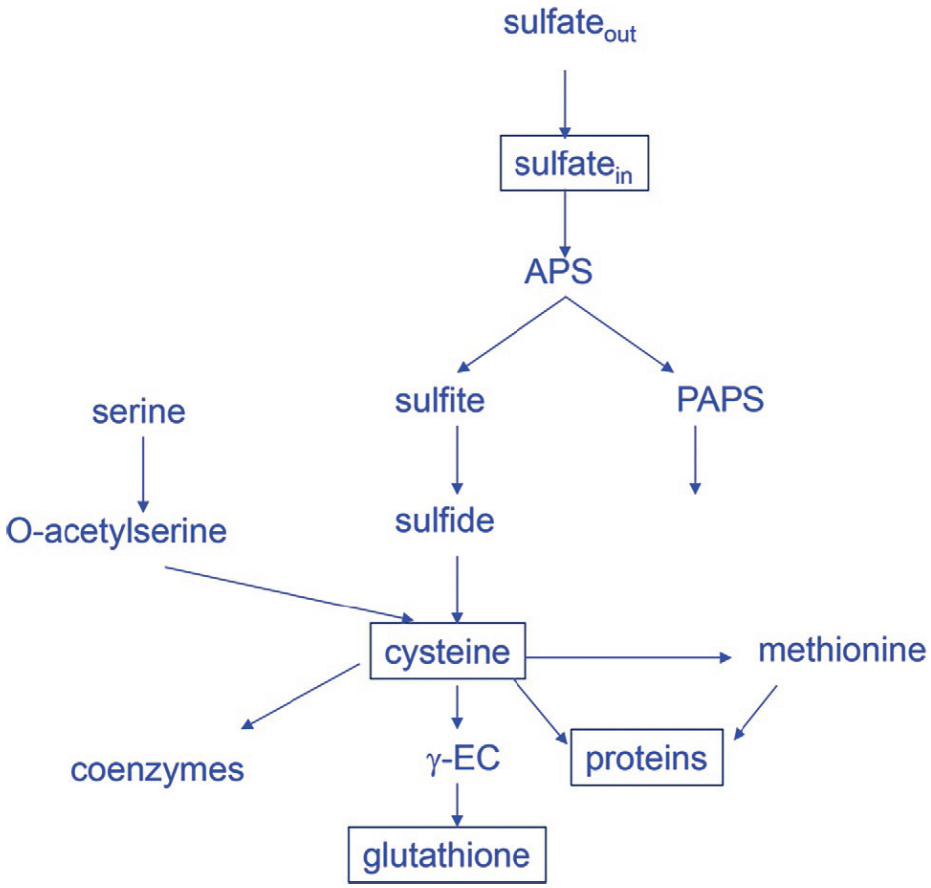

Figure.5: Scheme of sulfate assimilation. The pools measured in the flux protocol are boxed. Sulfate uptake, Cysteine, glutathione and total proteins can be calculated with ^{35}S (Günal & Kopriva, 2022).

Nutrient solution

- 0.6M $Ca(NO_3)_2$ X 4 H_2O
- 0.4M KNO3
- 0.3M KH_2PO_4
- 0.2M $MgSO_4$ X 7H_2O
- 40mM Na Ethylenediaminetetraacetic acid Fe(III)
- 10mM $MnCl_2$ X 4H_2O
- 50mM H_3BO_3
- 1.75mM $ZnCl_2$
- 0.5mM $CuCl_2$
- 0.8mM Na_2MoO_4
- 0.1mM $CoCl_2$ X 6H_2O

- 1mM KI
- 4-Morpholineethanesulfonic acid hydrate (MES)

2.12.1 [^{35}S] Labeling

The labelling solution was prepared, containing the nutrient solution adjusted to sulfate concentration of 0.2mM. To a 50mL falcon tube place at least 1mL of the nutrient solution per well was added. Further steps were performed in a room certified for work with radioactive substances. 0.5µL of the [35S] sulfate stock was added per ml of nutrient solution to the labelling solution in Falcons, close and mix. 2mL scintillation cocktail was added into a scintillation vial. Then 10µL of the labelling solution were added, mixed, and the radioactivity was determined by scintillation counting. The activity should reach at least 100,000cpm per 10µL of the labelling solution. In case of too low activity additional volume of the [^{35}S] sulfate stock was added, mixed and re-measured. This measurement gives the specific activity of sulfate in the experiment (cpmsulf) as the measured cpm/2 per nmol sulfate. (10µL of 0.2mM solution correspond to 2nmol sulfate). 1mL of the labeling solution was added to the plants in the wells. Subsequently, the plates were kept under a light source for 4h. After this incubation plants were washed with water and the whole seedlings were placed in weighted 1.5 ml tubes. Fresh weight was recorded and samples were frozen with liquid nitrogen.

Plants were homogenized and centrifuged for 5 min at maximum speed. 2mL scintillation cocktail were added into a scintillation vial, 10µL of the supernatant were added to tubes with 1ml scintillation cocktail and the radioactivity was determined by scintillation counting. This measurement gives the radioactivity of [^{35}S]sulfur in 1mg of plant material (10µL after 1:10 extraction correspond to 1mg FW). For determination of [^{35}S] in proteins 100µL of supernatant was pipetted into a new tube, for determination in thiols 50µL of supernatant was used (Figure.5).

2.12.2 Homogenisation and determination of sulfate uptake

Plants homogenized in 10-fold (V/w) volume of 0.1M HCl using micro pestles. For volumes above 300µL homogenize first in a smaller volume (300µL), add the rest volume, and shortly homogenized with the full volume. After homogenization keep tubes on ice till all extractsare finished. Samples were centrifuged 5min maximum speed in a microfuge. 2mL scintillation

cocktail added into a scintillation vial, add 10µL of the supernatant, mix, and determine the radioactivity by scintillation counting. This measurement gives the radioactivity of [35S]sulfur in 1mg of shoot (cpmS) or root (cpmR) (10µL after 1:10 extraction correspond to 1mg FW).For determination of [^{35}S] in proteins pipette 100µL of supernatant into a new tube. For determination of [^{35}S] in thiols, pipette 50µL of supernatant into a new tube. To calculate sulfate uptake in the plants, determine first the uptake into roots (UP-R) and shoots (UP-S) in nmol/h/g FW according to following formula: 1000cpmR/cpmsulf/4 or 1000cpmS/cpmsulf/4, respectively. From these values calculate the total amount of sulfate taken up into the plant per hour (TOT): (UP-R x FWR)+(UP-S x FWS). This value divided by FWR gives the sulfate uptake in nmol/h/g root.The UP-S value represents the rate of sulfate root-to-shoot translocation.The allocation of sulfate in the shoot can be calculated as percentage of sulfate taken up found in the shoot, i.e., (UP-S x FWS)/TOT.

2.12.3 Determination of incorporation into proteins

1. 25µL 100% TCA solution added to the 100µL extract from 2.2.1 and keep on ice for 15min. Centrifuge for 10min at maximum speed in a microfuge, discard the supernatant.Wash the pellet in 100µL 1% TCA, centrifuge for 5min, discard supernatant.Wash the pellet in 200µL 96% EtOH, centrifuge for 5min, discard supernatant, and leave air dry for 10min.Dissolve the pellet in 100µL 0.1M NaOH. Add 2mL scintillation cocktail into a scintillation vial, add the whole 100µL protein solution, mix, and determine the radioactivity by scintillation counting. This measurement, after division by cpmsulf, division by 4 (for 4h), division by 10 (for 10mg tissue), and multiplication by 1000 (to adjust for g FW) gives the incorporation of [^{35}S]sulfur per hour and g of shoot (PROTS) or root (PROTR). Relative incorporation into proteins can be calculated as PROTS/UP-S or PROTR/UP-R.

2.12.3 Determination of incorporation into thiols

50µL extract from homogenized samples taken add 50µL 0.1M NaOH to neutralize and 1µL 0.1M DTT to reduce the thiols and incubate in dark at 37 °C for 15min.Add 11.5µL 1M Tris-HCl pH8.0 and 5µL 100mM monobromobimane to label the thiols, mix and incubate in dark at 37 °C for 15min. We added 11.5µL 50% acetic acid, mix and centrifuge for 10min at maximal speed and transfer the supernatant into HPLC vials. Inject 100µL into high-performance liquid

chromatography (HPLC) system, where the thiol conjugates are separated and quantified. Any HPLC system can be used with a reverse phase column (Spherisorb ODS2, 250 X 4.6mm, 5µm), fluorimetric detector (excitation: 390nm, emission: 480nm) and radiodetector (e.g., FlowStar). Two solvents are used in a linear gradient from 5 to 18% B (90% methanol, 0.25% acetic acid, pH3.9) in A (10% methanol, 0.25% acetic acid, pH3.9) over 20min with a constant flow rate of 1mL/min. The first radioactive peak coming with the front represents sulfate, later peaks correspond to cysteine and glutathione and another peak is detected after the column is washed with 100% solvent B. The output of the Chromatography Data System Software should be set to peak relative area.To determine the incorporation into the individual sulfur pools (in nmol S/h/g FW), use the peak percentage area (PPA), using this guide:

$GSH_{R\ or\ S} = ¼1000 * PPA_{GSH}$ X cpm_R or S/cpmsulf/$_4$ and analogically,

$Cys_{R\ or\ S} = ¼1000 * PPA_{GSH}$ X cpm_R or S/cpmsulf/$_4$

The flux through primary assimilation is calculated by addition of the incorporations into proteins and thiols—$PROT_{R\ or\ S}$+$Cys_{R\ or\ S}$+$GSH_{R\ or\ S.}$ The flux is dependent both on sulfate uptake and assimilation rate.The relative flux is the percentage of the primary flux in the total ^{35}S uptake. The relative flux is dependent only on the assimilation rate.

2.13 Cysteine and glutathione analysis

Low-molecular weight thiols were analyzed as described in with a similar method described in section 2.12.4 without radioactive labeling or detection.

2.14 Statistical analysis

Statistical analysis was performed using R (R Development Core Team, 2008) and Microsoft Office Excel 365. The data was tested for normality (with Shapiro-Wilk test) and homoscedasticity (with Levene's test), if null hypothesis for both tests could be confirmed, an ANOVA test was performed to test for significant differences in means of the groups. For experiments with 2 independent variables two-way ANOVAS were performed, for on variable a one-way ANOVA or one-tailed, unpaired Student’s t tests were performed. After the ANOVA indicated significant differences (null hypothesis rejected), a post-hoc Tukey-Duckworth test was carried out to identify which specific groups differed from each other. All statistical tests were

conducted at a 95% confidence level, with a p-value below 0.05 considered statistically significant, leading to rejection of the null hypothesis. Respective statistical tests are indicated below each graph. Plots were created using libraries ‘tidyverse’ and ‘ggpubr’ (Kassambara et al., 2020; Wickham et al., 2019).

For the metabolomics analysis mean values were calculated from 4-5 biological replicates. The outliers were detected by calculating Interquartile Range 1.5. The values below (Q1-1.5.IQR) and values above (Q3+1.5.IQR) were labeled as outliers. Mean values of the response rates of the wild type at the given condition were compared to mean values of the mutants for the graphs. The mean value changes of the metabolites illustrated as log2 fold change. Two-tailed, unpaired Student’s t test used for significance analysis in Microsoft Office Excel 365. Asterisks mark values significantly different from WT *:$P \leq 0.05$,**:$P \leq 0.01$,***:$P \leq 0.001$.

3. RESULTS I

3.1 Analysis of sulfur metabolism mutants impaired in both primary and secondary pathway

3.1.1 Extremely high Cysteine accumulation in *apk1apk2cad2* mutant

A big part of our knowledge about sulfur metabolism is derived from studies of knock-out and knock-down mutants. It has been previously shown before that mutants in APS reductase, such as *apr2*, result in reduced flux through primary assimilation and accumulation of sulfate (Vauclare et.al 2002). Another mutant in primary sulfur metabolism is *sir1-1*, a knock down mutant of a single gene *SiR*, which shows defects in growth and also accumulates sulfate and OAS. Interestingly, crossing this mutant with *cad2*, a knock down of the first enzyme GSH1 of the glutathione synthesis pathway, decreased the reductive cellular redox state of the mutant and that increased the flux to primary sulfur metabolism as a result partially rescued its dwarf phenotype (Speiser et. al 2018).

The *apk1apk2* mutant is a double mutant of *APK*, the key enzyme at the diverging point of sulfur metabolism. The *apk1apk2* mutant accumulates significantly higher concentrations of primary sulfur compounds Cys and GSH and has significantly lower amounts of glucosinolates (Mugford et al 2009). Even though glucosinolates belong to secondary metabolites, APK is a vital enzyme for Arabidopsis. Knocking-out all the isoforms of the gene is lethal, knocking-out the main isoforms *APK1* and *APK2* cause growth attenuation and dwarf phenotype.

To test if the reason for the growth impairment of *apk1apk2* is the GSH accumulation and change in redox properties similar as in *sir1_1*, we crossed *apk1apk2* mutant with *cad2* mutant. In particular, we investigated how decreasing the high concentrations of GSH in *apk1apk2* impacts the flux through sulfur metabolism, using radioactive sulfur isotope ^{35}S tracing. We observed around 6% of the sulfate taken up being incorporated into primary sulfur metabolites in the wild type (Figure.6). In addition, we showed that *apk1apk2* mutants incorporated around 3-fold more sulfate into cysteine and GSH (Figure.6). While *cad2* mutants did not show any significant difference in total primary assimilation, they exhibited 3.5-fold increased cysteine synthesis rate and 3-fold decreased incorporation into GSH. The double mutant *apk1apk2* and triple mutant *apk1apk2cad2* both had 2.5-fold increase in primary sulfur assimilation. All three

mutants showed around 2-fold higher labeled sulfur detected in their proteins compared to Col-0 (Figure.6). We also found that ^{35}S incorporation into GSH in the *apk1apk2* mutant was reduced closer to wild type levels in *apk1apk2cad2* as a consequence of crossing with *cad2* (Figure.6). Finally, our most striking finding was cysteine synthesis levels in the triple mutant, *apk1apk2cad2,* which incorporated 15-fold more ^{35}S compared to wild type (Figure.6).

Crossing *apk1apk2* with *cad2* did not rescue the dwarf phenotype, even though it decreased the GSH levels. However, cysteine levels were still higher compared to WT (Figure.6, Figure.7 & Figure.11). Notably, another mutant accumulating Cys, *des1*, did not exhibit the dwarf phenotype. Furthermore, crossing *apk1apk2* with *apr2* was also not sufficient to completely rescue the phenotype (Figure.11). The levels of primary sulfur metabolites in *apk1apk2apr2* mutant were still significantly higher than WT. Therefore, our results showed that the growth attenuation of *apk1apk2* mutant is likely related to the secondary sulfur metabolism related (Mugford et al., 2009).

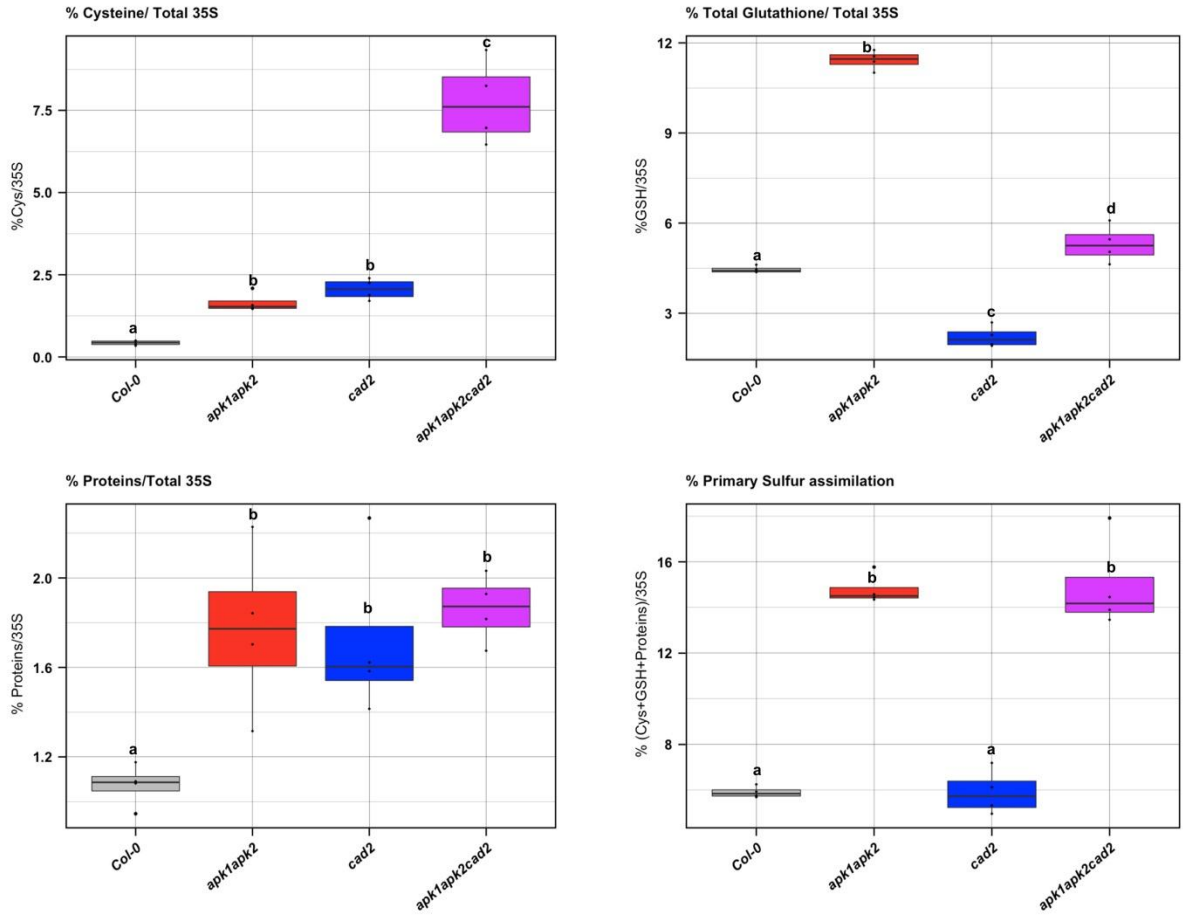

Figure.6: Analysis of flux of the sulfur metabolism in *apk1apk2*, *cad2* and *apk1apk2cad2* mutants
Incorporation of ^{35}S into, Cysteine, Glutathione, proteins and total primary sulfur assimilation metabolites shown as a percentage of ^{35}S incorporated from ^{35}S taken up (Günal & Kopriva, 2022). The data is shown as box plots, each point representing one biological one of 4 biological replicates. The significance analyses between each genotype were calculated with Student's t-test and different letters represent values that are significantly different ($P < 0.05$).

3.1.2 New sulfur mutants with broad range of cysteine and glutathione concentrations

The *apk1apk2cad2* results, which showed much higher cysteine values than previously considered toxic (Romero et al., 2014) intrigued us to investigate more mutants around the branching point of sulfur metabolism. We crossed *apk1apk2* with another well studied primary sulfur metabolism mutant *apr2*, and obtained a triple mutant *apk1apk2apr2* to further analyze this interplay. We hypothesized that crossing these mutants would decrease the S assimilation and Cys and GSH concentration which would in return rescue the dwarf phenotype similar to the *sir1-1* mutant (Speiser et al., 2018).

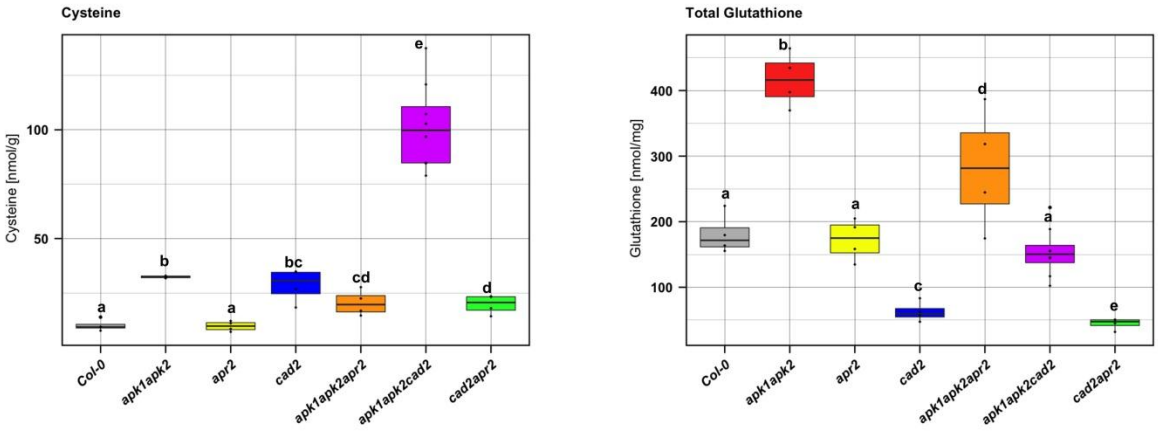

Figure.7: Cysteine and glutathione in mutants in primary and secondary sulfur metabolism
Plants were grown on ½ MS media for 2.5 weeks and thiols in whole seedlings were analyzed with HPLC. The collected data is shown as box plots, each point representing one of 4-6 biological replicates. The significance analyses between each genotype were calculated with Student's t-test and different letters represent values that are significantly different ($P < 0.05$).

We also crossed *apr2* with *cad2* to combine the impact of these two primary sulfur enzyme mutants. Extraction and quantification of thiols showed that the *apr2* mutation did not impact the concentration of cysteine or GSH on its own. However, when combined with other mutations, it decreased their primary sulfur assimilation. *cad2apr2* had only 20-25% of the wild type GSH, which was lower than *cad2*. The crossing with *apr2* brought down the cysteine and GSH levels of *apk1apk2*. However, *apk1apk2apr2* still showed higher concentrations of GSH and Cys compared to WT even though it was significantly lower than *apk1apk2*. The thiols results suggested that the effect of these mutations was additive when two sulfur metabolism mutants were combined. It also showed that the loss of APR2 alone does not have an impact on thiols under normal conditions, but only when the demand for sulfate reduction is increased.

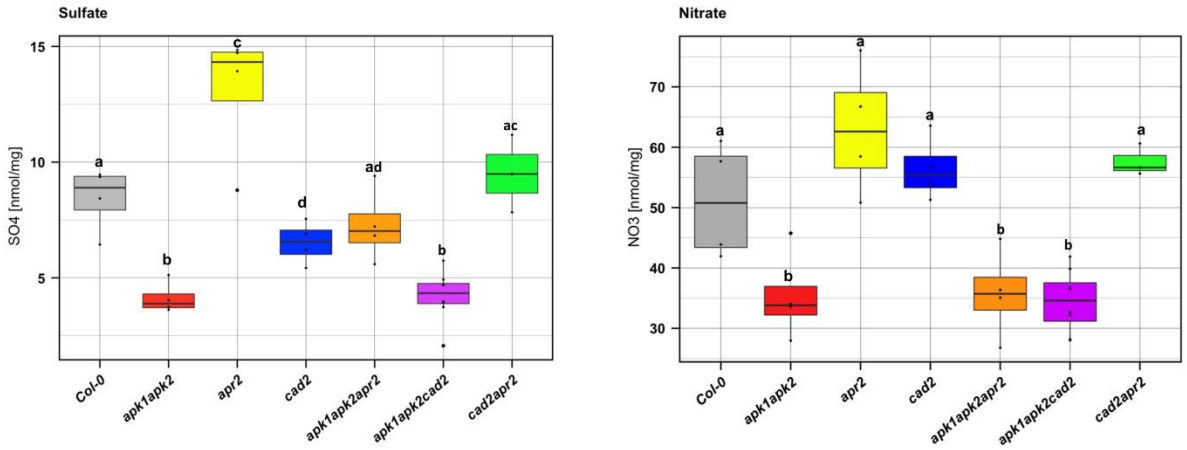

Figure.8: Measurement of anions sulfate and nitrate in the set of primary and secondary sulfur metabolism mutant seedlings.

Whole seedlings grown on ½ MS media for 2.5 weeks were analyzed**.** The collected data is fully shown as box plots, each point representing a sample. 4 biological replicate have been used. The significance analyses between each genotype were calculated with Student's t-test and different letters represent values that are significantly different ($P < 0.05$).

We then measured the anions, i.e., sulfate, phosphate, and nitrate, in these mutants (Figure.8, Supplementary Figure.1). The *apk1apk2* and *apk1apk2cad2* mutants showed significantly lower sulfate and nitrate contents compared to WT. *apk1apk2cad2* also had significantly lower sulfate and nitrate. However, *apr2* accumulated sulfate to higher levels, as described previously (Chao et al., 2014). Interestingly, sulfate levels of *apk1apk2apr2* were higher compared to *apk1apk2* revealing the dominant impact of *apr2* on sulfate accumulation in this genotype. Nonetheless, the nitrate levels remained significantly lower than WT and closer to *apk1apk2* levels in *apk1apk2apr2* triple mutant (Figure.8). The GSH synthesis impaired *cad2* mutant showed significantly lower sulfate levels. Crossing this mutant with sulfate accumulating *apr2* brought the sulfate levels of *cad2apr2* back up to WT levels in the double mutant (Figure.8). Phosphate analysis only showed significant increase in *apk1apk2apr2* and *apk1apk2cad2* mutants compared to WT (Supplementary Figure.1).

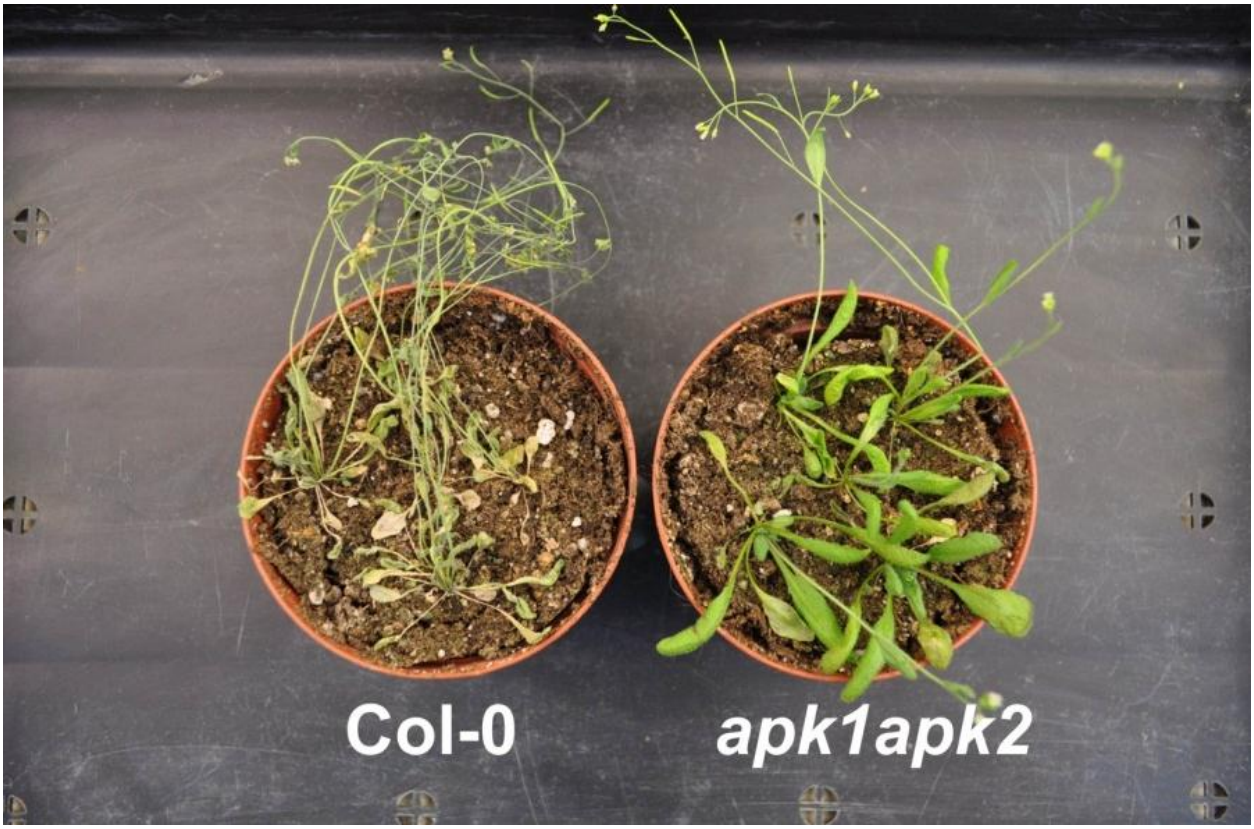

Figure.9: Drought resistance of *apk1apk2* mutant
4-week-old greenhouse grown plants were placed in a high light chamber for 5 days under high temperatures (30°C) and high light (600 $\mu Em^{-2}s^{-1}$)

3.2 Primary sulfur compounds providing drought protection

A critical observation was made in AG Kopriva on the drought resistance of *apk1 apk2* mutants in the greenhouse The *apk1apk2* mutants were left to dry and not watered during an extended holiday period of 14 days but survived, while WT plants had already dried out (Figure.9 & Figure.10). This led us to focus on the contribution of S metabolism to abiotic stress tolerance. First, we tested the survival of *apk1apk2* and related mutants in the high light chamber at 30°C and 600 $\mu Em^{-2}s^{-1}$. The WT plants dried rapidly, whereas *apk1apk2* mutant and its triple crosses *apk1apk2apr2* and *apk1apk2cad2* survived even after 5 days in the chamber without water (Figure.9, Figure.10 & Supplementary Figure. 2). *apk1apk2* mutants preserved 70-80% water content while WT had long dried out (Figure.9 & Figure.10). *apr2, cad2, des1* and *cad2apr2* mutants all contained significantly less water than WT after stress treatment. *apk1apk2* was significantly higher than all the other genotypes while *des1* was significantly lower.

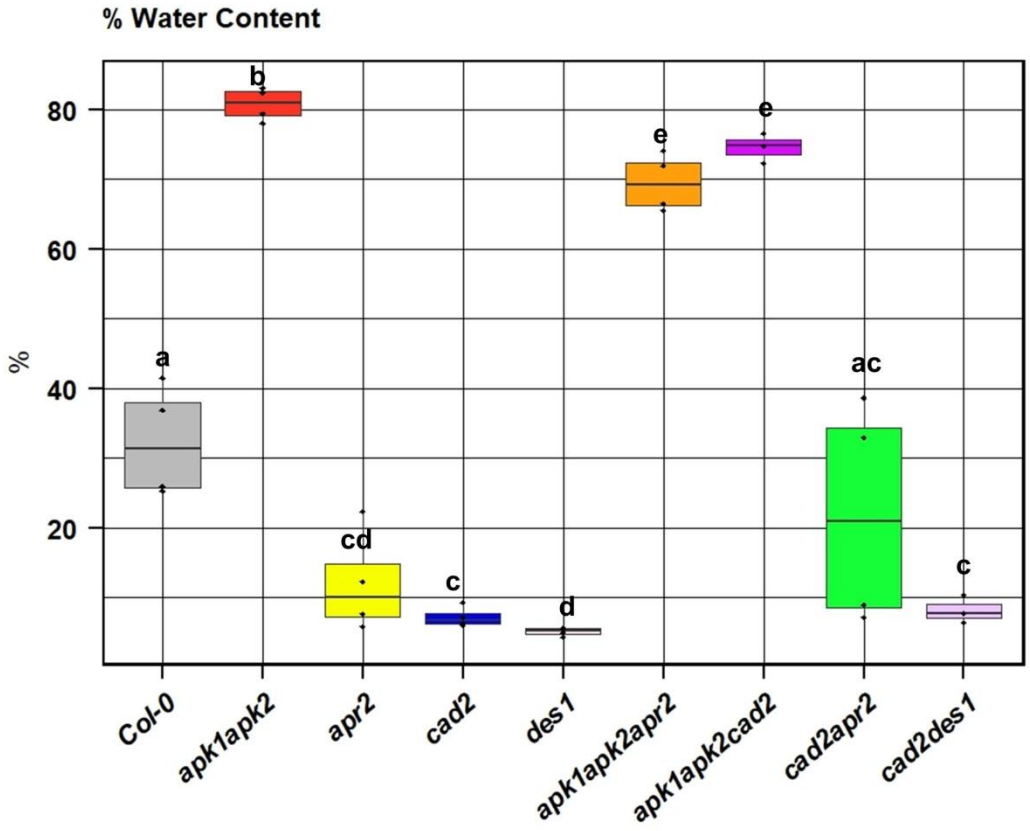

Figure.10: Water content of the sulfur metabolism mutants after extreme drought and heat stress.
5 weeks old plants grown in green house under long day conditions were subjected to water withdrawal for 5 days in high light chamber at 30°C and 600 $\mu Em^{-2}s^{-1}$. Full rosette samples were collected and fresh weight, as well as dry weight and water content were measured. The data is shown as box plots, each point representing one of 4 biological replicates. Asterisks mark values significantly different from their respective control treatment (*:$P \leq 0.05$,**:$P \leq 0.01$,***:$P \leq 0.001$ Student t-test). Significance analyses between each genotypes calculated with Student's t-test are shown as different letters.

To understand the role of sulfur metabolism in drought tolerance in more detail, we created additional sulfur metabolism mutants. We included *des1* mutant in the main cysteine degrading enzyme DES1 (Álvarez et al., 2010). DES1 is located in the cytoplasm, converting cysteine to sulfide and, therefore, accumulates higher levels of cysteine and GSH while having reduced levels of the gaseous signaling molecule H_2S (Álvarez et al., 2010). *des1* knock-out mutant is not able to produce sufficient sulfide which acts as a signaling molecule to trigger stomata closure, accumulation of osmolytes and antioxidant molecules under drought stress (Thakur & Anand,

2021). The connection of sulfide to stomatal closure and ABA signaling makes sulfide directly related to drought response (Scuffi et al., 2014).

To create another cysteine accumulating mutant we crossed *des1* with *cad2* mutant and created the *cad2des1* double mutant. Theoretically, this mutant cysteine cannot effectively degrade cysteine or utilize it for GSH synthesis and it is expected to accumulate cysteine more than *cad2* or *des1*. The four different sulfur metabolism mutants in the different key points of the pathway and their combinations were grown at short days and their growth was compared. Our results showed that the dwarf phenotype of *apk1apk2* mutant was not rescued when crossing with *cad2* or with *apr2* (Figure.11). In addition, no significant differences between the triple mutants were detected under short day conditions and they were all less than 50% of the surface area of WT. However, under long day conditions *apk1apk2cad2* was found to be significantly smaller than other *apk1apk2* mutants. Finally, we observed that *des1* rosette areas were around 17% larger than WT while the *cad2des1* values were around 24% smaller. The double mutant *cad2apr2* plants were also significantly smaller with a 30% smaller rosette surface area compared to WT (Figure.11).

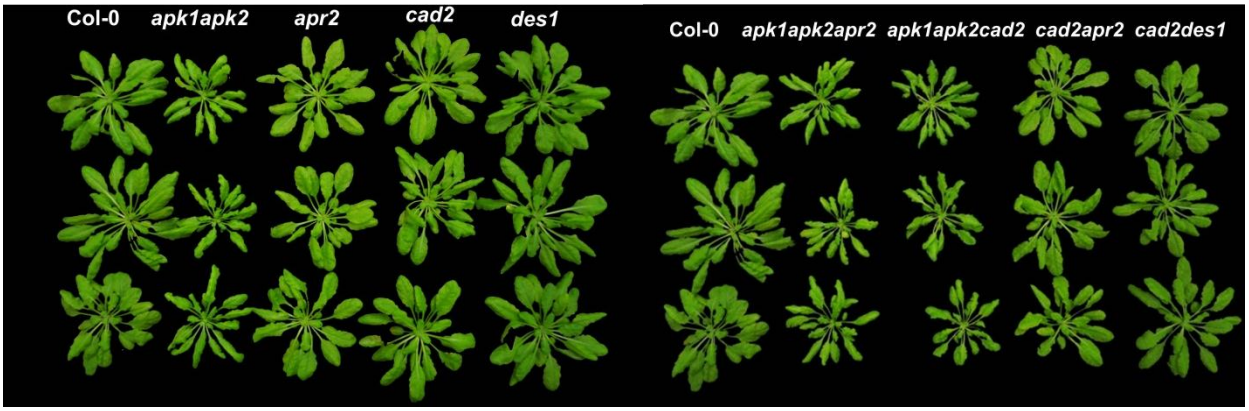

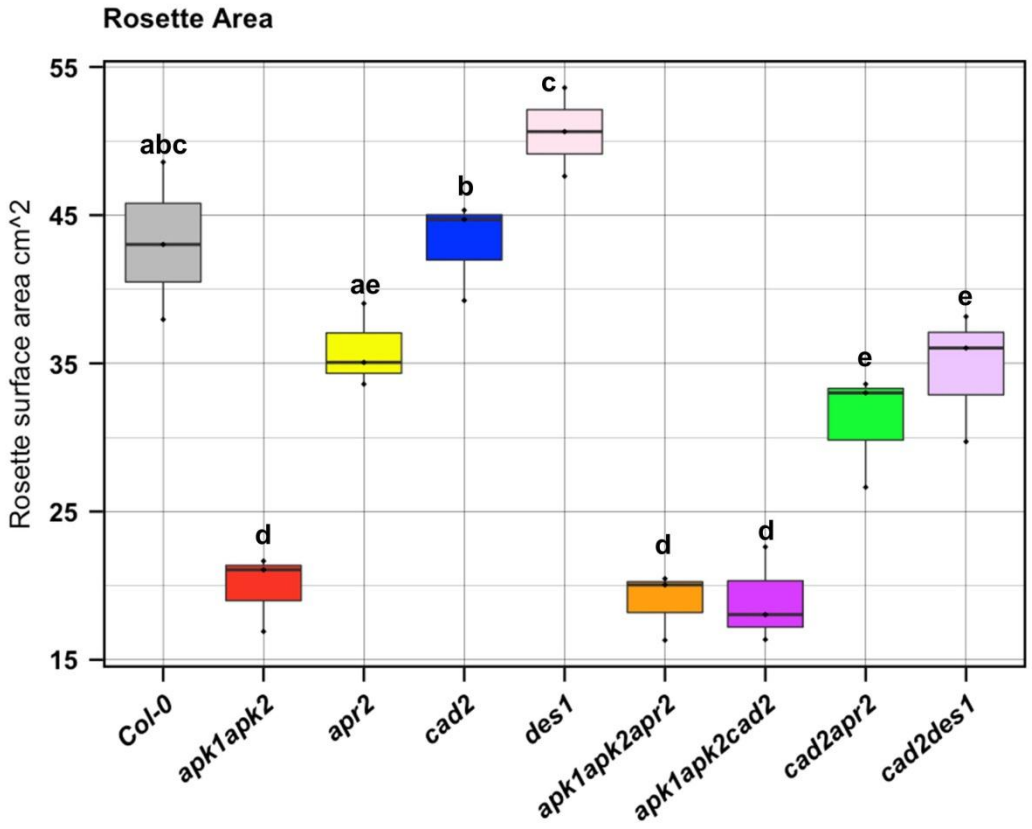

Figure.11: Rosette surface area of the sulfur metabolism mutants.
Plants were grown for 8 weeks in a growth chamber in short day conditions. Surface area is calculated with ImageJ from photographs. The collected data is fully shown as box plots, each point representing a sample. 3 biological replicate were used. The significance analyses between each genotype were calculated with Student's t-test and different letters represent values that are significantly different ($P < 0.05$).

3.2.1 Differentiating the role of cysteine and glutathione under drought stress

The set of mutants offered a great opportunity to further dissect the importance of different sulfur compounds in response to drought stress. In our toolbox we had mutants with altered levels of cysteine and GSH as well as secondary sulfur compounds. We carried out a water withdrawal experiment with our set of mutants under controlled conditions in sterile growth chambers to avoid any other stresses. We tested our previous findings from the high light chamber and were aiming to provide milder stress conditions for further metabolic analyses.

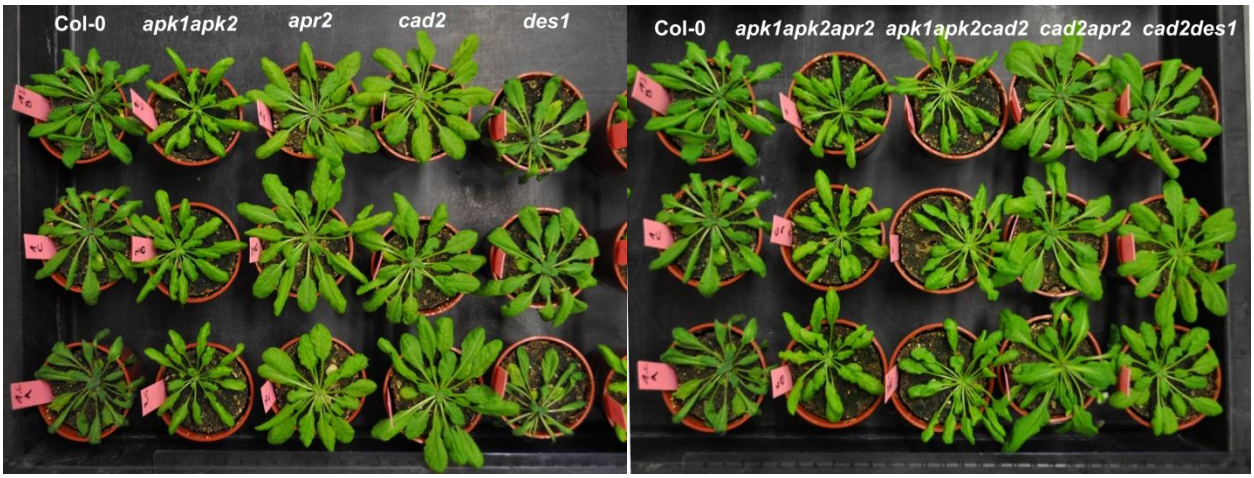

Figure.12: Water withdrawal experiment of sulfur metabolism mutants.
5 weeks old plants were used for this experiment and water was withdrawn for 3 weeks for the drought treatment group. At the time of the photograph plants were 8 weeks old; they were grown in a growth chamber under short day conditions.

While the *des1* mutant showed a better growth performance at control conditions, it was the first plant that started to wilt after 3 weeks of water withdrawal (Figure.12). Thus, we collected leaf samples from all genotypes. First, we quantified the water content of the leaves after freeze drying. Notably, *apk1apk2* mutant and its crosses showed lower water content already in well-watered conditions. Under control conditions Col-0 had 90% water content in the leaves while *apk1apk2* mutant had significantly less water, around 80% and *apk1apk2cad2* showed even lower water content values with around 70% (Figure.13). Because of the initial difference in the water contents, comparing the final water content after drought treatment can be misleading. Therefore, the comparison of the drought treatment samples of the mutants with their respective control conditions explains the drought stress response better than the absolute values. However, only the water content of Col-0, *des1* and *cad2* was significantly reduced, while the water

content of other mutants was not affected. This was especially surprising in *apr2*, which had a lower capacity to reduce sulfate (Figure.13).

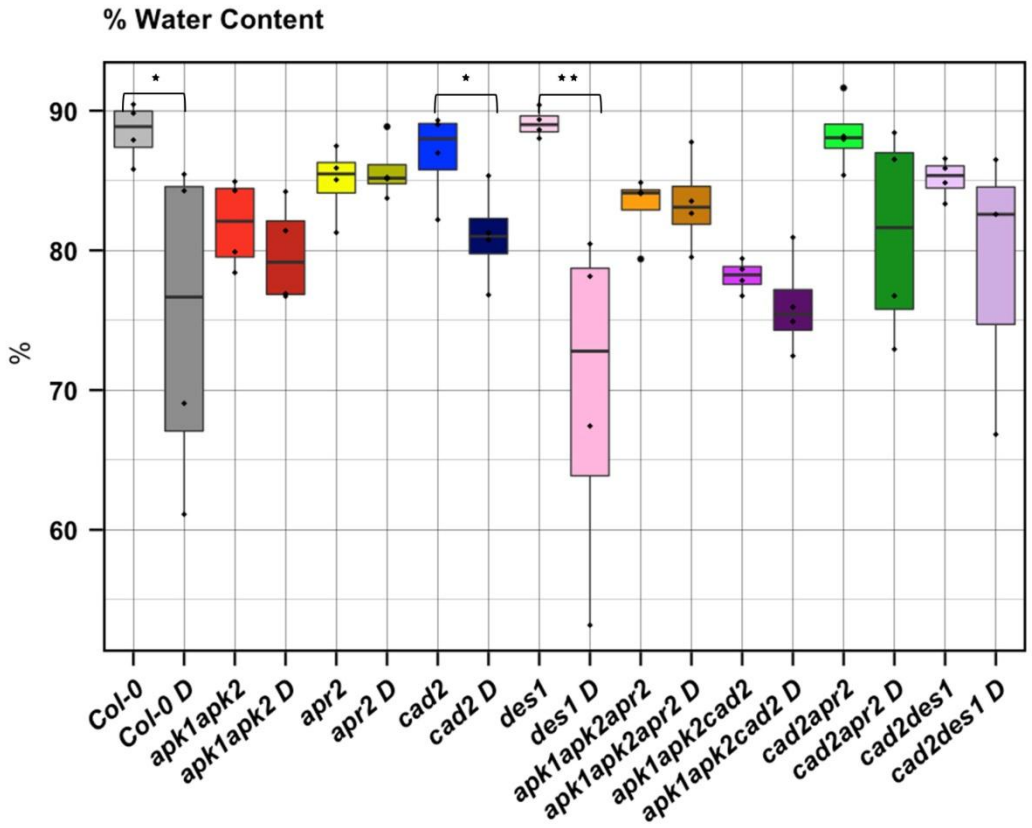

Figure.13: Water content of the sulfur metabolism mutants

5 weeks old plants grown in a growth chamber under short day conditions were subjected to water withdrawal for 3 weeks. Samples of fully expanded leaves were collected and fresh weight, as well as dry weight and water content, was measured. The data is shown as box plots, each point representing one of 4 biological replicates (3 replicates in case of *cad2de* due to germination problems). Asterisks mark values significantly different from their respective control treatment (*:P $\leq$ 0.05,**:P $\leq$ 0.01,***:P $\leq$ 0.001 Student t-test). Significance analyses between each genotype calculated with Student's t-test are shown in the Supplementary table 1.

For a better visualization of the response to drought stress, we calculated the mean value change of water content under drought stress compared to control conditions in each genotype as a percentage (Figure.14). We found that *des1* mutant lost more than 20% of its water, compared to control conditions. *apr2* mutant and *apk1apk2* and its crosses maintained water very well in these 3 weeks. *cad2apr2* and *cad2des1* mutants lost as much water as the *cad2* mutant; however,

the water content reduction was not significant. Strikingly, the effect on *cad2des1* mutant was considerably smaller than *des1* mutant.

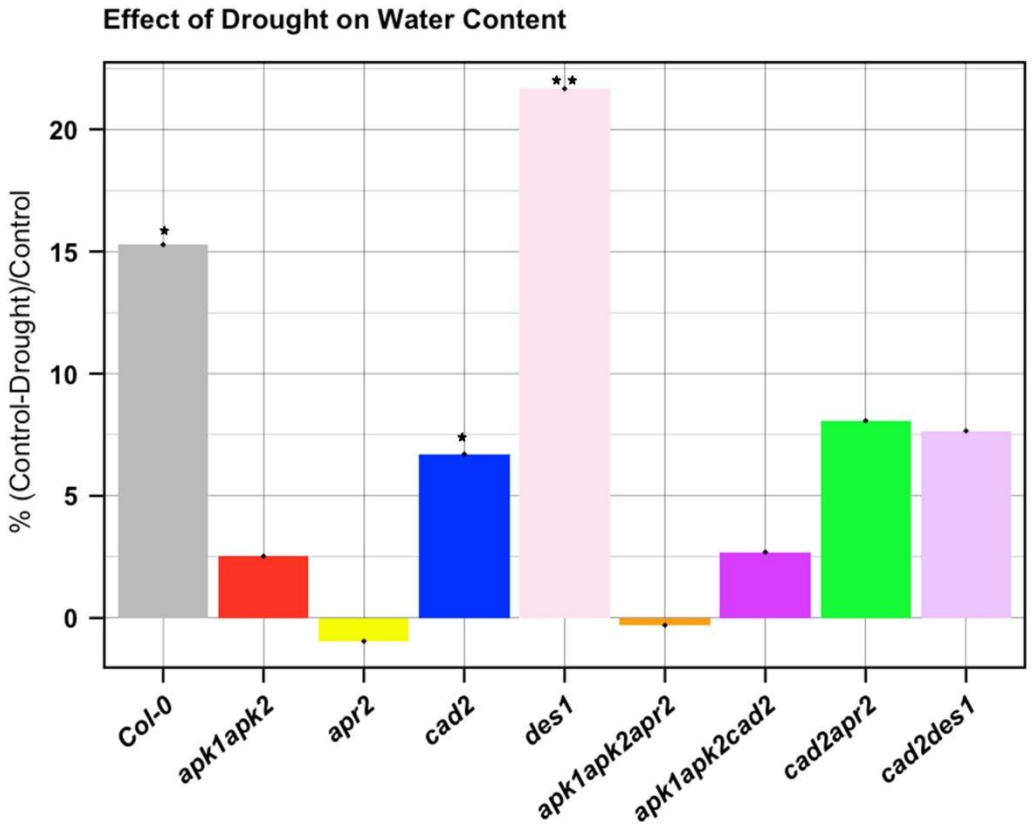

Figure.14: Effect of drought treatment on average water content.
5 weeks old plants grown in growth chamber under short day conditions were subjected to water withdrawal for 3 weeks. Samples of fully expanded leaves were collected and fresh weight, as well as dry weight and water content were measured. To calculate the effect, water content after drought treatment compared to water control under control conditions. Asterisks mark values significantly different from their respective control treatment (*:P ≤ 0.05,**:P ≤ 0.01,***:P ≤ 0.001 Student t-test).

3.2.2 δC^{13} calculation as an indicator of drought

Another well-established method to determine water use efficiency (WUE) and tolerance to drought stress in plants is δC^{13} analysis (Dittberner et al., 2018)**.** Because of kinetic isotope effect ^{13}C ratios from photosynthetic plants are lower compared to inorganic carbon sources (Hayes, 2001). The lighter isotope ^{12}C has a higher energy state which allows it to be the preferred isotope by RUBISCO for carbon assimilation in plants, ^{12}C also diffused faster through stomata

(Von Caemmerer et al., 2014). So an increased $\delta^{13}C$ indicates that the plant was not fully transpiring (low stomata conductance) and was forced to incorporate more ^{13}C. This value gets higher when stomata are closed or stomata density is lower. Therefore, higher $\delta^{13}C$ values indicate reduced WUE (Dittberner et al., 2018).

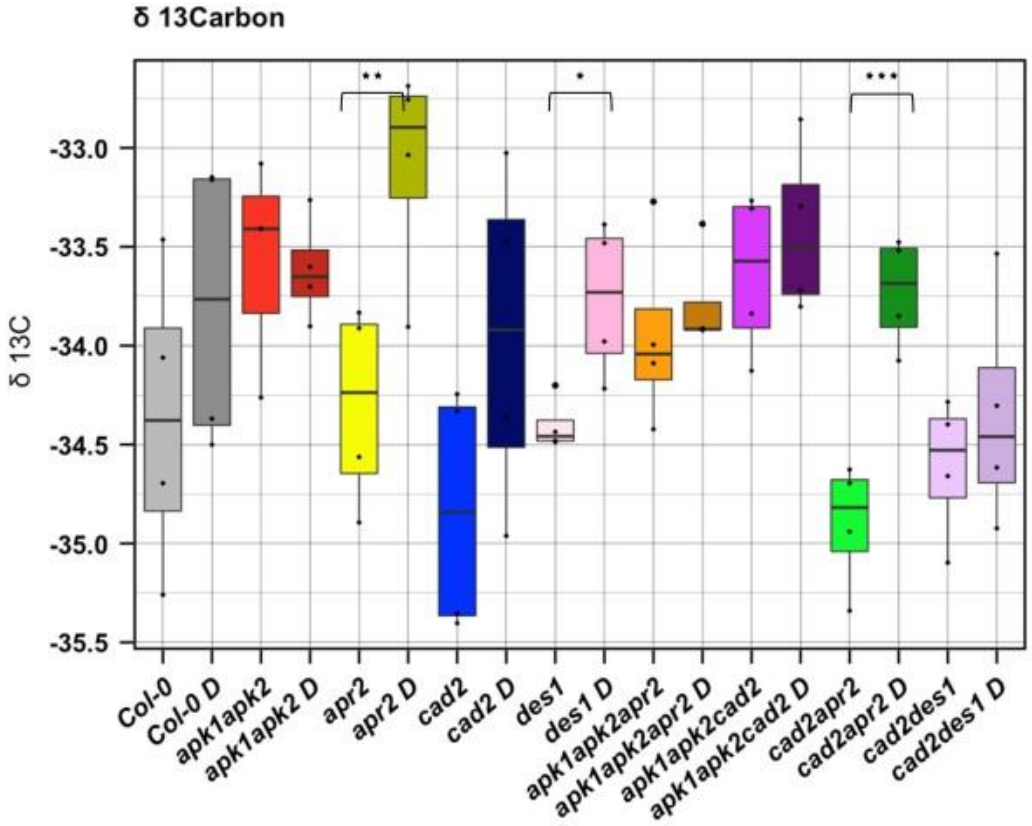

Figure.15: **δ13C values of the sulfur metabolism mutants.**
5 weeks old plants grown in growth chamber under short day conditions were subjected to water withdrawal for 3 weeks. Samples of fully expanded leaves were collected and fresh leaves were freeze dried and 1mg dry sample packed into tin foils send for the analysis. The samples were analyzed with EA-IRMS done by Philipp Westhoff. The data is shown as box plots, each point representing one of 4 biological replicates. Asterisks mark values significantly different from their respective control treatment (*:$P \leq 0.05$,**:$P \leq 0.01$,***:$P \leq 0.001$ Student t-test). Significance analyses between each genotypes calculated with Student's t-test are shown in the Supplementary Table 1.

$\delta^{13}C$ analysis with EA-IRMS showed an increase in ^{13}C isotope ratio under drought treatment in wild type as expected. However, this effect was not significant, indicating that our water withdrawal experiment was relatively mild. *apk1apk2* mutant and its crosses, corresponding to their observed drought tolerance, had higher $\delta^{13}C$ than WT already in control conditions and the

drought treatment did not significantly affect this phenotype (Figure.15). On the other hand, *apr2* and *cad2apr2* showed a significant and the highest increase in $\delta^{13}C$, more than 3% (Figure.16). The mutant affected the most from the water withdrawal treatment, *des1*, also showed significant increase in $\delta^{13}C$ (Figure.16). *cad2des1* did not exhibit a significant change in its ^{13}C ratio.

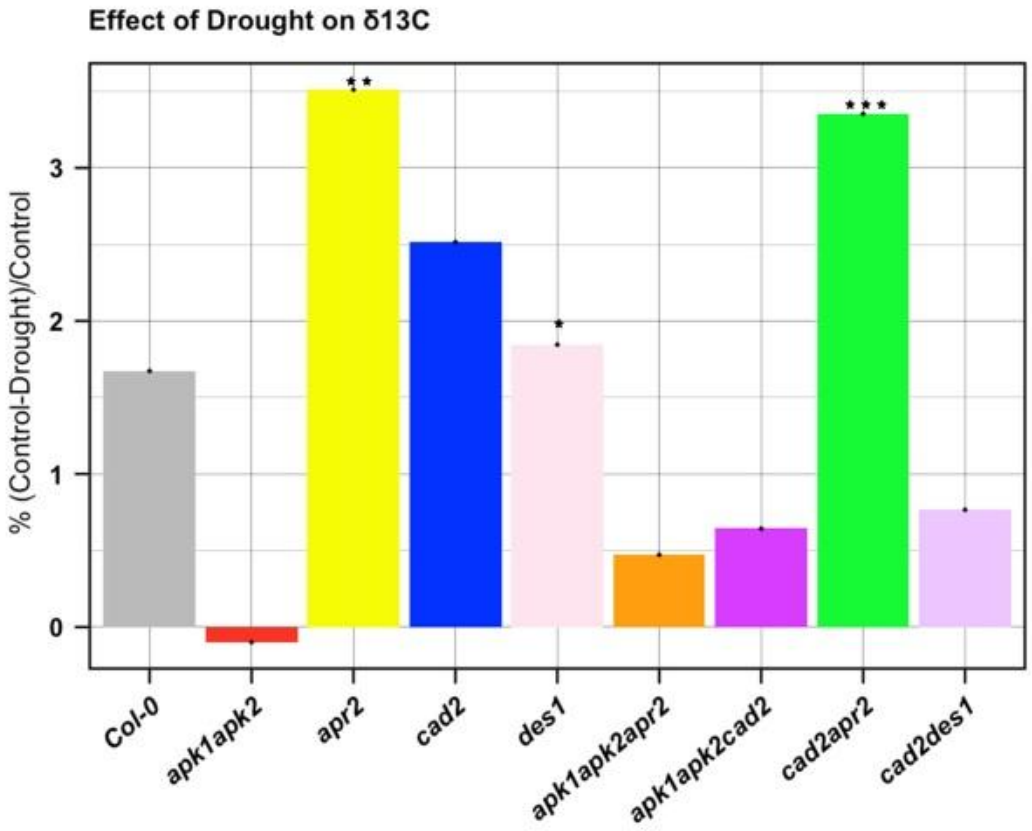

Figure.16: Effect of drought treatment on δ13C in the sulfur metabolism mutants
5 weeks old plants grown in a growth chamber under short day conditions were subjected to water withdrawal for 3 week. Samples of fully expanded leaves were collected and fresh leaves were freeze dried and 1mg dry sample packed into tin foils sent for the analysis. The samples were analyzed with EA-IRMS done by Philipp Westhoff. To calculate the effect, water content after drought treatment compared to water control under control conditions. Asterisks mark values significantly different from their respective control treatment (*:$P \leq 0.05$,**:$P \leq 0.01$,***:$P \leq 0.001$ Student t-test).

The results of water content and $\delta^{13}C$ led us to consider another factor that is highly important under drought stress, stomata. We counted and calculated stomata density from the imprints taken from the abaxial part of the fully grown leaves. The values were instrumental for understanding the imparities in the water content reduction and ^{13}C incorporation. *apk1apk2* and

its crosses in line with their ability to hold water better and already high $\delta^{13}C$ had significantly lower stomata density (Figure.17). *cad2* and *des1* showed significant decreases while *apr2* and *cad2apr2* had densities similar to WT levels (Figure.17). *cad2des1* also had very low stomata density consistent to its ability to keep water more consistently. However, the reason why this mutant with lower stomata density could also have low $\delta^{13}C$ under control conditions was not clear. Therefore, we decided to examine the key process for carbon assimilation: photosynthesis.

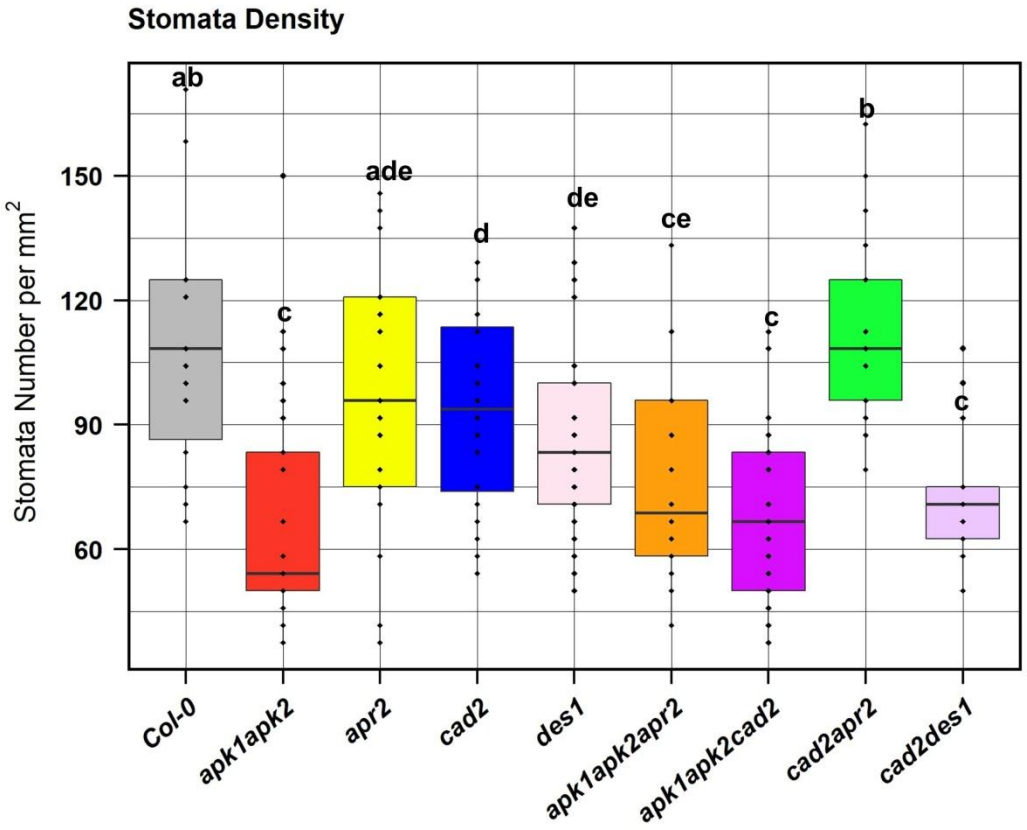

Figure.17: Stomata density of the sulfur metabolism mutants
Stomata numbers were counted from the abaxial part of 8 weeks old plants grown in short day control conditions. Bright field microscopy used for counting the stomata from leaf imprints. 4 biological replicates have been used. At least 5 different locations on the leaf surface were counted. The collected data is fully shown as box plots, each point representing a sample. The significance analyses between each genotype were calculated with Student's t-test and different letters represent values that are significantly different ($P < 0.05$).

3.2.3 Efficiency of Photosystem II heavily impacted in mutants under drought conditions

To analyze alterations in photosynthesis, we used pulse amplitude modulation (PAM) method. Our results indicated that drought treatment decreased PSII efficiency for almost all the

genotypes other than *apk1apk2* (Figure.18). The treatment decreased the PSII efficiency of *apr2* slightly but not significantly. Only *apk1apk2* possessed significantly higher efficiency of PSII under both control and drought conditions (Figure.18 & Supplementary Figure. 4). Under drought stress the difference between WT and *apk1apk2* got even greater, while under control conditions, crosses of *apk1apk2* showed slightly higher values of PSII efficiency. Unlike *apk1apk2*, the *apk1apk2apr2* and *apk1apk2cad2* did not preserve their efficiency in drought and their efficiency significantly lower under drought conditions.

The *apk1apk2* exhibited the highest PSII efficiency and was not affected by drought treatment. PSII levels of *cad2* and *des1* were not significantly different from WT under control conditions, whereas heavily affected in drought treatment. *cad2apr2* and *cad2des1* were also severely affected by stress. Two weeks of drought treatment made it possible to detect the differences between distinct responses of sulfur mutants more clearly (Figure.18 & Supplementary Figure. 4). PSII efficiency of *des1* and *cad2* mutants were especially damaged under drought. Lastly, *cad2, des1, cad2apr2* and *cad2des1* mutants were all showed significantly decreased maximum PSII efficiency under drought (Figure.18).

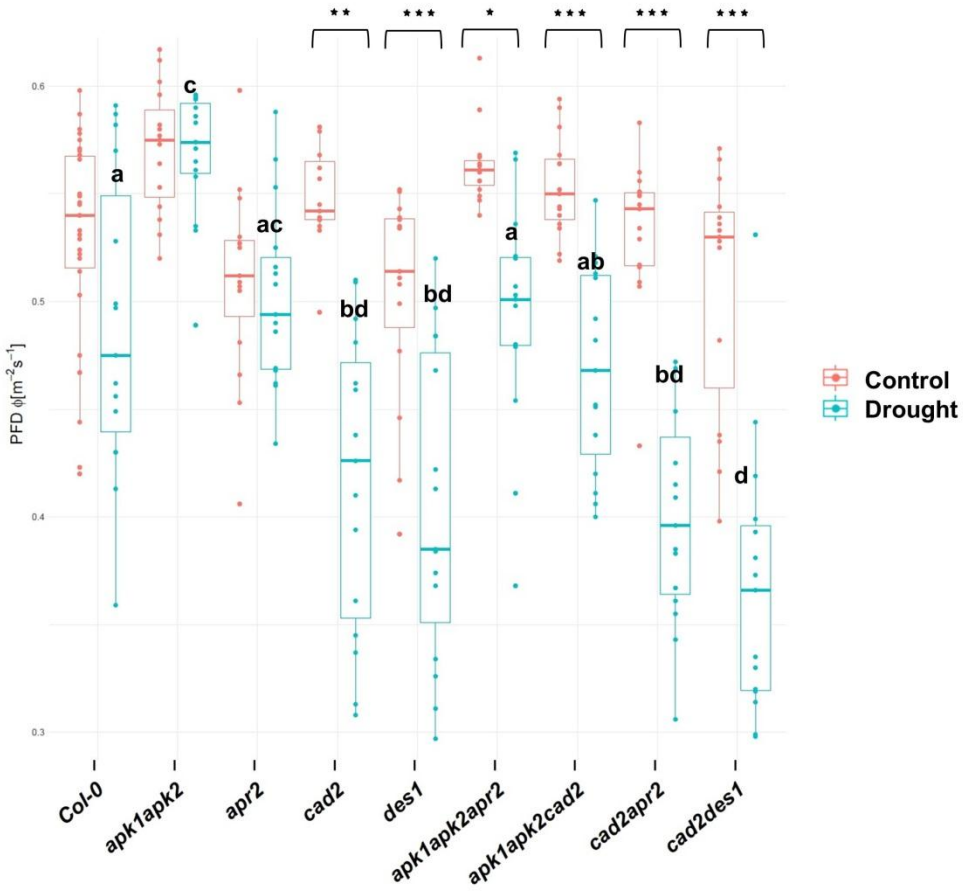

Figure.18: PSII efficiency of the sulfur metabolism mutants under control and drought conditions
Control plants were measured when 5 weeks old and drought samples were measured 2 weeks after water withdrawal. Plants were grown in short day conditions. 5 different leaves from 3 biological replicates analyzed for 5 minutes with PAM using 62 PAR. The data is shown as box plots, each point representing a measurement. Asterisks on top of brackets mark values significantly different from their respective control treatment. Asteriks on top of box plots mark values significantly different from Col-0. Significance analyses between each genotypes calculated with ANOVA test and Tukey post-hoc test (*:$P \leq 0.05$,**:$P \leq 0.01$,***:$P \leq 0.001$).

3.2.4 Glutathione concentrations reduced under drought stress

We measured thiols to understand if there is any correlation between the concentration of thiols and the plants ability to resist drought conditions or maintain their PSII efficiency. We wanted check that if thepreviously shown high GSH concentration (Figure.6 & Figure.7) could be the possible reason of the protection of PSII machinery under drought stress conditions. All genotypes, except *apk1apk2*, were found to have significantly increased cysteine concentration under drought stress (Figure.19). The crosses of *apk1apk2* once again showed higher cysteine contrations under control conditions, with *apk1apk2cad2* having the highest concentrations

(Figure.19). Notably, the mutant lacking one of the main cysteine degradation enzymes, *des1* also had very high cysteine levels and almost doubled its Cys under stress conditions (Figure.19).

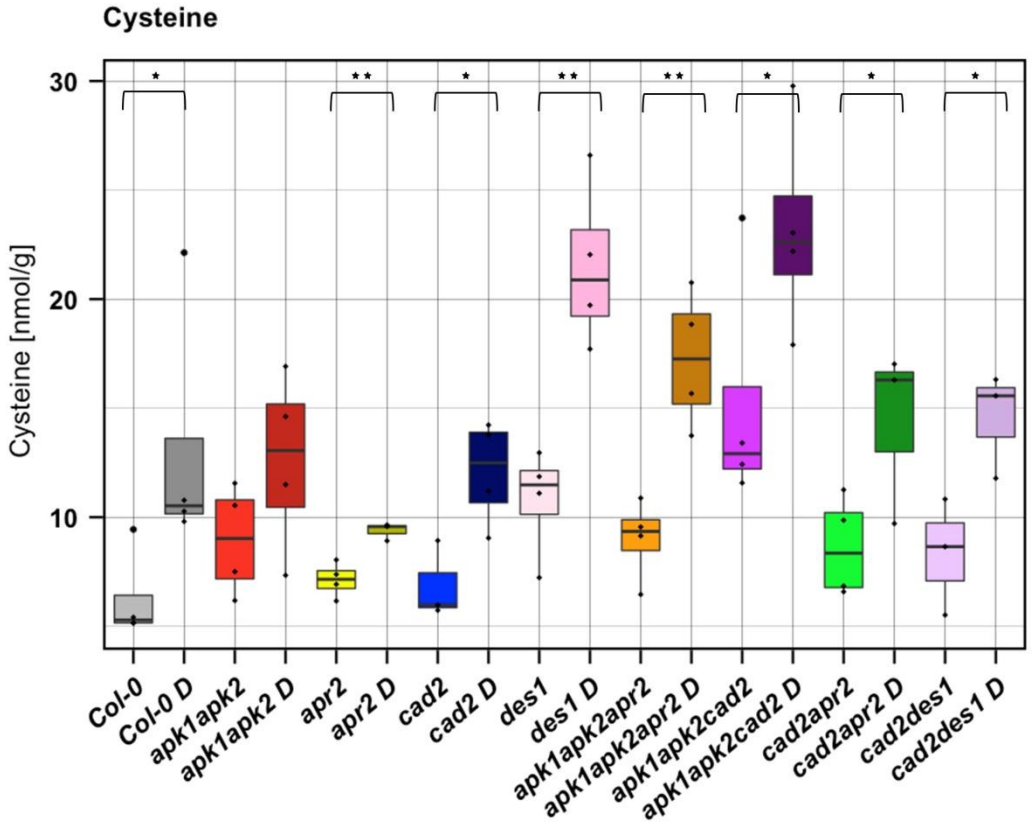

Figure.19: Cysteine concentrations of the sulfur metabolism mutants.
5 weeks old plants grown in growth chamber under short day conditions were subjected to water withdrawal for 3 weeks. Samples of fully expanded leaves were collected fresh and subsequently frozen. The data is shown as box plots, each point representing one of 4 biological replicates. Asterisks mark values significantly different from their respective control treatment (*:P ≤ 0.05,**:P ≤ 0.01,***:P ≤ 0.001 Student t-test). Significance analyses between each genotype calculated with Student's t-test are shown in the Supplementary table 1.

Furthermore, we analyzed the GSH concentrations from the fully grown rosette leaves of the plants. We observed that the concentrations were already quite low to begin with even under control conditions. We observed the reduction of GSH under drought conditions in all the genotypes except the double mutant *cad2apr2* (Figure.20).This mutant was previously shown to have exteremly low concentrations of GSH (Figure.7). Of WT, *apr2* and *apk1apk2* all three had significantly lower concentrations of GSH after drought stress (Figure.20).

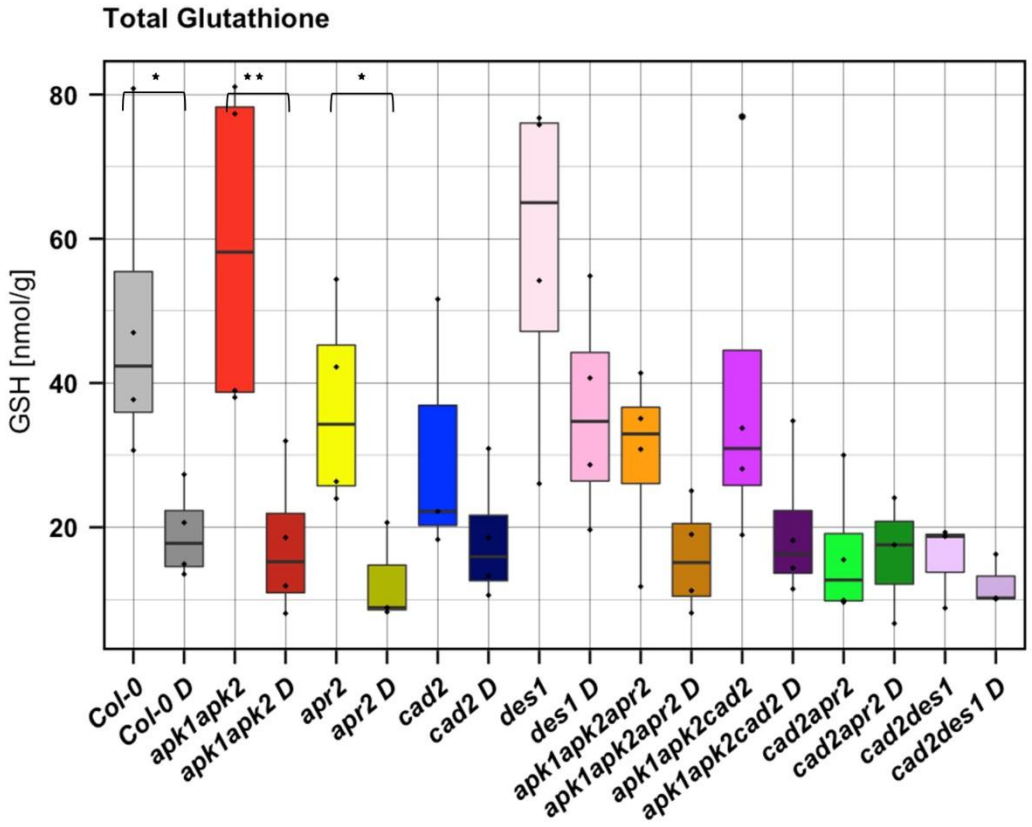

Figure.20: Glutathione concentrations of the sulfur metabolism mutants
5 weeks old plants grown in growth chamber under short day conditions were subjected to water withdrawal for 3 weeks. Samples of fully expanded leaves were collected fresh and subsequently frozen. The data is shown as box plots, each point representing one of 4 biological replicates. Asterisks mark values significantly different from their respective control treatment (*:$P \leq 0.05$,**:$P \leq 0.01$,***:$P \leq 0.001$ Student t-test). Significance analyses between each genotype calculated with Student's t-test are shown in the Supplementary table 1.

3.2.5 PAP concentrations were increased in response to drought

Since the best performing genotypes under drought stress in our set of mutants were *apk1apk2* and its crosses, which are attenuated in key sulfation metabolism enzyme APK, we measured PAP levels in all genotypes in both conditions. Consistent with the previous findings (Estavillo et al., 2011), the drought treatment increased the PAP concentrations. The only significant change we observed was in *apr2* and *cad apr2*. Even though it was not significant in WT, *apk1apk2, cad2 and des1* also reacted to drought with increased PAP concentrations. Interestingly, lower levels of PAP were detected in *apk1apk2apr2* and *apk1apk2cad2* in response

to drought (Figure.21). However, variations in PAP concentration were too high to clearly explain drought tolerance alone.

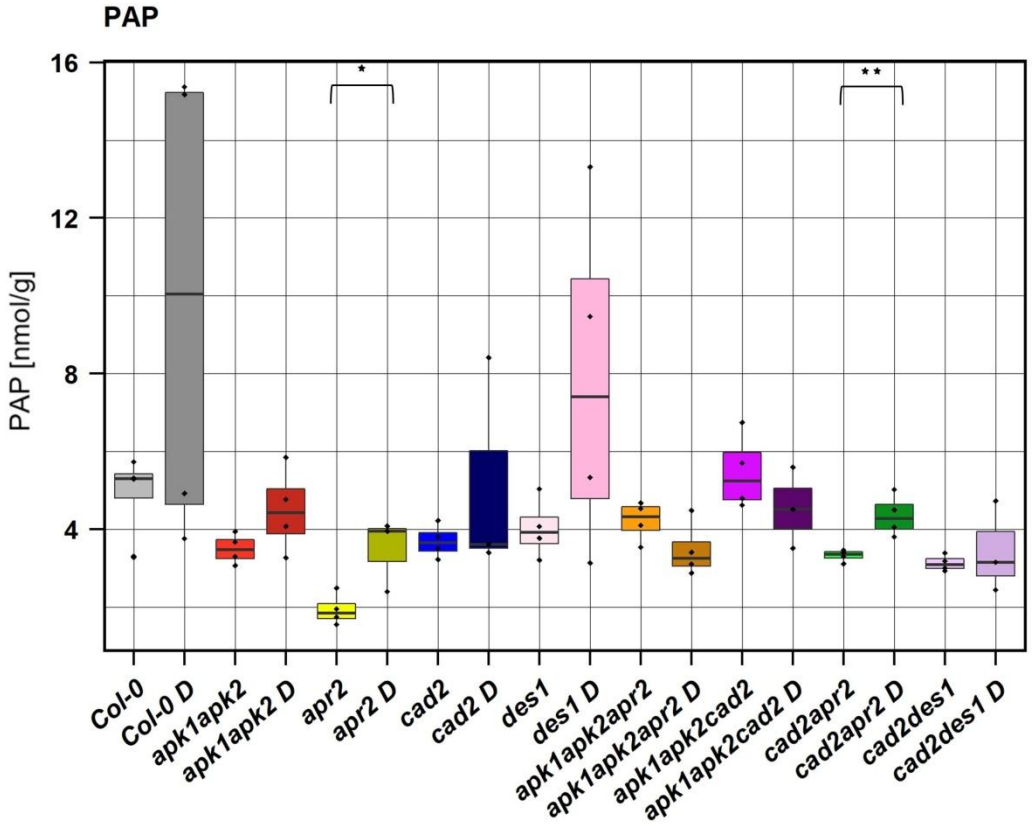

Figure.21: PAP concentrations of the sulfur metabolism mutants

. 5 weeks old plants grown in growth chamber under short day conditions were subjected to water withdrawal for 3 week samples of fully expanded leaves were collected fresh and directly frozen. The data is shown as box plots, each point representing one of 4 biological replicates. Asterisks mark values significantly different from their respective control treatment (*:P ≤ 0.05,**:P ≤ 0.01,***:P ≤ 0.001 Student t-test). Significance analyses between each genotype calculated with Student's t-test are shown in the Supplementary table 1.

3.3 Comparing drought resistance of the mutants in sulfation pathways

After the drought experiments with our first set of mutants, we observed drought resistance of secondary sulfur metabolism mutants *apk1apk2* and triple mutants derived from it. We wanted to dissect the impact of the sulfation pathway on abiotic stress in more detail. The drought tolerance and regulatory mechanism of the PAP degradation enzyme, SAL1, has been long established (Estavillo et al., 2011). We aimed to test whether the drought stress tolerance mechanism of

apk1apk2 and PAP accumulating *fou8* mutant are the same or different and additive. We also hypothesized that a lower stomata density of *apk1apk2* mutants could be connected with sulfated peptides. TYROSYLPROTEIN SULFOTRANSFERASE is an enzyme responsible for sulfation of small peptides (Komori et al., 2009). By including *tpst1*, we tested the potential role of sulfated peptides on the stomata density. For this purpose, we designed another water withdrawal experiment with *apk1apk2*, *fou8* and their cross *apk1apk2fou8,* and *tpst1*.

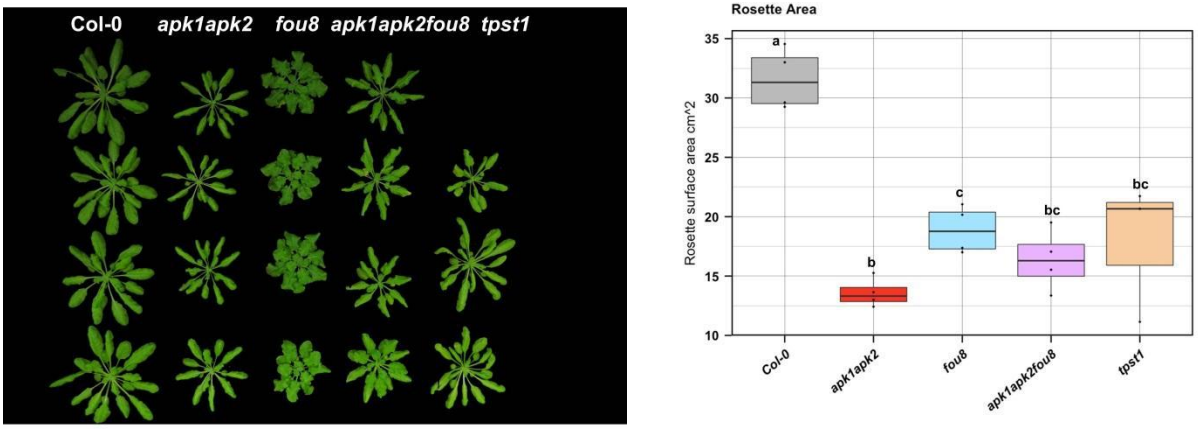

Figure.22: Rosette area of the sulfation pathway mutant
Rosette area of 7 weeks old plants. Plants have been grown in a growth chamber under short day conditions. The collected data is fully shown as box plots, each point representing a sample. 4 biological replicates were used. (3 replicates for *tpst1*). The significance analyses between each genotype were calculated with Student's t-test and different letters represent values that are significantly different ($P < 0.05$).

Following five weeks of growth under short-day conditions, water was withheld from the drought treatment group, whereas the control group continued to receive regular watering. The position of the trays in the chamber and the pots inside the trays was frequently shuffled. All mutants investigated in this experiment were smaller than WT. In addition, the *apk1apk2* mutant was significantly smaller than *fou8* (Figure.22). However, rosette structure and irregular leaf shapes made it difficult to calculate surface area from 2D image. *fou8* had very wavy, round and short leaves, while *apk1apk2* mutant had convex leaves which were bent inward at all times. Furthermore, *apk1apk2* has longer petioles compared to *fou8*. Their cross, *apk1apk2 fou8,* carried both of its parents' characteristics for the leaf shape; wavy, short and convex leaves. The average rosette surface area of the triple mutant was the average of its parents. *tpst1* also had a dwarf phenotype, but we did not observe extreme growth attenuation of this mutant (Komori et al., 2009). It had severe germination problems resulting in only 3 biological replicates.

3.3.1 Water withdrawal experiment with sulfation pathway mutants

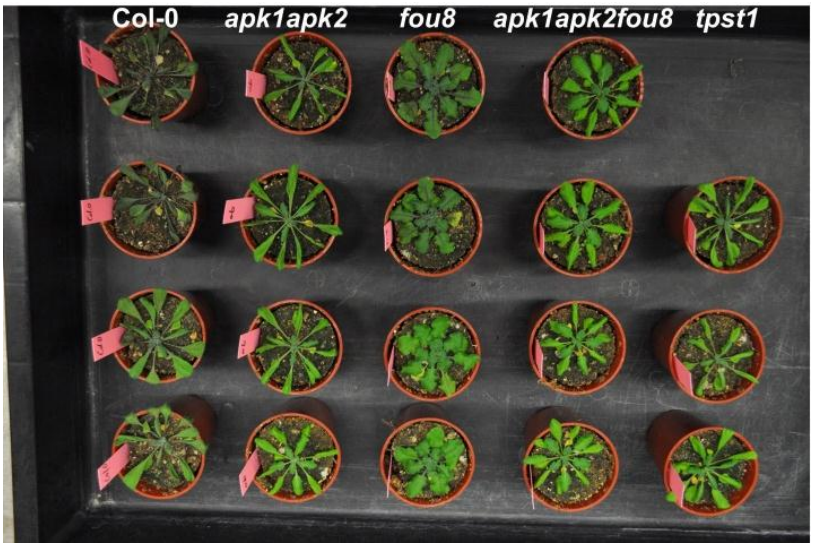

Figure.23: Water withdrawal experiment of sulfation mutants. WT severely wilted
5 weeks old plants used for this experiment and water was withdrawn for 2 weeks for the drought treatment group. Plants were 7 weeks old when the when the photo is taken; they have been grown in growth chamber under short day conditions.

After 2 weeks WT plants severely wilted but mutants were still quite green (Figure.23). *fou8* visibly turned purple near its leaf veins, sign of possible anthocyanin accumulation. We calculated the water content from the plants as previously described. WT had around 92% water under control conditions. *apk1apk2*, *fou8* and their cross had significantly lower water content under the same conditions. All mutants lost water less rapidly in the drought stress conditions compared to WT. *apk1apk2fou8* showed significantly higher water content compared to *apk1apk2* under stress (Figure.24). *tpst1* mutant also preserve its water at the very high levels efficiently.

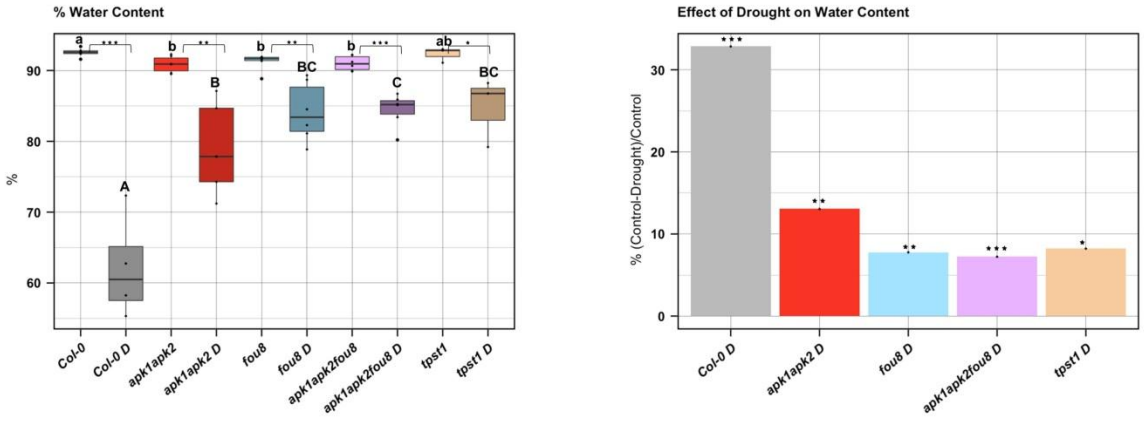

Figure.24: Water content of the sulfation mutants and effect of drought on the water content.
5 weeks old plants grown in growth chamber under short day conditions were subjected to water withdrawal for 3 weeks. Samples of fully expanded leaves were collected and fresh weight, as well as dry weight and water content were measured. The data is shown as box plots, each point representing one of 4 biological replicates (3 replicates in case of *cad2des1* due to germination problems). To calculate the effect, water content after drought treatment compared to water content under control conditions. Asterisks mark values significantly different from their respective control treatment (*:$P \leq 0.05$,**:$P \leq 0.01$,***:$P \leq 0.001$ Student t-test). Significance analyses between each genotypes calculated with Student's t-test are shown with letters.

For this set of mutants we also calculated the effect of drought on water content. Water content of WT and all the mutants water significantly reduced (Figure.24). The effect was more than 30% in case of WT, and around 12% for *apk1apk2* and other mutants water content were effected less than 10% (Figure.24).

3.3.2 Water use efficiency (δC^{13}) of the sulfation mutants

The δC^{13} values of the all genotypes were significantly increased under drought stress. Under control conditions *apk1apk2* again possessed higher δC^{13} levels than WT, whereas *fou8* had lower δC^{13} value. Other genotypes were not different from WT. Altogether, after 2 weeks of water retention, levels of δC^{13} in Col-0 increased around 7% while all the mutants had significant increase *apk1apk2fou8* had the smallest change. The δC^{13} rates of *apk1apk2fou8, fou8* and *tpst1* were significantly lower than WT (Figure.25).

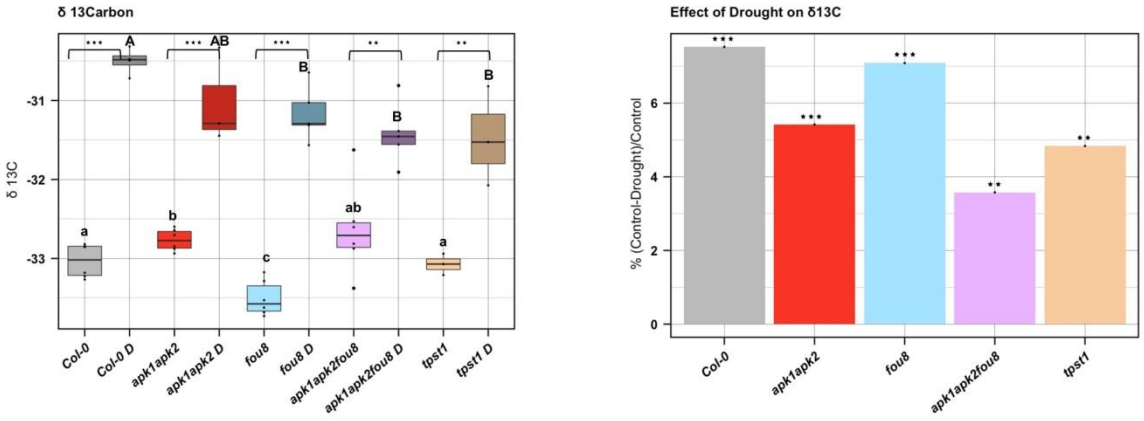

Figure.25: δ13C and effect of drought on the isotope ratio of the sulfation mutants.
5 weeks old plants grown in growth chamber under short day conditions were subjected to water withdrawal for 3 weeks. Samples of fully expanded leaves were collected and fresh leaves were freeze dried and 1mg dry sample packed into tin foils send for the analysis. The samples analyzed with EA-IRMS done by Philipp Westhoff. The data is shown as box plots, each point representing one of 4 biological replicates. To calculate the effect, water content after drought treatment compared to water content under control conditions. Asterisks mark values significantly different from their respective control treatment (*:$P \leq 0.05$,**:$P \leq 0.01$,***:$P \leq 0.001$ Student t-test). Significance analyses between each genotypes calculated with Student's t-test are shown in the as letters.

3.3.3 Stomata density of sulfur metabolism mutants

Stomata numbers counted from 7 weeks old plants as described before. *apk1apk2* mutant again showed a significantly lower stomata density than WT. *fou8* mutant also showed significantly lower stomata density compare to wild type (Figure.26). While the two mutants had the same density, their cross *apk1apk2fou8* had significantly higher stomata values than its parent genotypes, similar to WT levels. *tpst1* also had low stomata density parallel to its drought tolerance ability.

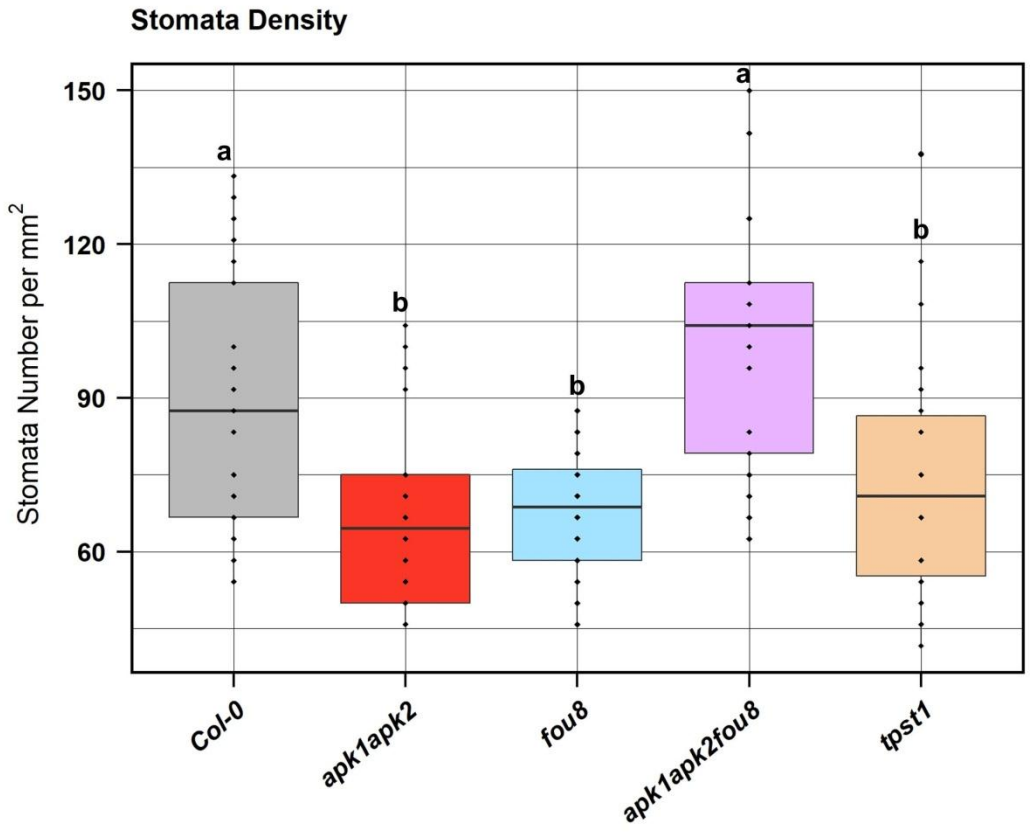

Figure.26: Stomata density of the sulfation mutants

Stomata number were count from the abaxial part of 7 weeks old plants grown in short day control conditions. The leaf imprints used for the counting with bright field microscopy. 4 biological replicate have been used .At least 5 different location on the leaf surface counted. The collected data is fully shown as box plots each point representing a sample. The significance analysis between each genotype calculated with Student's t-test and different letters represent values significantly different ($P < 0.05$).

3.3.4 Photosystem II efficiency of sulfation mutants under control conditions

After observing the fluctuations of PSII efficiency in the sulfur metabolism mutants in our previous experiment we decided to measure quantum yield of PSII and non-photochemical quenching. In parallel with previous PAM analysis *apk1apk2* mutant had higher PSII maximum efficiency but it was not significant. Other mutants were also not significantly different than WT. We also calculated the non-photochemical quenching in sulfation mutants, *apk1apk2* decreased *fou8* increased (Figure.27).

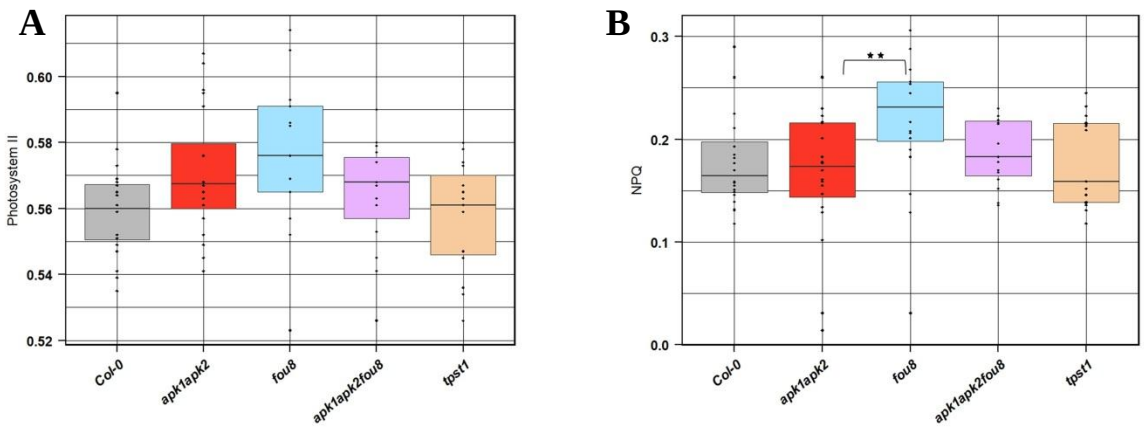

Figure.27: A: Analysis of maximum PSII efficiency B: Peak values of NPQ of sulfur metabolism mutants under control and drought conditions.

5 weeks old measured at when 5 weeks. Plants were grown in short day conditions. 5 different leaves from 3 biological replicates analyzed for 5 minutes with PAM using 62 PAR. Control plants were measured when 5 weeks old and drought samples were measured 2 weeks after water withdrawal. Plants were grown in short day conditions. 5 different leaves from 3 biological replicates analyzed for 5 minutes with PAM using 62 PAR. The data is shown as box plots, each point representing a measurement. Asterisks on top of brackets mark values significantly different from their respective control treatment. Asteriks on top of box plots mark values significantly different from Col-0 (*:$P \leq 0.05$,**:$P \leq 0.01$,***:$P \leq 0.001$ Student t-test). Significance analyses between each genotypes calculated with ANOVA test and Tukey post-hoc test. Statistical values are shown in the Supplementary table 2.

3.3.5 PAP measurement of sulfation mutants

PAP accumulation is hypothesized to be the main source of drought tolerance for *fou8* mutant. Therefore, we measured PAP content in the mutants by HPLC. Under control conditions *fou8* mutant had significantly higher concentrations of PAP than WT, as described and PAP concentration of *apk1apk2fou8* was lower than *fou8* as expected (Lee et al., 2012). PAP concentration in the WT plants was significantly increased after the drought stress. The mutants did not showed the same level of increase, however, *apk1apk2* and *apk1apk2fou8* PAP contents slightly but significantly increased. *fou8* PAP values did not increase and, surprisingly, *tpst1* was also not affected (Figure.28)**.**

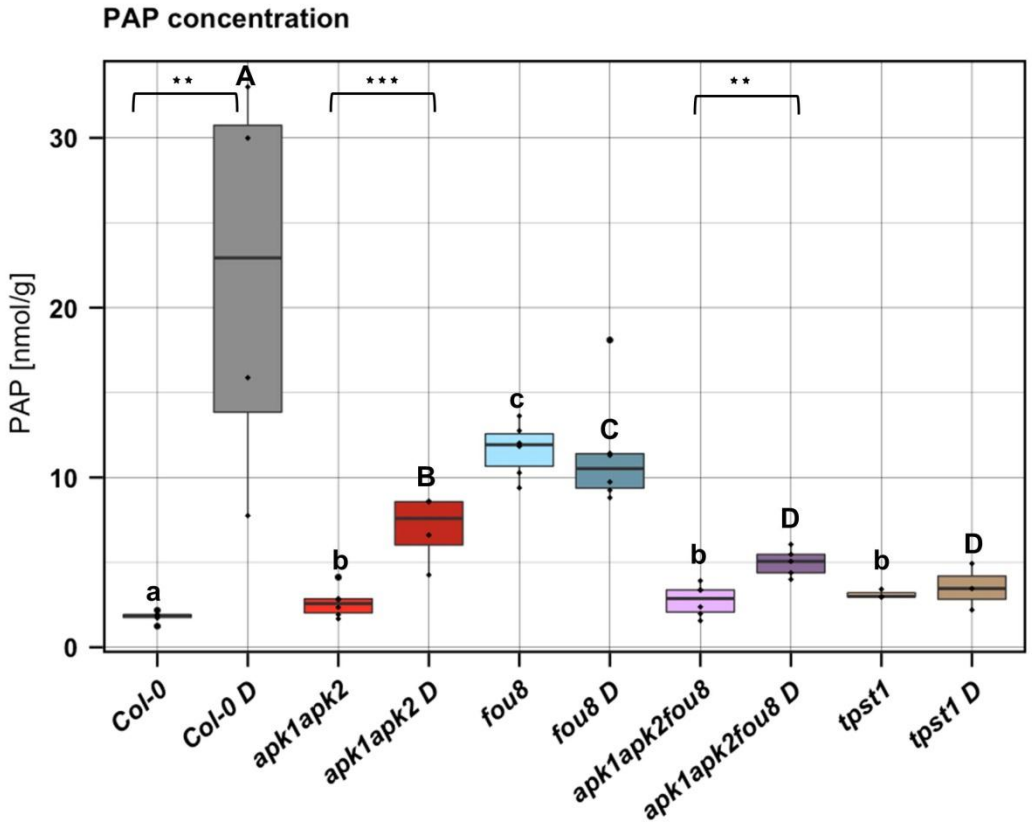

Figure.28: PAP concentrations of the sulfation mutants.
five-week-old old plants grown in growth chamber under short day conditions were subjected to water withdrawal for 2 weeks. Samples of fully expanded leaves were collected fresh and subsequently frozen. The data is shown as box plots, each point representing one of 4 biological replicates. Asterisks mark values significantly different from their respective control treatment (*:P ≤ 0.05,**:P ≤ 0.01,***:P ≤ 0.001 Student t-test). Significance analyses between each genotype calculated with Student's t-test are shown with letters

4. RESULTS II

4.1 Impact of PAP accumulation on photorespiration and mitochondria

Our hypothesis was that the dwarf phenotype of *fou8* mutant could be the consequence of PAP accumulation in mitochondria interfering with the mtFAS pathway through feedback mechanism of mtPPT enzyme. mtFAS mutants have reduced lipolylation of the glycine decarboxylase causing glycine accumulation under normal CO_2 which can be reversed when plants are transferred to high CO_2 (Guan et al., 2015). Therefore, we tested the photorespiratory phenotype

and glycine accumulation of the *fou8* mutants. We also used *apk1apk2*, which also shows a semi-dwarf phenotype and shares several metabolic alterations with *fou8*, and *shm1*, a mutant in photorespiratory serine hydroxymethyltransferase, as a control.

Exposing the semi dwarf *apk1apk2* and *fou8* mutants to high CO_2 concentration did not rescue the growth phenotypes of the mutants (Figure.29). Also, another photorespiratory phenotype, the wilting after transfer from high CO_2 to ambient air, was absent from the two mutants, but clearly visible in the photorespiratory *shm1* (Voll et al., 2006), which was used as a control (Figure.29).

As another photorespiratory phenotype, accumulation of glycine was observed in *mtppt-rnai* mutant lines due to reduction of GDC activity (Guan et al., 2015). To assess whether the *fou8* mutant might share this phenotype we performed a metabolomic analysis of leaves of plants grown initially in high CO_2 after 3 days in ambient air (AC) or high CO_2 (HC), using GC-MS. No significant differences in glycine levels of *fou8* or *apk1apk2* mutants could be found under normal CO_2 conditions or high CO_2 (Figure.30).

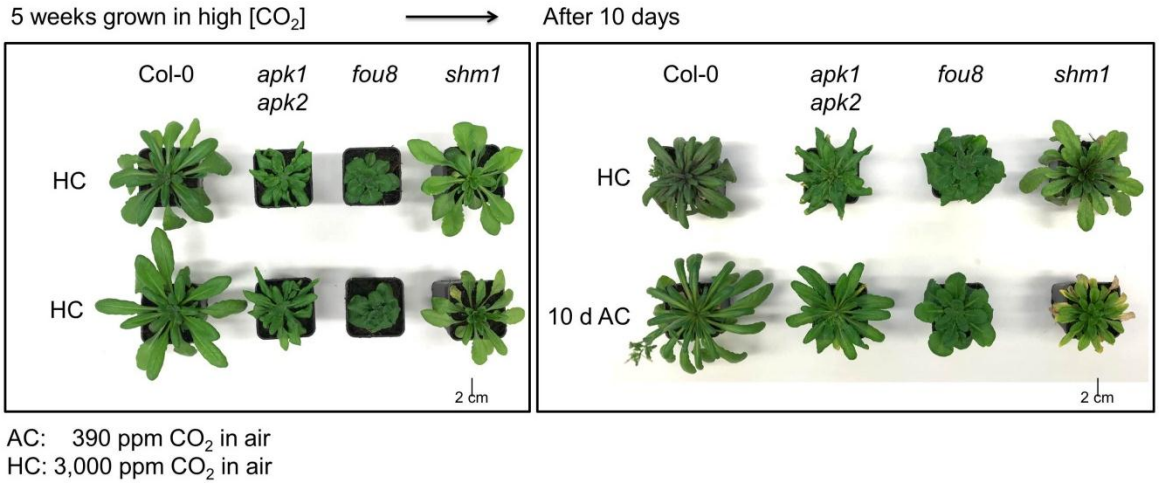

Figure.29: Phenotypes of *apk1apk2*, *fou8*, and *shm1* mutants.
The different genotypes were grown in high CO_2 for 5 weeks and either transferred to ambient air for 3 days (Samples collected for MS after 3 days but photo is taken after 10 days) or kept further in high CO_2. Representative plants from 5 biological replicates for each condition are shown. Ambient air (AC):390 ppm CO_2in air, High CO_2 (HC): 3,000 ppm CO_2 in air.

4.2 Amino acid alterations in *fou8* and *apk1apk2* mutants

To understand more about the impact of PAP accumulation on primary metabolism, we further analysed the GC-MS data. The metabolic analysis showed significant differences in

concentration of several amino acids in leaves. The biggest change was observed in cysteine, which accumulated to very high levels in *apk1apk2*, as described before (Mugford et al., 2009) (Figure.30). Reduction of secondary sulfur metabolism in this mutant caused approx. 10-fold increase in cysteine levels under both conditions. This makes *apk1apk2* mutant one of the highest cysteine accumulating mutants ever reported, with concentration much higher than previously described as toxic (Romero et al., 2014). Methionine levels were elevated in both of the mutants significantly after plants switch to AC conditions but in HC methionine levels were not significantly different from wild type. Serine levels were significantly reduced in *apk1apk2* ($log_2FC = -0.5$) after plants switch to AC and in *fou8* ($log_2FC = -0.7$) in HC conditions. Tyrosine and glutamate levels were increased in *apk1apk2* under both conditions but not different from wild type in *fou8.* Tryptophan levels were 4 times higher in *fou8* mutant than in wild type after plants switch to AC conditions. Growing the plants under high CO_2 did not affect tryptophan levels in Col-0 while they were decreased by 50% compared when they switched to normal conditions in *fou8* mutants (Figure.30). Interestingly, after switch to under normal conditions almost all amino acids in *fou8* and *apk1apk2* mutants were increased (Figure.30). High CO_2 treatment decreased the accumulation of few amino acids compared to Col-0 but the only amino acids which showed significant decrease were serine and phenylalanine in *fou8* and beta-alanine *apk1apk2*.

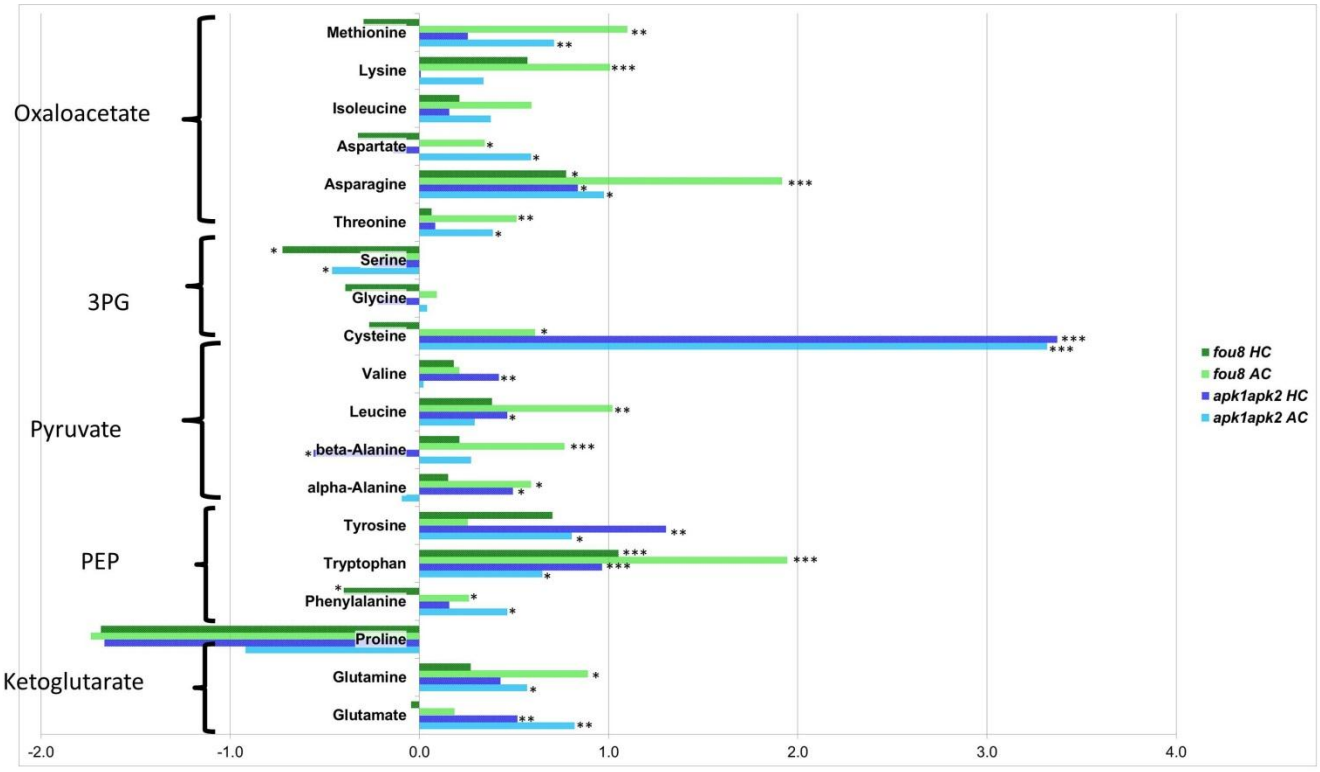

Figure.30: Accumulation of proteinogenic amino acids in *fou8* and *apk1apk2* mutants
Plants were grown for 5 weeks in high CO_2 and either transferred to ambient air for 3 days or kept further in high CO_2 Metabolites in leaves were analyzed by GC-MS. Shown are fold change differences to WT at the given condition. Proteinogenic amino acids were grouped according to where their carbon backbones are branching from central carbon metabolism; Oxaloacetate, 3-phosphoglycerate (3PG), Pyruvate, Phosphoenolpyruvate (PEP), Ketoglutarate. Ambient air (AC):390 ppm CO2in air, High CO2 (HC): 3,000 ppm CO2 in air.Asterisks mark values significantly different from WT *:$P \leq 0.05$,**:$P \leq 0.01$,***:$P \leq 0.001$ t-test.

4.3 Changes in carbohydrate levels in *fou8* and *apk1apk2* mutants

Carbohydrate profiles of the mutants were quite different compared to the WT. Large reductions relative to wild type were observed in the levels of glucose, which was decreased 24-fold (log2FC = -4.6) after plant switched to AC and 10-fold in HC in *fou8* and 6-fold (log2FC =-2.6) and 2.6-fold in *apk1apk2* mutants (Figure.31). Fructose, raffinose and mannose levels were all strongly and significantly reduced in *fou8* in both conditions (Figure.31). Additionally, concentrations of raffinose and sucrose were lower in *fou8*, this difference from wild type was more pronounced after switch to ambient air than in elevated CO_2. Interestingly, under high CO_2 conditions *apk1apk2* accumulated more sucrose than Col-0 and *fou8*. Mannitol was the only carbohydrate which was increased in both mutants after switch to normal CO_2 levels. After

switching to ambient air trehalose was not detected in the wild type, but only in the mutants, where it was unchanged in both conditions. However, under high CO_2 it was detectable in WT, which allowed revealing a 6-fold increase in *fou8* and a striking 60-fold increase in *apk1apk2* (Supplementary Table.3).

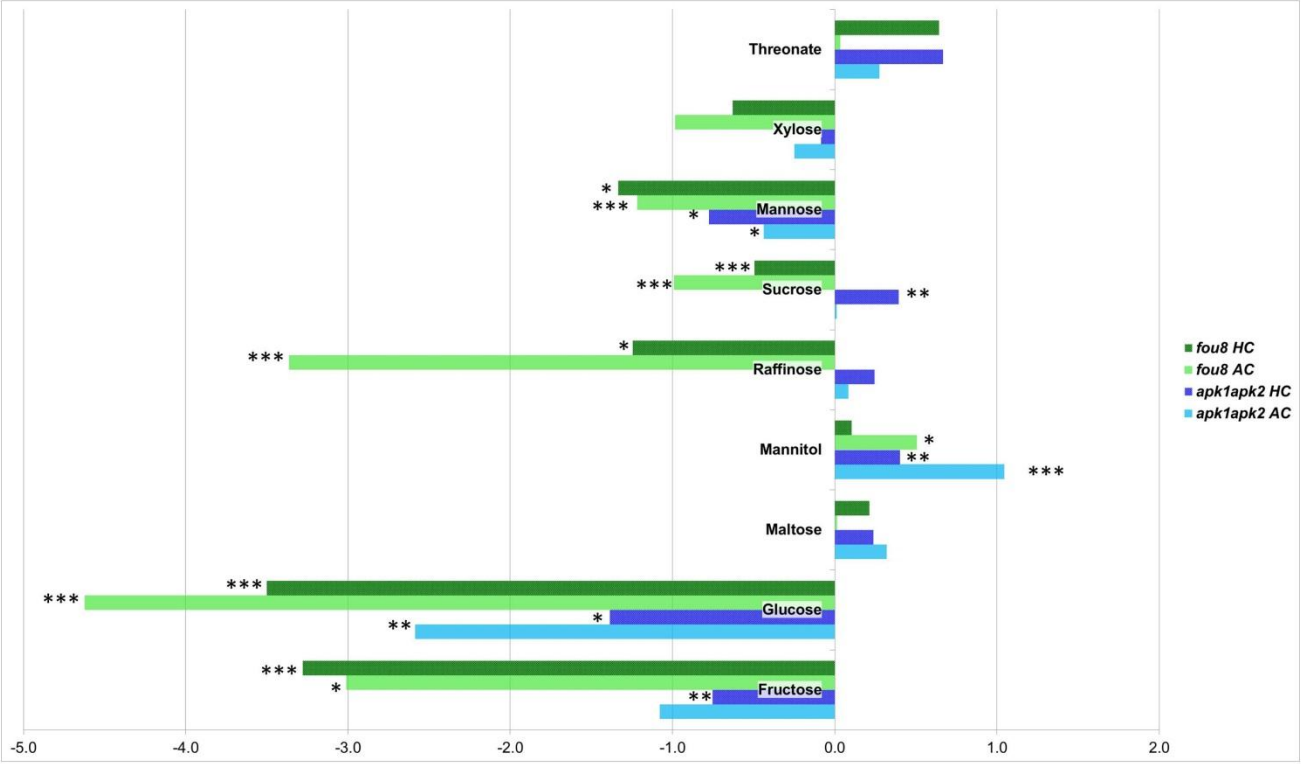

Figure.31: Reduction of carbohydrates in fou8 and *apk1apk2* mutants
Plants were grown for 5 weeks in high CO_2 and either transferred to ambient air for 3 days or kept further in high CO_2. Metabolites in leaves were analyzed by GC-MS. Shown are fold change differences to WT at the given condition. Ambient air (AC):390 ppm CO2in air, High CO2 (HC): 3,000 ppm CO2 in air. Asterisks mark values significantly different from WT *:$P \leq 0.05$,**:$P \leq 0.01$,***:$P \leq 0.001$ t-test.

In addition, notable differences were observed in accumulation of organic acids, particularly the TCA cycle intermediates. Remarkably, compared to WT the two mutants showed almost completely opposite alterations in TCA cycle intermediates. Loss of SAL1 resulted in coordinated reduction in accumulation of the TCA cycle intermediates α-ketoglutarate, succinate, fumarate and malate in both conditions (Figure.32). Only citrate+isocitrate were not significantly affected in *fou8*. High CO_2 treatment did not alter the observed TCA cycle metabolic profile of these mutants compare to wild type. On the other hand, *apk1apk2* significantly accumulated citrate+isocitrate, α-ketoglutarate, succinate and malate while only

fumarate did not show any difference to WT (Figure.32).In addition, pyruvate and glycolate were less abundant in *fou8* than WT after switch to ambient air.

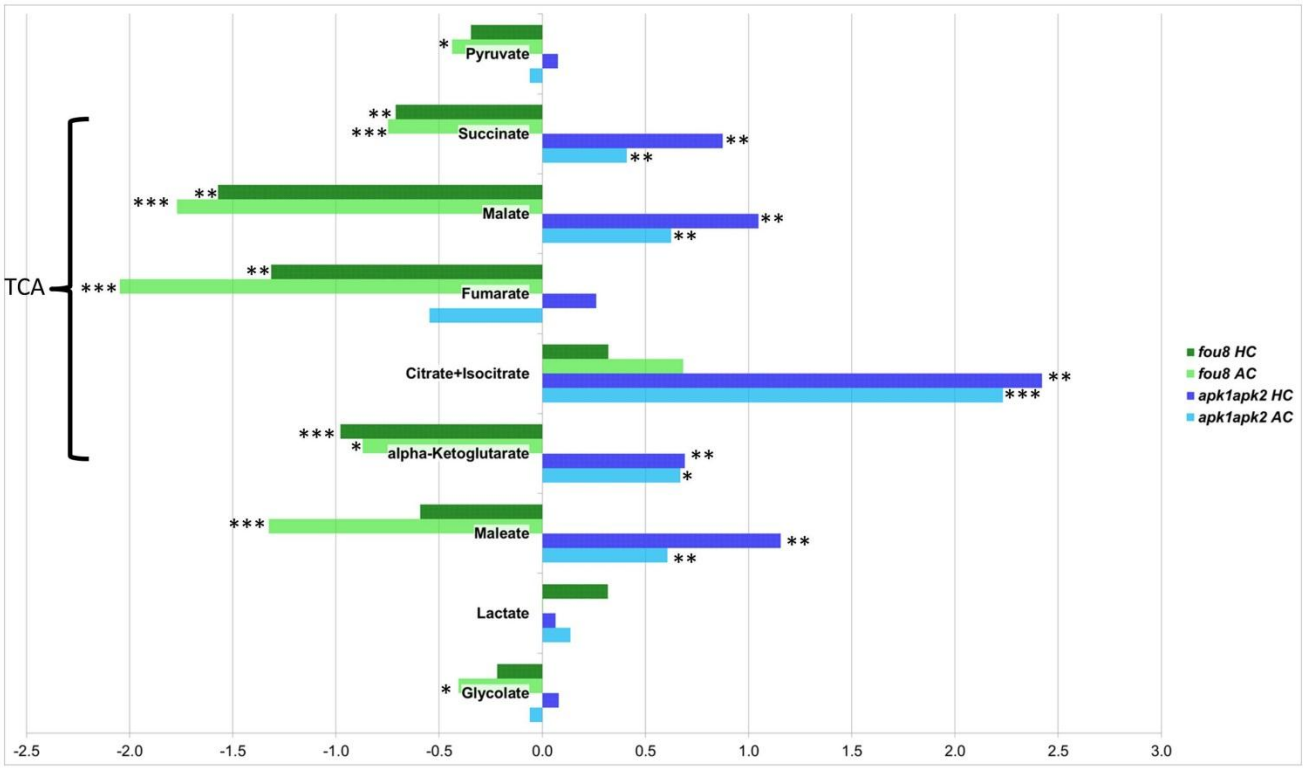

Figure.32: Contrasting effect on TCA cycle intermediates in *fou8* and *apk1apk2* mutants
Plants were grown for 5 weeks in high CO_2 and either transferred to ambient air for 3 days or kept further in high CO_2. Metabolites in leaves were analyzed by GC-MS. Ambient air (AC):390 ppm CO2in air, High CO2 (HC): 3,000 ppm CO2 in air. Shown are fold change differences to WT at the given condition. Asterisks mark values significantly different from WT *:$P \leq 0.05$,**:$P \leq 0.01$,***:$P \leq 0.001$ t-test.

4.4 Regulation of TCA cycle genes in *fou8*

In an attempt to explain the differences in TCA cycle in *fou8* mutant, we analyzed existing RNA-Seq data set and differentially expressed genes (DEG) lists (Crisp et al., 2017). In the *sal1-8* mutant four genes for TCA cycle enzymes showed a slight downregulation with lower than two-fold change and one gene, *c-NAD-MDH3*, was downregulated to a higher degree (log2FC = -1.34) (Table.3). In contrast *SDH1-2* showed increased transcript levels at log2FC = 1.88 (Table.3). These differences seem not to be sufficient to explain the differences of TCA cycle intermediates in *fou8* mutant. We also checked the expression of Coenzyme A (CoA) transporters since it is an important cofactor for the TCA cycle enzymes. CoA transporter CoA

Carrier 2(COAC2) was upregulated in *sal1-8* mutant while COA Carrier 1(COAC1) was not differentially expressed (Table.3).

Table.3: Differentially expressed TCA cycle and CoA transporter genes in sal1-8 mutant

Expression data from RNA-Seq and differentially expressed genes list used (Crisp et al., 2017). Genes written red downregulated; written green upregulated.

Gene Model Description	Locus Identifier	Primary Gene Symbol	Log_2 Fold Change	P Value
SUCCINATE DEHYDROGENASE 1-2	AT2G18450.1	SDH 1-2	1.88	2.369E-02
CITRATE SYNTHASE 3	AT2G42790.1	CSY3	-0.63	6.268E-05
ACONITASE 1	AT4G35830.1	ACO1	-0.63	1.989E-06
SUCCINATE DEHYDROGENASE 8	AT2G46390.1	SDH8	-0.67	2.573E-05
CYTOSOLIC NADP+ DEPENDENT ISOCITRATE DEHYDROGENASE	AT1G65930.1	cICDH	-0.93	1.472E-07
CYTOSOLIC NAD DEPENDENT MALATE DEHYDROGENASE 3	AT5G56720.1	c-NAD-MDH3	-1.34	2.104E-03
CoA CARRIER 2	AT4G26180.1	COAC2	0.78	2.032E-04

In addition, we reanalyzed the DEG list of *sal1-8* mutant to assess the effect of the mutation on transcription of genes associated with mitochondria. We compared the DEG list of *sal1-8* to complete list of genes located in mitochondria (GO:0005739) (Crisp et al., 2017). We found that 18% (966 genes) of the total 5450 genes encoding proteins with function in mitochondria are differentially expressed in *sal1-8* mutant, 62% (601 out of 966)of them were upregulated (Figure.33 A). Gene enrichment analysis with g:profiler (Raudvere et al., 2019) of these 601 genes revealed that the biological process most significantly affected is mitochondrial RNA metabolic process (GO:0000959) (Figure.33 B). In Arabidopsis mitochondrial RNA metabolic processing gene network consist of 75 genes, and 22 of them are upregulated in *sal1-8* mutant. We compared this list with the DEG list from *xrn2xrn3* (Crisp et al., 2017) to investigate whether the differential regulation of genes for mitochondrial RNA processing might be caused by the

inhibition of XRN2 and XRN3 by PAP. This was suspected because PAP binds to XRN exoribonucleases in the nucleus and regulates RNA polymerase II by RNA degradation which causes drastic changes in transcription of many genes (Estavillo et al., 2011). However, only 3 genes overlapped in these datasets while the other 19 genes were only differentially expressed in *sal1-8* mutant (Figure.33 C). Remarkably, one of the 3 overlapping genes is AT5G14580, which encodes an RNA processing enzyme with a putative 3´-5´ exoribonuclease activity. This gene is upregulated in both *sal1-8* and *xrn2xrn3* and might have an important and undiscovered role in post transcriptional regulation of mitochondria associated transcripts.

A

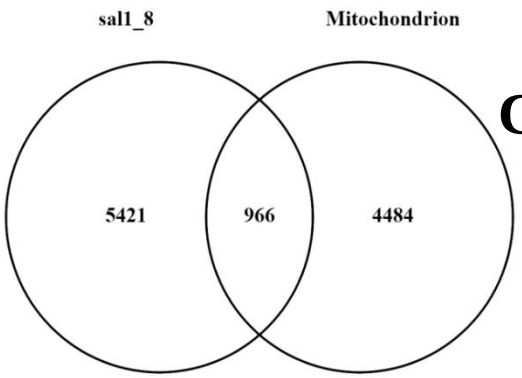

C

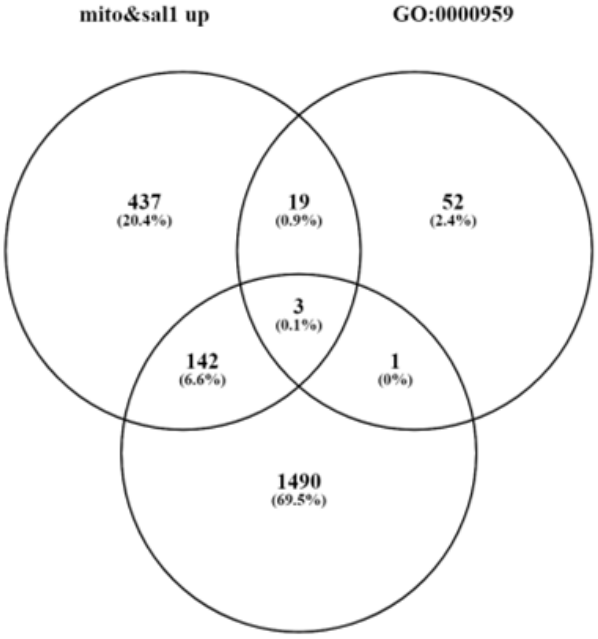

B

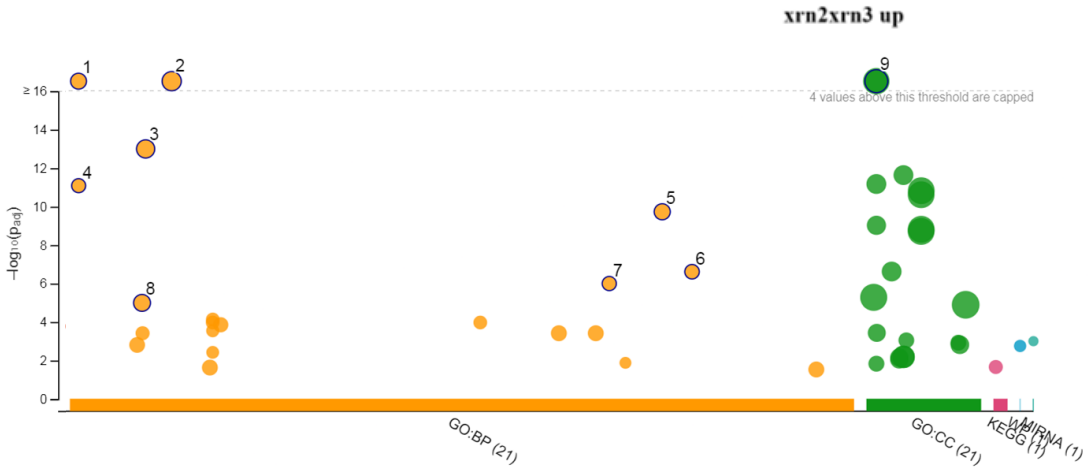

ID	Source	Term ID	Term Name	p_{adj} (query_1)
1	GO:BP	GO:0000959	mitochondrial RNA metabolic process	2.734×10^{-19}
2	GO:BP	GO:0009451	RNA modification	6.415×10^{-24}
3	GO:BP	GO:0007005	mitochondrion organization	1.047×10^{-13}
4	GO:BP	GO:0000963	mitochondrial RNA processing	8.497×10^{-12}
5	GO:BP	GO:0140053	mitochondrial gene expression	1.927×10^{-10}
6	GO:BP	GO:1900864	mitochondrial RNA modification	2.514×10^{-7}
7	GO:BP	GO:0080156	mitochondrial mRNA modification	1.032×10^{-6}
8	GO:BP	GO:0006839	mitochondrial transport	1.044×10^{-5}
9	GO:CC	GO:0005739	mitochondrion	1.818×10^{-139}

Figure.33 Gene set enrichment analysis of mitochondrial DEGs of sal1-8 mutant.

A. Venn diagram of *sal1-8* DEG list with genes compared with complete list of genes located in mitochondria (Mitochondrion; GO:0005739). RNA-Seq dataset (Crisp et al., 2017) **B**. Gene ontology analysis with g:profiler, analysis of upregulated genes in *sal1-8* mutant in mitochondria (GO: Gene Ontology BP: Biological Process, CC: Cellular component.) C. Venn diagram of upregulated *sal1-8* genes in mitochondria compared to upregulated genes in *xrn2xrn3* (Crisp et al., 2017) mutant and mitochondrial RNA metabolic process (GO:0000959).

5. DISCUSSION

Our findings proved the importance of sulfur metabolites and their unique roles under drought stress conditions. New crosses of sulfur metabolism mutants gave us the chance to test intriguing combinations of different concentrations of sulfur metabolites and their functions in response to abiotic stress. We observed drought tolerance of secondary sulfur metabolism mutant *apk1apk2* and tried to decipher the underlying reason. Our experiments found new possible connection between cysteine and stomata development. Our set of mutants also provided us with a new tool to analyze key roles of cysteine degradation and glutathione synthesis under drought stress.

In the second part of our study we investigated the role of secondary sulfur metabolism under drought. We compared the newly discovered drought resistance of *apk1apk2* to another drought resistant mutant related to secondary sulfur pathway, knock-out mutant of *SAL1* gene, *fou8*. We analyzed these two mutants and their crosses to find out if the drought response mechanism of these two mutants is different and possibly additive.

Lastly, we tested the *SAL1* mutant *fou8* and *apk1apk2* under non-photorespiratory conditions. Metabolomic analysis revealing big alterations of TCA cycle intermediates in *fou8* gave us an appealing clue about a relation between mitochondria and the metabolite PAP. We explored the existing transcriptional studies in *SAL1* mutants and the PAP related processes in mitochondria literature from human and animal studies. We proposed new connections between PAP and mitochondrial transport, biosynthesis and RNA processing mechanisms.

5.1 Connections of sulfur metabolites to drought tolerance

Drought stress is one of the biggest environmental factors that affect plant growth, development, and productivity. As global climate change intensifies, the frequency and severity of drought events are increasing, posing increasing risks on agriculture and food security. Understanding the drought response mechanisms and using that knowledge for breeding drought resistant crops becoming increasingly critical.

Plants have adapted various morphological, metabolomic and physiological strategies to survive water scarcity. The management of stress and this strategies can be divided into three category; avoidance, tolerance and escape (Oguz et al., 2022). To avoid drought stress plants decrease

water loss and increase water uptake with smaller leaf surface, thicker cuticle, tight regulation of stomata aperture and deeper root growth (Ullah et al., 2017). To endure drought periods plants accumulate osmoprotectant molecules and antioxidants against increasing oxidative stress. Another mechanism plant developed is to quicken their life cycle, flower early and develop seeds before drought intensifies (Fang & Xiong, 2015; Seleiman et al., 2021).

Connection of sulfur metabolites and drought response has long attracted the attention of research. Sulfur containing metabolites are central to response to oxidative stress conditions like drought (Chan et al., 2019). Almost all the sulfur containing molecules found in plant cell have been proposed to play a role in drought stress; sulfate, sulfite, sulfide, cysteine, glutathione or glucosinolates (Álvarez et al., 2010; Bangash et al., 2019; Batool et al., 2018; Bekturova et al., 2021; Salehin et al., 2019b). It was previously suggested that the key molecules in sulfur metabolism are sulfate, as signal from root to shoot, and cysteine for promoting stomatal closure under drought stress (Batool et al., 2018). Cysteine regulates the ABA mediated stomata closure with its role in synthesis of the Moco (Molybdenum Cofactor) needed for ABA synthesis (Batool et al., 2018; Ren et al., 2022). Antioxidant role of GSH and signaling functions of H_2S also makes sulfur metabolism key for drought stress (Mirza Hasanuzzaman et al., 2020; Ren et al., 2022). GSH is a scavenger of ROS under stress conditions and important redox balancer (Locato et al., 2017). Recently, another sulfur containing metabolite H_2S has been under the spot lights due to its proposed signaling role in stomatal closure under drought conditions (Álvarez et al., 2010; Aroca et al., 2021). On the other hand the different types of aliphatic, indolic and aromatic secondary sulfur metabolites GSL have shown different responses to drought in Arabidopsis and other *Brassicaceae* species (Abdelsoud et al., 2016). The by-product of secondary sulfur reactions PAP, the retrograde signaling molecule from chloroplast to nucleus, was proven to be highly connected to drought tolerance (Estavillo et al., 2011). However the impact of partitioning of the sulfur between primary and secondary metabolisms on drought response has never been investigated.

The first set of experiments was performed to understand the drought tolerance mechanism of *apk1apk2* mutant. This mutant possessed high concentrations of cysteine and glutathione (Figure.6 & Figure.7). We crossed *apk1apk2* with one the key enzyme of primary sulfur metabolism mutant *apr2*, in an attempt to decrease the flux of sulfur and change the reducing

redox state of *apk1apk2* mutant. The triple mutant showed decrease in both of the metabolites, however, they both were still significantly higher than in Col-0 (Figure.6). We also crossed the *apk1apk2* with *cad2* leading to decrease of GSH values to wild type levels, however, cysteine reached unprecedentedly high concentrations in this triple mutant (Figure.6). *cad2* has already low GSH, but after crossing with *apr2* the *cad2apr2* had even lower GSH values (Figure.6). We also included *des1* mutant which also has high Cys and GSH, to test the role of cysteine degradation and H_2S production (Álvarez et al., 2010). Lastly we crossed *des1* with *cad2* to create another cysteine accumulating mutant that theoretically would have lower amount of GSH and higher Cys compared to *des1*.

We used our set of mutants to understand drought stress mechanism of sulfur metabolism mutants if they avoid or endure the stress.

5.1.1 Sulfur metabolites give plants ability to avoid drought with better control of water

To be able to avoid stress, plants close their stomata and try to contain their water under drought. We first designed a drought experiment combined with high light and high temperate, and the results showed improved resistance of *apk1apk2* and its triple crosses. These genotypes were the only ones surviving the stress while maintaining around 70% water content (Figure.10). *des1* and *cad2des1* mutants wilted first, which might be explained by their reduced ability to produce H_2S and close their stomata (Scuffi et al., 2014). Higher cysteine and GSH levels in *des1* mutant were not enough to save this plant under stress because of its inability to close stomata properly (Álvarez et al., 2010; Scuffi et al., 2014). *apk1apk2cad2* also survived the drought even though this mutant had only WT levels of GSH. The resistance of this triple mutant with normal levels of GSH showed that GSH is not playing a pivotal role in keeping the water (Bangash et al., 2019).

Second drought experiment was in more controlled, slow but long stress conditions to see which sulfur metabolite has the key role in mitigating the effects of drought. *apk1apk2* retained its water extremely well again (Figure.12 & Figure.13). We showed that *des1* was the most effected genotype from drought and was not able to maintain its water at the same level like WT, as previously described (Figure.11, Figure.12 & Figure.13) (Jin et al., 2013). This proved that the accumulation of Cys and GSH alone is not enough for the closure of stomata. On the other hand

apk1apk2 and its crosses were able to maintain their water levels under drought even though they had different levels of GSH and cysteine (Figure.7). *cad2* mutant with higher cysteine and lower GSH lost water content significantly under drought compared to control conditions (Figure.7 & Figure.13). This showed the importance of maintaining standard levels of GSH being enough for the drought tolerance of *apk1apk2cad2*, but possessing lower than WT concentrations might cause significantly reduced water content under drought.

Next we measured the carbon isotope discrimination (δC^{13}) from samples collected from water withdrawing experiment. That gave us a more detailed view of the water content retaining abilities of different mutants. δC^{13} is an indirect way of calculating the balance between water loss and carbon assimilation (Dittberner et al., 2018). Lower $\delta^{13}C$ values indicate higher water use efficiency (WUE), in our experiment *apk1apk2* mutants were not affected by drought stress while other mutants increased their $\delta^{13}C$. This shows that the *apk1apk2* mutants maybe have not perceived the stress and did not close their stomata which would cause an increase in $\delta^{13}C$. Interestingly high $\delta^{13}C$ values already in control treatment of *apk1apk2* indicated lower water use of these mutants (Figure.15). The reason for the delay of the stress response might be due to the high GSH and Cys, which provide higher resilience against oxidation in the cell (Kopriva et al., 2024). $\delta^{13}C$ of *cad2des1* double mutant was low and did not increase with drought stress (Figure.15). That was also unexpected from double mutant carrying *des1* mutation and having imparities in stomata closure. However, *cad2des1* had lower stomata density compared to *des1* (Figure.17), which might explain the different behaviour.

Previous drought experiment with *des1* mutant also showed increased susceptibility of this mutant to drought treatment (Jin et al., 2013). The connection between H_2S and ABA mediated stomata closure makes sulfide very critical for drought avoidance strategies (Scuffi et al., 2014). The stomata closure problems of *des1* caused by lacking proper H_2S signaling makes this mutant to lose its water very easily (Romero et al., 2014). Recently a number of studies indicating the signaling role of H_2S to response to abiotic stress conditions are gaining traction (Aroca et al., 2021; García-Calderón et al., 2023; Gotor et al., 2019; Liu et al., 2021; Zhang et al., 2024). he connection between GSH and stomata closure has also been suggested before, however, experimental finding favors the key role of H_2S lately (Okuma et al., 2011; Pantaleno et al., 2021). Previously sulfide was suggested to have impact on stomatal closure only as a precursor

of cysteine biosynthesis which has attested main role (Rajab et al., 2019). Sulfide also feedback regulates DES1 enzyme and causes its persulfidation. Posttranslational persulfidation of key proteins on ABA signaling pathway results in increase in of the closure of stomata in response to by sulfide under drought conditions (Liu et al., 2021) (Figure.2). *des1* mutant with reduced H_2S levels also has lower levels of protein persulfidation (Gotor et al., 2019).

The water content and δC^{13} values were not enough to explain drought tolerance we observed. Because of that we focused to another factor important for the drought avoiding mechanism, the stomata density and size.

5.1.2 Cysteine causes lower stomata density

We found significant decrease in stomata density in all drought resistant *apk1apk2* crosses. Other cysteine accumulating mutants *cad2, des1* and *cad2des1* also had significantly lower stomata density compared to WT (Figure.17). This showed a possible correlation between cysteine accumulation and stomata development which was not proposed or investigated before. The ability of retaining water in *apk1apk2* and its crosses were parallel with their lower stomata density. However, lower stomata densities were not enough to withstand the drought in *des1* and *cad2*, possibly, because *des1* is not able to close its stomata and *cad2* does not have enough GSH to fight oxidative stress caused by drought. Previous studies also suggested reduced stomata density decreases the water loss which provides increased drought tolerance (Franks et al., 2015). An interesting new study cloned and overexpressed *GSH1* gene from *Caragana korshinskii* in Arabidopsis resulting in higher GSH content and lower stomata density in overexpressed lines, which led to better drought tolerance (B. Lu et al., 2021). Another recent study suggested that increased concentrations of H_2O_2 , a reactive oxygen species, in meristemoid cells initiates stomatal development (Shi et al., 2022). *apk1apk2* mutant also had high levels of GSH and lower stomata density. However GSH and stomata connection cannot be suggested for *apk1apk2cad2* which had WT level GSH but lower stomata density.

There is another interesting connection between sulfur metabolism and stomata development. Small peptides called EPIDERMAL PATTERNING FACTOR/EPIDERMAL PATTERNING FACTOR-LIKE (EPF/EPFL) are distinguished by abundant cysteine residues (S. Lu & Xiao, 2024). EPF peptides negatively regulate stomata development (Lin et al., 2017). EPF1 and EPF2

are secreted from stomatal lineage cells and block other cells to entry into stomatal fate which keep stomata density under control (Hara et al., 2007; Hunt & Gray, 2009). New study found that ABA is required for the fine-tuning of transcription of *EPF1* and *EPF2* and control of stomata density and spacing (Mohamed et al., 2023). A recent study with triploid poplar trees overexpressing stomatal density inhibitors *PagEPF2*, *PagEPF4* and *PagEPF9* had lower stomata density (Xia et al., 2024). Plants with lower stomata density had larger guard cells and better drought tolerance (Xia et al., 2024). We observed similar trend in *apk1apk2* mutants which has also larger stomata size, lower density and better drought tolerance (Peter Wolf, Bachelor Thesis, University of Cologne, 2020). Stomata density was also shown to be connected with better water use efficiency (Guo et al., 2019).The small peptides EPFs might explain the reason for lower stomata density in *apk1apk2* mutant in our experiments. Abundant cysteine concentration and high GSH concentration of this mutant could be the cause of excess amount of small peptide EPF secretion and decrease in stomata density. Another possibility is higher cysteine concentrations might protect the active cysteine residues of this small peptides. The connection between sulfur metabolism and EPFs has never been investigated yet.

To test the endurance against the drought stress we then tested how different concentrations of sulfur metabolites in our mutants affect their ability to protect photosynthetic efficiency.

5.1.3 Glutathione provides endurance under drought stress

To be able to understand the physiological consequences of GSH and Cys concentration changes we also measured PSII efficiency of our mutants under control and stress conditions. We observed a great variety of PSII efficiency difference especially under drought stress. All genotypes other than *apk1apk2* had reduced PSII efficiency under drought (Figure.18). This effect was bigger in mutants with lower GSH content or lacking the cysteine degradation enzyme DES1. Photosynthesis is one of the most important metabolic activity in plants and is affected greatly by drought and stomata closure, which leads to decreased CO_2 (Pinheiro & Chaves, 2011). The protection mechanism of the photosynthetic machinery results from thermal dissipation in the xanthophyll cycle and lutein cycle of the light harvesting complex (Demmig-Adams et al., 2006, Garcia-Plazaola et al., 2003). Photosynthesis is commonly downregulated under drought stress, as shown by a decreased quantum yield in PSII, when the photo protective

mechanisms compete with photochemistry over the absorbed energy (Genty et al., 1989; Giardi et al., 1996).

Interestingly PSII efficiency is affected in the mutants lacking sufficient GSH. Under oxidative stress and heavy metal stress conditions maximum PSII efficiency significantly reduced in *cad2* mutant seedlings in Arabidopsis (Hoang et al., 2021) Another study also proved that mutants in GSH synthesis had reduced PSII efficiency after 72 hours treatment with 10 µM cadmium (Sobrino-Plata et al., 2014). Also, external GSH application protected the PSII efficiency in *Solanum lycopersicum L* under salt stress conditions (Cong et al., 2024). Another experiment with external GSH application protected wheat seedlings photosynthetic abilities-with increasing *cholorphhyll a* and *chlorphyll b* content from heat and drought stress (Suliman et al., 2024). Application of GSH also protected photosynthesis of cucumber seedlings (Ding et al., 2016). GSH-Ascorbate cycle is an important cycle for eliminating ROS H_2O_2 and facilitates the conversion of excess excitation energy.

Lower stomata density and better ability to keep water content, together with higher GSH concentration yields up to better PSII efficiency in *apk1apk2* mutant. This is even more prominent under drought stress in *apk1apk2*. The reason of its higher drought tolerance might be rooted in its ability to protect the cell against oxidative stress under drought with antioxidant GSH content. Triple mutants created with *apk1apk2* crosses could not maintain their PSII efficiency under drought (Figure.18). This might be caused by their lower GSH concentrations compared to *apk1apk2*. *cad2* and *des1* mutants had significantly reduced PSII efficiency under drought conditions, this might be explained by their lower GSH content and lack of stomata regulation by H_2S respectively.

Sulfur metabolism enzymes are regulated to produce more GSH under stress conditions. The primary sulfur metabolism enzymes are mostly redox regulated and increased oxidative stress during drought increases the activity of these enzyme, while it decreases the secondary sulfur metabolism enzyme APKs activity (de Bont et al., 2022; Ravilious et al., 2012).

Alternatively cysteine was also suggested to have a protective role for photosynthetic machinery role against photooxidation (Orf et al., 2016). A study exogenously applied Cys to wheat plants before the drought treatment and that caused increase in carotenoids under drought (Elkelish et

al., 2021). Carotenoids are important in the xanthophyll cycle which dissipates the exceeding light energy to protect the plants and improve photosynthesis efficiency under drought (Elkelish et al., 2021). The impact of photorespiration on stomatal closure was shown previously (Eisenhut et al., 2017; Duminil et al., 2019) Up to 41% serine produced from photorespiration leaves the cycle to be used in sulfur assimilation (Fu et al., 2023; Abadie and Tcherkez, 2019) Thus recent study formulated a hypothesis that sulfate induced stomatal regulation by cysteine biosynthesis could be the possible reason of connection between stomatal closure and photorespiratory serine production (Eckardt et al., 2024).

5.1.4 Balance in the partitioning of sulfur is important for drought response

We can hypothesize from our findings and existing literature that regular levels of Cys, GSH and H_2S are all necessary for drought stress mechanisms. Cys is needed for proteins and regulation of stomata development, GSH needed for protection under stress conditions and H_2S is important for stomata closure under drought stress. Cysteine accumulation in *apk1apk2* and its crosses were not observed at the same level as in studies with *des1* mutant before (Figure.6 & Figure.7)(Álvarez et al., 2010; Scuffi et al., 2014; Shen et al., 2020). Thus we can say blocking the flux of sulfur to the secondary sulfur reactions is a bigger driver for the accumulation of primary sulfur compounds. The first partitioning of sulfur between sulfide and PAPS causes bigger effect on the divergence of sulfur pool compared to the second fork of cysteine degradation or GSH synthesis. The flux was increased 2.5times in *apk1apk2* and *apk1apk2cad2* compared to WT, which shows the impact of channeling the sulfur from sulfation pathways to sulfur reduction (Figure.1). GSH levels were decreased under drought stress possibly due to consumption and need of these ROS scavenger molecules in combat against drought. We observed that *des1* also had slightly but significantly lower stomata density but since it is unable to close them properly, this is not providing any drought tolerance to the *des1* as it does to *apk1apk2* (Figure.17). However lower stomata density also correlates with higher cysteine concentration of *des1* mutant and possible cysteine rich small peptide EPF connection to hinder stomata density. The lower concentration of GSH in *cad2* is causing problems in this mutant's ability to protect photosynthetic machinery under drought conditions. Under drought conditions *cad2* mutant was able to keep its water content better than *des1* and WT and probably it can

close its stomata properly but cannot continue high functioning photosynthesis due to reduced GSH content (Figure.18).

5.2. Sulfation pathway mutants under drought

We observed drought resistance of secondary sulfur metabolism mutant *apk1apk2* and triple mutants *apk1apk2apr2* and *apk1apk2cad2*. To elucidate further the importance of sulfation pathway on drought stress, we included long established drought resistant *SAL1* mutant *fou8 to* our new drought experiments. We tested whether the mechanisms of drought tolerance of *fou8* and *apk1apk2* are the different. We also included the cross of these two mutants, a triple mutant *apk1apk2fou8* for the purpose of understanding if these mechanisms are different and additive (Rodríguez et al., 2010). To investigate another important component of sulfated metabolites, we included *TYROSYLPROTEIN SULFOTRANSFERASE* mutant *tpst1*. TPST1 is located in golgi and responsible for sulfation of small peptides in the plants (Komori et al., 2009). Sulfated peptides such as the phytosulfokines (Matsubayashi & Sakagami, 1996), root growth factors (Matsuzaki et al., 2010), or Casparian strip integrity factors (Nakayama et al., 2017) have critical roles in cell elongation and differentiation. We wanted to test the importance of sulfated small peptides on stomata formation and drought stress response.

Our drought experiment with sulfation mutants included *fou8, apk1apk2*, their cross *apk1apk2fou8,* and *tpst1*. Previous study showed that *apk1apk2fou8* accumulated less PAP compared *fou8* but it was still significantly higher than WT (Lee et al., 2012). Water content of *apk1apk2fou8* and *fou8* was significantly higher than *apk1apk2* after drought treatment (Figure.24). Effect of drought on water content and δC^{13} decreased in triple mutant (Figure.25). That indicated that the mechanisms of the drought resistance of two mutants might be distinct and additive. All the sulfation mutants used in our second set of mutants showed attenuation of growth at control conditions and better water retaining abilities (Figure.23 & Figure.24).PAP accumulation in *fou8* mutant triggers a great change in its transcriptome and activates ABA signaling pathway and it can stomata closure independent from OST1 and ABI1 (Crisp et al., 2017; Pornsiriwong et al., 2017). PAP accumulation in plants alter auxin and gibberellic acid concentrations which impacts all the phytohormonal crosstalk in plants, however exact reason why *sal1* mutants are dwarf is not known (Phua et al., 2018). We also could not explain the exact reason of dwarfism in *apk1apk2* phenotype.

apk1apk2, *fou8* and *tpst1* had significantly lower stomata density however stomata density of *apk1apk2fou8* was unexpectedly not significantly different than WT (Figure.26). We calculated the stomatal density of abaxial leaf surface and found lower stomatal density of howeer previous study counted the number of epidermal cells and number of stomata and found unchanged stomatal index in *fou8* mutants compared to wild type (Wilson et al., 2009). The main mechanism underlying the drought resistant phenotype of *fou8* is the initiation of expression of oxidative stress response genes by accumulation of PAP (Estavillo et al., 2010). PAP concentration increase up to 30-fold in Arabidopsis under drought stress conditions (Estavillo et al., 2010). SAL1 is inhibited in its oxidized form which explains the high accumulation of PAP under drought (Chan et al., 2016). In the mutants of key ABA pathway members, *ABA INSENSITIVE 1(abi1)* and *OPEN STOMATA 1 (ost1)* , endogoneous or exogenous PAP is inducing ABA responsive genes with separate pathway independent from ABA which causes stomatal closure and drought tolerance (Pornsiriwong 2017) *sal1* mutant crossed with ABA insensitive mutants still possessed drought tolerance indicating the response to PAP accumulation is independent from canonical ABA pathway (Pornsiriwong 2017) Our analysis of PAP under both stress and control conditions have not provided us with further details about these mutants than previously described (Lee et al., 2012; Rodríguez et al., 2010). The results of *tpst1* mutant were quite unexpected, but due to germination problems only three biological replicates were used for this mutant. However they grew much bigger than previously described (Komori et al., 2009). The mechanism of this mutant's water retention ability and lower stomata number could be related with sulfation and maturation of phytosulfokines (Li et al., 2024).

5.3 PAP and Mitochondria connection

The aim of our next research was to address an intriguing question: Why is SAL1 localized in the mitochondria in plants? In this study we found large changes in accumulation of amino acids, TCA intermediate metabolites and carbohydrates in *fou8* mutant. Analysis of overlapping transcriptomic changes in *fou8* mutants and mitochondria and possible impacts of PAP accumulation on mitochondrial processes encouraged us to search the existing literature. We found several exciting but overlooked connections between PAP and mitochondria.

Subcellular target specific complementation of *SAL1* in *sal1* mutant background to the exclusively in mitochondria (mitSAL1) rescued most aspect of the phenotype (Ashykhmina et

al., 2022). However targeting SAL1 to cytoplasm or chloroplast did not rescue the phenotype fully, showing the importance of the PAP degradation in mitochondria (Ashykhmina et al., 2022). Furthermore, double mutants of *SAL1* and PAP transporters *sal1papst1* and *sal1papst2* were also complemented with *mitSAL1*. Complementation of *salpapst1* with *mitSAL1* rescued the phenotype while *sal1papst2* complementation could not, and the plants remained small (Ashykhmina et al., 2019).

The PAP generating reaction, phosphopantetheinylation of ACP by mtPPT gave an appealing clue. We hypothesized that SAL1 in mitochondria is needed for the removal of PAP molecules produced by mtFAS, since PAP accumulation might inhibit mtPPT and thus availability of acylated ACP for production of fatty acids. Indeed, such feedback regulation of the activity of PPTase by high concentrations of PAP which strongly inhibits the enzyme was shown before in bacterial and animal systems (Foley & Burkart, 2009). In plants, deficiency in mtPPT and other components of mtFAS leads to a distinct photorespiratory phenotype and a strong reduction in growth (Fu et al., 2020; Guan et al., 2015). Since *sal1* mutants are also semi-dwarf, similar to the *apk1apk2*, it seemed plausible to expect a complementation of this growth defect by elevated CO_2. However, neither the growth of the two mutants was complemented by high CO_2, nor did the plants exhibit any injury after transfer from high to ambient CO_2 (Figure.29), both of which are well described general photorespiratory phenotypes. We also compared the accumulation of glycine, which was highly elevated in *mtppt-rnai* plants (Guan et al., 2015), since it is possible that the effect of PAP is first observable on the metabolite level, before the morphology. However, the GC-MS analysis revealed that there is no typical metabolic photorespiratory phenotype (Figure.30, Figure.31 & Figure.32).

Because there seem not to be any major effects of PAP on mtFAS, we investigated the connections between PAP and other mitochondrial processes. We observed extraordinary reduction in concentrations of TCA cycle intermediates in both ambient air and high CO_2 conditions (Figure.32). A slight reduction of TCA cycle intermediates, was also observed in a previous metabolomic analysis in *sal1* mutant (Wilson et al., 2009). However, the effect of PAP accumulation on mitochondria has not been the focus of research before. The change in the concentration of TCA cycle intermediates can alter several key processes in the cell such as; cellular signaling, chromatin re-modification and DNA methylation (Martínez-Reyes & Chandel,

2020). Furthermore, they affect many physiological processes like immune systems and stem cell functions and are their conctrations are altered in many different diseases in animals like tumorogenesis and neurodegenerative disorders (Martínez-Reyes & Chandel, 2020).

While we did not observe the expected accumulation of glycine in *fou8,* almost all other amino acids were elevated in the mutant (Figure.30), which is very similar to the metabolic profile of the mutants of PDC subunit E2 enzyme (Yu et al., 2012). This is worth noting, because E2 subunit uses lipoic acid as a cofactor similar to H-protein of GDC which had decreased function in mtFAS mutant *mtPPT* causing accumulation of glycine (Guan et al., 2015).

The reduced levels of glucose and fructose and the semi dwarf phenotype of the mutants pointed to a possible lower efficiency of CO_2 fixation. However, these phenotypes could not be reverted under high CO_2 conditions. It is plausible to suggest that reduced levels of pyruvate and other TCA cycle intermediates in *fou8* are the consequence of the lower concentrations of glucose and other monosaccharides. The reduction of glucose and fructose levels has also been shown previously in several different metabolomic analyses of *SAL1* mutants (Robles et al., 2010; Wilson et al., 2009). But even though *apk1apk2* and *fou8* both have decreased levels of glucose; they show opposite responses in the TCA cycle (Figure.32). To be able to interpret the unique metabolomic profile of *fou8,* we revisited the possible connections between PAP and the mitochondria in different organisms in the literature (Figure.34).

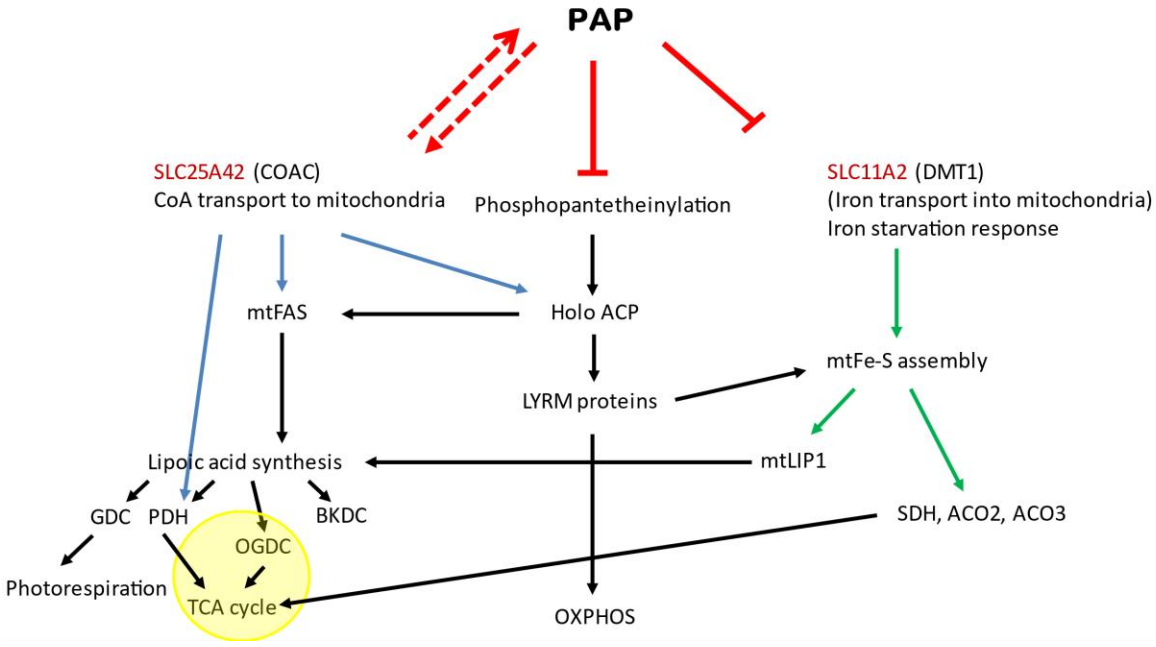

Figure.34: Biological interactions of PAP with CoA, mtFAS and mtFe-S assembly
Red arrows: PAP interactions. Blue arrows: CoA related biological pathways and enzymes. Green arrows: Iron related biological reactions BLACK: other biological interactions. ACO2: Aconitase2, ACO3: Aconitase3, BKDC: Branched-chain a-Keto Acid Dehydrogenase Complex, COAC: CoA Carrier, DMT1: Divalent Metal Transporter 1, GDC: Glycine Decarboxylase Complex , LYRM: Leu-Tyr-Arg Motif proteins, mtLIP1: Mitochondrial Lipoyl Synthase, OGDC: 2-oxoglutarate Dehydrogenase Complex , OXPHOS: Oxidative phosphorylation complexes, PDC: Pyruvate Dehydrogenase Complex, SDH: Succinate Dehydrogenase, SLC: Solute carrier family proteins.

5.3.1 Phosphopantetheinylation produce PAP in mitochondria

PAP is a toxic by-product molecule in human cells which needs to be degraded. Accumulation of PAP causes problems in DNA repair, chromatin structure, DNA methylation and cell death (Toledano et al., 2012). Two possible source of PAP accumulation are sulfation reactions and phosphopantetheinylation in fatty acid synthesis. The feedback inhibition of PPTase enzyme by its own by-product PAP was previously described in bacteria (Foley & Burkart, 2009).

A recent metabolomic study on human glioma brain tumors revealed that human ortholog of *SAL1*, *BPNT-1*, was significantly down-regulated in cancer cells (Li et al., 2018). Strikingly, BPNT-1 enzyme is dual localized in cytosol and in mitochondria in human cells (Li et al., 2018). The brain cancer tissue had significantly higher PAP concentrations compared to healthy brain tissue. The transcription levels of PAPS synthases (*PAPSS-1 & PAPSS-2*) and human

phosphopantetheine transferase *AASDHPPT* were also upregulated (Li et al., 2018). The experimental findings in human tumor cells indicating possible upregulation mechanism of PAPS sytheases and mtFAS when the PAP accumalition increased.

mtPPT enzyme is essential for synthesis of holoACP which is the key enzymatic reaction for mtFAS. Holo ACP also has a critical role in mtFe-S assembly and oxidative phosphorylation complexes (OXPHO) through its interaction with Leu-Tyr-Arg Motif (LYRM) proteins (Nowinski et al., 2018). It was also discovered that holoACP is needed for Fe-S cluster biogenesis, where it physically interacts with LYRM proteins and helps the formation Fe-S cluster with acylation (Van Vranken et al., 2016). All these connections of phosphopantetheinylation with mtFAS and mtFe-S assembly increase the possible impact of PAP accumulation in mitochondria.

5.3.2 Iron transport into mitochondria is impacted by PAP

DMT1 is a metal transporter localized on the outer mitochondrial membrane and the inhibition of this transporter leads to decreased iron uptake to the mitochondria in mice (Wolff et al., 2014). Work with intestine specific knockout lines of *bpnt1* mutant mice revealed that accumulation of PAP leads to iron deficiency (Hudson et al., 2018). Wild type mice responded to iron starvation stress with up-regulating Divalent Metal Transporter 1 (DMT1), while PAP accumulating *bpnt1* mutants were not able to increase their DMT1 transcript or protein levels (Hudson et al., 2018). The iron deficiency anemia phenotype of mice mutants was rescued by reducing PAP synthesis.

These studies could explain the effect of PAP accumulation on iron deficiency in the mitochondria and subsequently mtFe-S assembly. Iron sulfur clusters are indispensable cofactors for numerous enzymes in mitochondrial biological processes. Mitochondrial lipoic acid synthesis enzyme lipoyl synthase (mtLIP1) and TCA cycle enzymes Aconitase2 (ACO2), Aconitase3 (ACO3) and succinate dehydrogenase (SDH) are the enzymes which also require iron sulfur clusters for function (Moseler et al., 2021). The possible inhibition of iron transporter genes in mitochondrial membrane by PAP, might lead to lower efficiency of iron sulfur cluster assembly machinery in plants mitochondria.

There are also new studies in plants focusing on *SAL1* mutants under iron deficiency and their capacity of iron accumulation. *fry1* mutant has been shown to accumulate higher concentrations

of iron under control conditions and to be more tolerant to iron deficiency (Balparda et al., 2020). Also same study suggested a connection between PAP pathway, ethylene signaling and iron metabolism (Balparda et al., 2020). However, another study in Arabidopsis focusing on the effect of sulfur starvation on iron deficiency response, concluded PAP was not involved in this interplay (Robe et al., 2020).

5.3.3 Coenzyme A transport in mitochondria counter exchange PAP

The coordinated reduction of the TCA cycle intermediates in *fou8* mutant could indicate a lack of CoA in mitochondria, which is an essential cofactor for pyruvate dehydrogenase, the gatekeeping enzyme for pyruvate to enter the TCA cycle. Reduction in PDC activity due to low availability of CoA could be an alternative explanation of the metabolic phenotype of *fou8* (Figure.32). Interestingly, in the animal kingdom, PAP acts as a counter exchange transport molecule for uptake of CoA into the mitochondria by SLC25A42 protein (Fiermonte et al., 2009). In Arabidopsis two CoA transporters have been partially characterized, CoA Carrier1 (COAC1) and COAC2 (Zallot et al., 2013). COAC2 belongs to the same subclass of transporters like SLC25A42. If COAC2 has the same counter exchange specificity as SLC25A42, accumulation of PAP in cytoplasm of *fou8* could inhibit the transporter and decrease the CoA import in mitochondria. *COAC2* transcript levels in *sal1* RNA seq is slightly increased (log2FC = 0.78) which might indicate possible malfunctioning of the transport when PAP over accumulates (Table.3). Another Arabidopsis CoA transporter, PXN (Peroxisomal NAD+ carrier, AT2G39970) is located in the peroxisome and characterized as a NAD+ transporter but it is also able to transport CoA, dephospho-CoA, acetyl-CoA and PAP (Agrimi et al., 2012).

In the literature, connection between some neurodegenerative diseases and CoA dependent phosphopantetheinylation of mitochondrial acyl carrier proteins has been shown. (Lambrechts et al., 2019). Dysfunctions in the activities of mitochondrial enzymes triggered by defects of CoA pathway genes were reversed by feeding the cells with phosphopantetheine (Jeong et al., 2019). Intriguingly, PAP accumulation caused by lithium inhibition or mutation of BPNT-1 also caused the dysfunction of ASJ neurons in *C. elegans* (Meisel & Kim, 2016). CoA transporters connection with PAP still need to be further analyzed in plant kingdom.

5.3.4 Mitochondrial RNA processing could be regulated by PAP accumulation

Remarkably, the most significant biological process upregulated in PAP accumulating *sal1-8* mutants was mitochondrial RNA processing (Figure.33). Plant mitochondria have a circular genome which is transcribed by specific phage type RNA polymerases (Liere et al., 2011). After transcription, mitochondrial RNAs undergo an extensive post-transcriptional processing, which gives rise to very complicated transcription patterns (Hammani & Giegé, 2014). One of the promising candidate genes for RNA processing is AT5G14580, with a putative exoribonuclease activity. We found this mitochondria affiliated gene to be upregulated in both *sal1-8* and *xrn2xrn3.* The role of this gene and how PAP affects mitochondrial RNA processing, however, still needs to be assessed. Indeed, it is known that PAP inhibits XRN exoribonucleases in the nucleus and alters the RNA degradation of RNA polymerase II which causes drastic changes in transcription of many genes (Estavillo et al., 2011). Parallel to these findings, complementation of *sal1* with SAL1 with nuclear localization sequence rescued the mutant phenotype (Ashykhmina et al., 2022).

5.4 CONCLUSIONS & OUTLOOK

5.4.1 Sulfur and Drought

Our results presented a new and promising connection between sulfur metabolism and drought tolerance. Analysis of the different endogenous combinations of sulfur metabolites is important to elucidate the role of each metabolite in drought response**.** We created novel mutant crosses in sulfur metabolism with up to 15- fold cysteine accumulation and with GSH concentrations ranged from 25% up to 250% of WT. The unexpected drought resilience of *apk1apk2* provided us insights on required collection of sulfur metabolites to survive the drought stress. An unprecedented accumulation of cysteine in *apk1apk2cad2* and huge fluctuations of GSH in the different mutants showed us the importance of the sulfur flux into the secondary pathway. Interestingly, the cysteine accumulating mutants seem to possess lower stomata density. We showed that the combination of lower stomata density with adequate levels of GSH and ability to close stomata through H_2S provided *apk1apk2* mutant not only drought tolerance but also ability to retain PSII efficiency under drought stress. Cysteine rich stomata development repressors, EPF small peptides, are the great candidate for connecting the high cysteine with low stomata density (Hara et al., 2007; Hunt & Gray, 2009).

Transcriptional analysis of mutants accumulating different amounts of sulfur compounds can provide new candidates for drought response mechanism. To complete the picture *apk1apk2des1* mutant should be added to this mutant tool box, to investigate further how *in vivo* increase on both Cys and GSH concentrations will impact the phenotype and drought resistance when sulfide production is reduced. Since the connection between sulfide and autophagy is well established, the impact of cysteine accumulation on autophagy might be worth investigating using our mutants set. The cellular compartment specific accumulation and degradation of sulfur metabolites especially in mitochondria should be further investigated. Recently new study showed the importance of sulfide in mitochondria for of stomatal immunity against flg22 (Pantaleno et al., 2024).Sulfide-generating enzymes in mitochondria and their impacts on drought tolerance might also provide an interesting research topic between sulfur metabolism and mitochondria.

For the future our findings can have interesting applications for breeding drought tolerant plants. Testing drought tolerance of different natural *APK* alleles from economically important *Brassicaceae* members can help finding drought resistant natural accessions and cultivars. On the other hand blocking APK and GSH1 in sulfur pathway could be the new innovative way of creating cysteine accumulating organisms for commercial purposes. Effect of cysteine accumulation on seed development, germination, flower development, venation of leaves were all observed preliminary in the greenhouse for *apk1apk2cad2* mutant and should be investigated further

5.4.2 PAP and mitochondria

Our hypothesis was that PAP accumulation in mitochondria of *sal1* mutants inhibit phosphopantetheinylation reaction in mtFAS, leading to reduced synthesis of lipoic acid and photorespiratory phenotype. Metabolomic and transcriptomic analyses of *fou8* mutant, however, did not yield the results we expected, but provided us new directions towards intriguing mitochondria-PAP connections for example mtFe-S assembly, iron and CoA transport to mitochondria and mitochondrial RNA processing all have connecting points with PAP .

We discovered that accumulation of PAP affects mitochondrial processes, inhibits TCA cycle in *fou8* mutant, while it leads to accumulation of the TCA cycle intermediates in *apk1apk2*. It is

appealing to hypothesize, that accumulation of PAP could be affecting the lipoic acid synthesis through mtFAS and iron sulfur cluster dependent enzymes through iron transporters which at the end results an accumulation of TCA intermediates. Other reason for the *fou8* phenotypes could be the impaired CoA transport into the mitochondria because of PAP accumulation. Our experimental findings and previous studies suggest that accumulation of PAP in mitochondria might play an important role on coordination of mtFAS, mtFe-S assembly and CoA transport. The interactions between these processes might be the reason of distinct metabolic profile we have observed (Figure.34).

We also observed lower carbohydrate levels in PAP accumulating *fou8* mutant. This might be due to reduced effectiveness of light harvest complex or water use efficiency during photosynthesis but these needs to be investigated further. Indeed, among the down regulated biological processes in *sal-1* chloroplast, photosynthesis light reactions and light harvesting in photosystem I were significantly enriched (Supplementary Figure. 9).

Our re-analysis of existing RNA data suggested that it is very likely that PAP is affecting the RNA processing in the mitochondria. Among the 3 genes upregulated in both *sal1* and *xrn2xrn3*, the AT5G14580 is the most interesting as the corresponding protein is located in the mitochondria and is suggested to have 3'-5'-exoribonuclease activity. Another gene upregulated by both mutations is a putative endonuclease AT5G09840. These two genes deserve closer attention for their possible role in causing the mitochondrial transcriptomic and metabolic alterations by PAP.

Further research needs to be carried out to illuminate potential effects of PAP as an intraorganellar signaling molecule in plants and animal kingdom. Effects of PAP on all the mitochondrial processes need to be addressed and clarify in vitro experiments. That will help us to understand numerous interactions between different pathways in mitochondria and different organelles.

REFERENCES

Abuelsoud, W., Hirschmann, F., & Papenbrock, J. (2016). Drought stress tolerance in plants, vol 1: Physiology and biochemistry. Drought Stress Tolerance in Plants, Vol 1: Physiology and Biochemistry, May, 1–526. https://doi.org/10.1007/978-3-319-28899-4

Agrimi, G., Russo, A., Pierri, C. L., & Palmieri, F. (2012). The peroxisomal NAD+ carrier of Arabidopsis thaliana transports coenzyme A and its derivatives. Journal of Bioenergetics and Biomembranes, 44, 333-340.

Amano, Y., Tsubouchi, H., Shinohara, H., Ogawa, M., & Matsubayashi, Y. (2007). Tyrosine-sulfated glycopeptide involved in cellular proliferation and expansion in Arabidopsis. Proceedings of the National Academy of Sciences, 104(46), 18333-18338.

Anoman, A. D., Flores-Tornero, M., Benstein, R. M., Blau, S., Rosa-Téllez, S., Bräutigam, A., Fernie, A. R., Muñoz-Bertomeu, J., Schilasky, S., Meyer, A. J., Kopriva, S., Segura, J., Krueger, S., & Ros, R. (2019). Deficiency in the phosphorylated pathway of serine biosynthesis perturbs sulfur assimilation. Plant Physiology, 180(1), 153–170. https://doi.org/10.1104/pp.18.01549

Álvarez, C., Calo, L., Romero, L. C., García, I., & Gotor, C. (2010). An O-Acetylserine(thiol)lyase homolog with l-Cysteine desulfhydrase activity regulates cysteine homeostasis in arabidopsis. Plant Physiology, 152(2), 656–669. https://doi.org/10.1104/pp.109.147975

Álvarez, C., García, I., Moreno, I., Pérez-Pérez, M. E., Crespo, J. L., Romero, L. C., & Gotor, C. (2012). Cysteine-generated sulfide in the cytosol negatively regulates autophagy and modulates the transcriptional profile in arabidopsisw. Plant Cell, 24(11), 4621–4634. https://doi.org/10.1105/tpc.112.105403

Aroca, A., & Gotor, C. (2022). Hydrogen Sulfide: A Key Role in Autophagy Regulation from Plants to Mammalians. Antioxidants, 11(2). https://doi.org/10.3390/antiox11020327

Aroca, A., García-Díaz, I., García-Calderón, M., Gotor, C., Márquez, A. J., & Betti, M. (2023). Photorespiration: regulation and new insights on the potential role of persulfidation. Journal of Experimental Botany, 74(19), 6023–6039. https://doi.org/10.1093/jxb/erad291

Aroca, A., Zhang, J., Xie, Y., Romero, L. C., & Gotor, C. (2021). Hydrogen sulfide signaling in plant adaptations to adverse conditions: Molecular mechanisms. Journal of Experimental Botany, 72(16), 5893–5904. https://doi.org/10.1093/jxb/erab239

Ashykhmina, N., Chan, K. X., Frerigmann, H., Van Breusegem, F., Kopriva, S., Flügge, U. I., & Gigolashvili, T. (2022). Dissecting the Role of SAL1 in Metabolizing the Stress Signaling Molecule 3′-Phosphoadenosine 5′-Phosphate in Different Cell Compartments. Frontiers in Molecular Biosciences, 8(January), 1–16. https://doi.org/10.3389/fmolb.2021.763795

Ashykhmina, N., Lorenz, M., Frerigmann, H., Koprivova, A., Hofsetz, E., Stührwohldt, N., Flügge, U. I., Haferkamp, I., Kopriva, S., & Gigolashvilia, T. (2019). Papst2 plays critical roles in removing the stress signaling molecule 39-phosphoadenosine 59-phosphate from the cytosol and its subsequent degradation in plastids and mitochondria. Plant Cell, 31(1), 231–249. https://doi.org/10.1105/tpc.18.00512

Baek, D., Pathange, P., Chung, J. S., Jiang, J., Gao, L., Oikawa, A., ... & Lee, I. J. (2010). A stress-inducible sulphotransferase sulphonates salicylic acid and confers pathogen resistance in Arabidopsis. Plant Cell and Environment, 33(8), 1383–1392. https://doi.org/10.1111/j.1365-3040.2010.02156.x

Ball, L., Accotto, G. P., Bechtold, U., Creissen, G., Funck, D., Jimenez, A., ... & Mullineaux, P. M. (2004). Evidence for a direct link between glutathione biosynthesis and stress defense gene expression in Arabidopsis. The Plant Cell, 16(9), 2448-2462.

Balparda, M., Armas, A. M., Estavillo, G. M., Roschzttardtz, H., Pagani, M. A., & Gomez-Casati, D. F. (2020). The PAP/SAL1 retrograde signaling pathway is involved in iron homeostasis. Plant Molecular Biology, 102(3), 323–337. https://doi.org/10.1007/s11103-019-00950-7

Bangash, S. A. K., Müller-Schüssele, S. J., Solbach, D., Jansen, M., Fiorani, F., Schwarzländer, M., Kopriva, S., & Meyer, A. J. (2019). Low-glutathione mutants are impaired in growth but do not show an increased sensitivity to moderate water deficit. PLoS ONE, 14(10). https://doi.org/10.1371/journal.pone.0220589

Batool, S., Uslu, V. V., Rajab, H., Ahmad, N., Waadt, R., Geiger, D., Malagoli, M., Xiang, C. Bin, Hedrich, R., Rennenberg, H., Herschbach, C., Hell, R., & Wirtz, M. (2018). Sulfate is incorporated into cysteine to trigger ABA Production and stomatal closure. Plant Cell, 30(12), 2973–2987. https://doi.org/10.1105/tpc.18.00612

Beinert, H. (2000). A tribute to sulfur. European Journal of Biochemistry, 267(18), 5657-5664.;

Bekturova, A., Oshanova, Di., Tiwari, P., Nurbekova, Z., Kurmanbayeva, A., Soltabayeva, A., Yarmolinsky, D., Srivastava, S., Turecková, V., Strnad, M., & Sagi, M. (2021). Adenosine 5′

phosphosulfate reductase and sulfite oxidase regulate sulfite-induced water loss in Arabidopsis. Journal of Experimental Botany, 72(18), 6447–6466. https://doi.org/10.1093/jxb/erab249

Bick, J. A., Setterdahl, A. T., Knaff, D. B., Chen, Y., Pitcher, L. H., Zilinskas, B. A., & Leustek, T. (2001). Regulation of the plant-type 5′-adenylyl sulfate reductase by oxidative stress. Biochemistry, 40(30), 9040–9048. https://doi.org/10.1021/bi010518v

Bohrer, A. S., Kopriva, S., & Takahashi, H. (2014). Plastid–cytosol partitioning and integration of metabolic pathways for APS/PAPS biosynthesis in Arabidopsis thaliana. Frontiers in Plant Science, 5, 751. https://doi.org/10.3389/fpls.2014.00751

Bohrer, A. S., Yoshimoto, N., Sekiguchi, A., Rykulski, N., Saito, K., & Takahashi, H. (2015). Alternative translational initiation of ATP sulfurylase underlying dual localization of sulfate assimilation pathways in plastids and cytosol in Arabidopsis thaliana. Frontiers in Plant Science, 5, 750.

Cairns, N. G., Pasternak, M., Wachter, A., Cobbett, C. S., & Meyer, A. J. (2006). Maturation of Arabidopsis seeds is dependent on glutathione biosynthesis within the embryo. Plant physiology, 141(2), 446-455.

Calderwood, A., Morris, R. J., & Kopriva, S. (2014). Predictive sulfur metabolism–a field in flux. Frontiers in Plant Science, 5, 646.

Cao, M.-J., Wang, Z., Zhao, Q., Mao, J.-L., Speiser, A., Wirtz, M., Hell, R., Zhu, J.-K., & Xiang, C.-B. (2014). Sulfate availability affects ABA levels and germination response to ABA and salt stress in rabidopsis thaliana. The Plant Journal, 77(4), 604–615. https://doi.org/https://doi.org/10.1111/tpj.12407

Chan, K. X., Mabbitt, P. D., Phua, S. Y., Mueller, J. W., Nisar, N., Gigolashvili, T., Stroeher, E., Grassl, J., Arlt, W., Estavillo, G. M., Jackson, C. J., & Pogson, B. J. (2016). Sensing and signaling of oxidative stress in chloroplasts by inactivation of the SAL1 phosphoadenosine phosphatase. Proceedings of the National Academy of Sciences of the United States of America, 113(31), E4567–E4576. https://doi.org/10.1073/pnas.1604936113

Chan, K. X., Phua, S. Y., & Breusegem, F. Van. (2019). Secondary sulfur metabolism in cellular signalling and oxidative stress responses. Journal of Experimental Botany, 70(16), 4237–4250. https://doi.org/10.1093/jxb/erz119

Chao, D. Y., Baraniecka, P., Danku, J., Koprivova, A., Lahner, B., Luo, H., Yakubova, E., Dilkes, B.,

Kopriva, S., & Salt, D. E. (2014). Variation in sulfur and selenium accumulation is controlled by naturally occurring isoforms of the key sulfur assimilation enzyme ADENOSINE 5'-PHOSPHOSULFATE REDUCTASE2 across the arabidopsis species range. Plant Physiology, 166(3), 1593–1608. https://doi.org/10.1104/pp.114.247825

Chen, H., & Xiong, L. (2010). The bifunctional abiotic stress signalling regulator and endogenous RNA silencing suppressor FIERY1 is required for lateral root formation. Plant, Cell & Environment, 33(12), 2180–2190. https://doi.org/10.1111/j.1365-3040.2010.02218.x

Chen, S., Jia, H., Wang, X., Shi, C., Wang, X., Ma, P., Wang, J., Ren, M., & Li, J. (2020). Hydrogen Sulfide Positively Regulates Abscisic Acid Signaling through Persulfidation of SnRK2.6 in Guard Cells. Molecular Plant, 13(5), 732–744. https://doi.org/10.1016/j.molp.2020.01.004

Cobbett, C. S., May, M. J., Howden, R., & Rolls, B. (1998). The glutathione-deficient, cadmium-sensitive mutant, cad2-1, of Arabidopsis thaliana is deficient in gamma-glutamylcysteine synthetase. The Plant Journal : For Cell and Molecular Biology, 16(1), 73–78. https://doi.org/10.1046/j.1365-313x.1998.00262.x

Cong, Y., Chen, X., Xing, J., Li, X., Pang, S., & Liu, H. (2024). Nitric oxide signal is required for glutathione-induced enhancement of photosynthesis in salt-stressed Solanum lycopersicum L. Frontiers in Plant Science, 15(June), 1–14. https://doi.org/10.3389/fpls.2024.1413653

Cooper, M., & Messina, C. D. (2023). Breeding crops for drought-Affected environments and improved climate resilience. Plant Cell, 35(1), 162–186. https://doi.org/10.1093/plcell/koac321

Corpas, F. J., González-Gordo, S., Muñoz-Vargas, M. A., Rodríguez-Ruiz, M., & Palma, J. M. (2021). The modus operandi of hydrogen sulfide (H2S)-dependent protein persulfidation in higher plants. Antioxidants, 10(11), 1686.

Coughtrie, M. W. H. (2016) Function and organization of the human cytosolic sulfotransferase (SULT) family. Chem. Biol. Interact. 259, 2–7 CrossRef Medline Dias et al.,

Crisp, P. A., Ganguly, D. R., Smith, A. B., Murray, K. D., Estavillo, G. M., Searle, I., Ford, E., Bogdanović, O., Lister, R., Borevitz, J. O., Eichten, S. R., & Pogson, B. J. (2017). Rapid recovery gene downregulation during excess-light stress and recovery in arabidopsis. Plant Cell, 29(8), 1836–1863. https://doi.org/10.1105/tpc.16.00828

de Bont, L., Donnay, N., Couturier, J., & Rouhier, N. (2022). Redox regulation of enzymes involved in

sulfate assimilation and in the synthesis of sulfur-containing amino acids and glutathione in plants. Frontiers in Plant Science, 13(August), 1–12. https://doi.org/10.3389/fpls.2022.958490

Demmig-Adams, B., & Adams III, W. W. (2006). Photoprotection in an ecological context: the remarkable complexity of thermal energy dissipation. New phytologist, 172(1), 11-21.

Ding, X., Jiang, Y., He, L., Zhou, Q., Yu, J., Hui, D., & Huang, D. (2016). Exogenous glutathione improves high root-zone temperature tolerance by modulating photosynthesis, antioxidant and osmolytes systems in cucumber seedlings. Scientific reports, 6(1), 35424.

Dittberner, H., Korte, A., Mettler-Altmann, T., Weber, A. P., Monroe, G., & de Meaux, J. (2018). Natural variation in stomata size contributes to the local adaptation of water-use efficiency in Arabidopsis thaliana. Molecular ecology, 27(20), 4052-4065.

Duminil, P. (2019). Characterization of two primary metabolism enzymes in Arabidopsis thaliana: phosphoglycerate mutase and phosphoglycolate phosphatase (Doctoral dissertation, Université Paris Saclay (COmUE)).

Eisenhut, M., Bräutigam, A., Timm, S., Florian, A., Tohge, T., Fernie, A. R., ... & Weber, A. P. (2017). Photorespiration is crucial for dynamic response of photosynthetic metabolism and stomatal movement to altered CO2 availability. Molecular plant, 10(1), 47-61.

Estavillo, G. M., Crisp, P. A., Pornsiriwong, W., Wirtz, M., Collinge, D., Carrie, C., ... & Pogson, B. J. (2011). Evidence for a SAL1-PAP chloroplast retrograde pathway that functions in drought and high light signaling in Arabidopsis. The Plant Cell, 23(11), 3992-4012.Foley & Burkart, 2009

Eckardt, N. A., Allahverdiyeva, Y., Alvarez, C. E., Büchel, C., Burlacot, A., Cardona, T., Chaloner, E., Engel, B. D., Grossman, A. R., Harris, D., Herrmann, N., Hodges, M., Kern, J., Kim, T. D., Maurino, V. G., Mullineaux, C. W., Mustila, H., Nikkanen, L., Schlau-Cohen, G., … Yano, J. (2024). Lighting the way: Compelling open questions in photosynthesis research. The Plant Cell, 36(10), 3914–3943. https://doi.org/10.1093/plcell/koae203

Elkelish, A., El-Mogy, M. M., Niedbała, G., Piekutowska, M., Atia, M. A. M., Hamada, M. M. A., Shahin, M., Mukherjee, S., El-Yazied, A. A., Shebl, M., Jahan, M. S., Osman, A., Abd El-Gawad, H. G., Ashour, H., Farag, R., Selim, S., & Ibrahim, M. F. M. (2021). Roles of exogenous α-lipoic acid and cysteine in mitigation of drought stress and restoration of grain quality in wheat. Plants, 10(11), 1–25. https://doi.org/10.3390/plants10112318

Estavillo, G. M., Crisp, P. A., Pornsiriwong, W., Wirtz, M., Collinge, D., Carrie, C., Giraud, E., Whelan, J., David, P., Javot, H., Brearley, C., Hell, R., Marin, E., & Pogson, B. J. (2011). Evidence for a SAL1-PAP chloroplast retrograde pathway that functions in drought and high light signaling in Arabidopsis. Plant Cell, 23(11), 3992–4012. https://doi.org/10.1105/tpc.111.091033

Fang, Y., & Xiong, L. (2015). General mechanisms of drought response and their application in drought resistance improvement in plants. Cellular and Molecular Life Sciences, 72(4), 673–689. https://doi.org/10.1007/s00018-014-1767-0

Farquhar, G. D., O'Leary, M. H., & Berry, J. A. (1982). On the Relationship Between Carbon Isotope Discrimination and the Intercellular Carbon Dioxide Concentration in Leaves. Functional Plant Biology, 9, 121–137. https://api.semanticscholar.org/CorpusID:84895827

Fiermonte, G., Paradies, E., Todisco, S., Marobbio, C. M., & Palmieri, F. (2009). A novel member of solute carrier family 25 (SLC25A42) is a transporter of coenzyme A and adenosine 3′, 5′-diphosphate in human mitochondria. Journal of Biological Chemistry, 284(27), 18152-18159.

Filipovic, M. R., Zivanovic, J., Alvarez, B., & Banerjee, R. (2018). Chemical biology of H2S signaling through persulfidation. Chemical reviews, 118(3), 1253-1337.

Finkelstein, R. (2013). Abscisic acid synthesis and response. The Arabidopsis Book, 11, e0166.

Foley, T. L., & Burkart, M. D. (2009). A homogeneous resonance energy transfer assay for phosphopantetheinyl transferase. Analytical Biochemistry, 394(1), 39–47. https://doi.org/10.1016/j.ab.2009.06.037

Franks, P. J., W. Doheny-Adams, T., Britton-Harper, Z. J., & Gray, J. E. (2015). Increasing water-use efficiency directly through genetic manipulation of stomatal density. New Phytologist, 207(1), 188–195. https://doi.org/10.1111/nph.13347

Fu, X., Guan, X., Garlock, R., & Nikolau, B. J. (2020). Mitochondrial fatty acid synthase utilizes multiple acyl carrier protein isoforms. Plant Physiology, 183(2), 547-557.

Fuentes-Lara, L. O., Medrano-Macías, J., Pérez-Labrada, F., Rivas-Martínez, E. N., García-Enciso, E. L., González-Morales, S., Juárez-Maldonado, A., Rincón-Sánchez, F., & Benavides-Mendoza, A. (2019). From elemental sulfur to hydrogen sulfide in agricultural soils and plants. Molecules, 24(12), 1–17. https://doi.org/10.3390/molecules24122282

García-Plazaola, J. I., Hernández, A., Olano, J. M., & Becerril, J. M. (2003). The operation of the lutein

epoxide cycle correlates with energy dissipation. Functional Plant Biology, 30(3), 319-324.Plazaola et al., 2003

García-Calderón, M., Vignane, T., Filipovic, M. R., Ruiz, M. T., Romero, L. C., Márquez, A. J., Gotor, C., & Aroca, A. (2023). Persulfidation protects from oxidative stress under nonphotorespiratory conditions in Arabidopsis. New Phytologist, 238(4), 1431–1445. https://doi.org/10.1111/nph.18838

Genty, B., Briantais, J. M., & Baker, N. R. (1989). The relationship between the quantum yield of photosynthetic electron transport and quenching of chlorophyll fluorescence. Biochimica et Biophysica Acta (BBA)-General Subjects, 990(1), 87-92.

Giardi, M. T., Cona, A., Geiken, B., Kučera, T., Masojidek, J., & Mattoo, A. K. (1996). Long-term drought stress induces structural and functional reorganization of photosystem II. Planta, 199(1), 118-125.

Gigolashvili, T., Geier, M., Ashykhmina, N., Frerigmann, H., Wulfert, S., Krueger, S., ... & Flugge, U. I. (2012). The Arabidopsis thylakoid ADP/ATP carrier TAAC has an additional role in supplying plastidic phosphoadenosine 5′-phosphosulfate to the cytosol. The Plant Cell, 24(10), 4187–4204. https://doi.org/10.1105/tpc.112.101964

Gil-Mascarell, R., López-Coronado, J. M., Bellés, J. M., Serrano, R., & Rodríguez, P. L. (1999). The Arabidopsis HAL2-like gene family includes a novel sodium-sensitive phosphatase. The Plant Journal, 17(4), 373-383.Guan et al., 2015

Gläser, K., Kanawati, B., Kubo, T., Schmitt-Kopplin, P., Grill, E., & Papenbrock, J. (2014). Exploring the Arabidopsis sulfur metabolome. The Plant Journal, 77(1), 31–45. https://doi.org/10.1111/tpj.12359

Goettsch, S., Badea, R. A., Mueller, J. W., & Bayer, P. (2006). Human TPST1 transmembrane domain triggers enzyme dimerisation and localisation to the Golgi compartment. Journal of Molecular Biology, 361(3), 436–449. https://doi.org/10.1016/j.jmb.2006.06.023

Gorgues, L., Li, X., Maurel, C., Martinière, A., & Nacry, P. (2022). Root osmotic sensing from local perception to systemic responses. 1–21. https://doi.org/10.1007/s44154-022-00054-1

Gotor, C., García, I., Aroca, Á., Laureano-Marín, A. M., Arenas-Alfonseca, L., Jurado-Flores, A., Moreno, I., & Romero, L. C. (2019). Signaling by hydrogen sulfide and cyanide through post-translational modification. Journal of Experimental Botany, 70(16), 4251–4265. https://doi.org/10.1093/jxb/erz225

Gotor, C., Laureano-Marín, A. M., Moreno, I., Aroca, Á., García, I., & Romero, L. C. (2015). Signaling in the plant cytosol: Cysteine or sulfide? Amino Acids, 47(10), 2155–2164. https://doi.org/10.1007/s00726-014-1786-z

Gromes, R., Hothorn, M., Lenherr, E. D., & Wirtz, M. (2008). The redox switch of γ-glutamylcysteine ligase via a reversible monomer-dimer transition is a mechanism unique to plants. The Plant Journal, 54(6), 1063–1075. https://doi.org/10.1111/j.1365-313X.2008.03477.x

Guan, X., Chen, H., Abramson, A., Man, H., Wu, J., Yu, O., & Nikolau, B. J. (2015). A phosphopantetheinyl transferase that is essential for mitochondrial fatty acid biosynthesis. Plant Journal, 84(4), 718–732. https://doi.org/10.1111/tpj.13034

Guo, X. Y., Wang, Y., Zhao, P. X., Xu, P., Yu, G. H., Zhang, L. Y., Xiong, Y., & Xiang, C. Bin. (2019). AtEDT1/HDG11 regulates stomatal density and water-use efficiency via ERECTA and E2Fa. New Phytologist, 223(3), 1478–1488. https://doi.org/10.1111/nph.15861

Günal, S., & Kopriva, S. (2022). Measurement of flux through sulfate assimilation using [35 S] sulfate. Methods in Enzymology, 1–13. https://doi.org/10.1016/bs.mie.2022.07.021

Günal, S., Hardman, R., Kopriva, S., & Mueller, J. W. (2019). Sulfation pathways from red to green. Journal of Biological Chemistry, 294(33), 12293–12312. https://doi.org/10.1074/jbc.REV119.007422

Gy, I., Gasciolli, V., Lauressergues, D., Morel, J. B., Gombert, J., Proux, F., ... & Mallory, A. C. (2007). Arabidopsis FIERY1, XRN2, and XRN3 are endogenous RNA silencing suppressors. The Plant Cell, 19(11), 3451-3461

Haink, G., & Deussen, A. (2003). Liquid chromatography method for the analysis of adenosine compounds. Journal of Chromatography. B, Analytical Technologies in the Biomedical and Life Sciences, 784(1), 189–193. https://doi.org/10.1016/s1570-0232(02)00752-3

Hara, K., Kajita, R., Torii, K. U., Bergmann, D. C., & Kakimoto, T. (2007). The secretory peptide gene EPF1 enforces the stomatal one-cell-spacing rule. Genes and Development, 21(14), 1720–1725. https://doi.org/10.1101/gad.1550707

Hartmann-Fatu, C., & Bayer, P. (2016). Determinants of tyrosylprotein sulfation coding and substrate specificity of tyrosylprotein sulfotransferases in metazoans. Chemico-Biological Interactions, 259, 17-22.

Hasanuzzaman, M., Bhuyan, M. H. M. B., Mahmud, J. A., Nahar, K., Mohsin, S. M., Parvin, K., & Fujita, M. (2018). Interaction of sulfur with phytohormones and signaling molecules in conferring abiotic stress tolerance to plants. Plant Signaling and Behavior, 13(5), 1–5. https://doi.org/10.1080/15592324.2018.1477905

Hasanuzzaman, Mirza, Bhuyan, M. H. M. B., Zulfiqar, F., Raza, A., Mohsin, S. M., Al Mahmud, J., Fujita, M., & Fotopoulos, V. (2020). Reactive oxygen species and antioxidant defense in plants under abiotic stress: Revisiting the crucial role of a universal defense regulator. Antioxidants, 9(8), 1–52. https://doi.org/10.3390/antiox9080681

Hayes, J. M. (2001). Fractionation of the Isotopes of Carbon and Hydrogen in Biosynthetic Processes* John. National Meeting of the Geological Society of America, March.

Heeg, C., Kruse, C., Jost, R., Gutensohn, M., Ruppert, T., Wirtz, M., & Hell, R. (2008). Analysis of the Arabidopsis O-acetylserine (thiol) lyase gene family demonstrates compartment-specific differences in the regulation of cysteine synthesis. The Plant Cell, 20(1), 168-185.

Herrmann, J., Ravilious, G. E., McKinney, S. E., Westfall, C. S., Lee, S. G., Baraniecka, P., ... & Jez, J. M. (2014). Structure and mechanism of soybean ATP sulfurylase and the committed step in plant sulfur assimilation. Journal of Biological Chemistry, 289(15), 10919-10929.

Hirschmann, F., Krause, F., & Papenbrock, J. (2014). The multi-protein family of sulfotransferases in plants: composition, occurrence, substrate specificity, and functions. Frontiers in Plant Science, 5, 556. https://doi.org/10.3389/fpls.2014.00556

Hoang, M. T. T., Doan, M. T. A., Nguyen, T., Tra, D. P., Chu, T. N., Dang, T. P. T., & Quach, P. N. D. (2021). Phenotypic characterization of arabidopsis ascorbate and glutathione deficient mutants under abiotic stresses. Agronomy, 11(4), 1–19. https://doi.org/10.3390/agronomy11040764

Hudson, B. H., Hale, A. T., Irving, R. P., Li, S., & York, J. D. (2018). Modulation of intestinal sulfur assimilation metabolism regulates iron homeostasis. Proceedings of the National Academy of Sciences, 115(12), 3000-3005.

Hunt, L., & Gray, J. E. (2009). The Signaling Peptide EPF2 Controls Asymmetric Cell Divisions during Stomatal Development. Current Biology, 19(10), 864–869. https://doi.org/10.1016/j.cub.2009.03.069

Ingrisano, R., Tosato, E., Trost, P., Gurrieri, L., & Sparla, F. (2023). Proline, Cysteine and Branched-

Chain Amino Acids in Abiotic Stress Response of Land Plants and Microalgae. Plants, 12(19), 3410. https://doi.org/10.3390/plants12193410

Jeong, S. Y., Hogarth, P., Placzek, A., Gregory, A. M., Fox, R., Zhen, D., ... & Hayflick, S. J. (2019). 4′-Phosphopantetheine corrects CoA, iron, and dopamine metabolic defects in mammalian models of PKAN. EMBO molecular medicine, 11(12), e10489.

Jez, J. M., Ravilious, G. E., & Herrmann, J. (2016). Structural biology and regulation of the plant sulfation pathway. Chemico-Biological Interactions, 259, 31–38. https://doi.org/10.1016/j.cbi.2016.02.017

Jin, Z., Xue, S., Luo, Y., Tian, B., Fang, H., Li, H., & Pei, Y. (2013). Hydrogen sulfide interacting with abscisic acid in stomatal regulation responses to drought stress in Arabidopsis. Plant Physiology and Biochemistry, 62, 41–46. https://doi.org/10.1016/j.plaphy.2012.10.017

Jobe, T. O., & Kopriva, S. (2018). Sulfur Metabolism in Plants. Encyclopedia of Life Sciences, 1–8. https://doi.org/10.1002/9780470015902.a0020126.pub2

Joshi, A. K., Zhang, L., Rangan, V. S., & Smith, S. (2003). Cloning, expression, and characterization of a human 4′-phosphopantetheinyl transferase with broad substrate specificity. Journal of Biological Chemistry, 278(35), 33142-33149.

Kawashima, C. G., Matthewman, C. A., Huang, S., Lee, B. R., Yoshimoto, N., Takahashi, H., ... & Kopriva, S. (2011). Interplay of SLIM1 and miR395 in the regulation of sulfate assimilation in Arabidopsis. The Plant Journal, 66(5), 863–876. https://doi.org/10.1111/j.1365-313X.2011.04547.x

Kehoe, J. W., & Bertozzi, C. R. (2000). Tyrosine sulfation: a modulator of extracellular protein–protein interactions. Chemistry & biology, 7(3), R57-R61.

Khan, M. S., Haas, F. H., Samami, A. A., Gholami, A. M., Bauer, A., Fellenberg, K., Reichelt, M., Hänsch, R., Mendel, R. R., Meyer, A. J., Wirtz, M., & Hell, R. (2010). Sulfite reductase defines a newly discovered bottleneck for assimilatory sulfate reduction and is essential for growth and development in Arabidopsis thaliana. Plant Cell, 22(4), 1216–1231. https://doi.org/10.1105/tpc.110.074088

Kim, B. H., & von Arnim, A. G. (2009). FIERY1 regulates light-mediated repression of cell elongation and flowering time via its 3′(2′),5′-bisphosphate nucleotidase activity. The Plant Journal, 58(2), 208–219. https://doi.org/10.1111/j.1365-313X.2008.03770.x

Klein, M., & Papenbrock, J. (2009). Kinetics and substrate specificities of desulfo-glucosinolate sulfotransferases in Arabidopsis thaliana. Physiologia Plantarum, 135(1), 140–149. https://doi.org/10.1111/j.1399-3054.2008.01182.x

Klughammer, C., & Schreiber, U. (2008). Complementary PS II quantum yields calculated from simple fluorescence parameters measured by PAM fluorometry and the Saturation Pulse method. PAM application notes, 1(2), 201-247.

Kocsy, G., Tari, I., Vanková, R., Zechmann, B., Gulyás, Z., Poór, P., & Galiba, G. (2013). Redox control of plant growth and development. Plant Science, 211, 77–91. https://doi.org/10.1016/j.plantsci.2013.07.004

Koffler, B. E., Luschin-Ebengreuth, N., Stabentheiner, E., Müller, M., & Zechmann, B. (2014). Compartment specific response of antioxidants to drought stress in Arabidopsis. Plant Science : An International Journal of Experimental Plant Biology, 227, 133–144. https://doi.org/10.1016/j.plantsci.2014.08.002

Komori, R., Amano, Y., Ogawa-Ohnishi, M., & Matsubayashi, Y. (2009). Identification of tyrosylprotein sulfotransferase in Arabidopsis. Proceedings of the National Academy of Sciences of the United States of America, 106(35), 15067–15072. https://doi.org/10.1073/pnas.0902801106

Kopriva, S., Mugford, S. G., Baraniecka, P., Lee, B. R., Matthewman, C. A., & Koprivova, A. (2012). Control of sulfur partitioning between primary and secondary metabolism in Arabidopsis. Frontiers in Plant Science, 3, 163.

Kopriva, S., Malagoli, M., & Takahashi, H. (2019). Sulfur nutrition: impacts on plant development, metabolism, and stress responses. Journal of Experimental Botany, 70(16), 4069-4073.

Kopriva, S. (2006). Regulation of sulfate assimilation in Arabidopsis and beyond. Annals of Botany, 97(4), 479–495. https://doi.org/10.1093/aob/mcl006

Kopriva, S., Karvansara, P. R., & Takahashi, H. (2024). Adaptive modifications in plant sulfur metabolism over evolutionary time. Journal of Experimental Botany, 75(16), 4697–4711. https://doi.org/10.1093/jxb/erae252

Kruse, C., Jost, R., Lipschis, M., Kopp, B., Hartmann, M., & Hell, R. (2007). Sulfur-enhanced defence: effects of sulfur metabolism, nitrogen supply, and pathogen lifestyle. Plant Biology, 9(05), 608-619.

Lambalot, R. H., Gehring, A. M., Flugel, R. S., Zuber, P., LaCelle, M., Marahiel, M. A., ... & Walsh, C.

T. (1996). A new enzyme superfamily—the phosphopantetheinyl transferases. Chemistry & biology, 3(11), 923-936.

Lambrechts, R. A., Schepers, H., Yu, Y., van der Zwaag, M., Autio, K. J., Vieira-Lara, M. A., ... & Sibon, O. C. (2019). CoA-dependent activation of mitochondrial acyl carrier protein links four neurodegenerative diseases. EMBO molecular medicine, 11(12), e10488.

Lappartient, A. G., & Touraine, B. (1996). Demand-driven control of root ATP sulfurylase activity and SO42-uptake in intact canola (the role of phloem-translocated glutathione). Plant Physiology, 111(1), 147-157.

Laxa, M., Liebthal, M., Telman, W., Chibani, K., & Dietz, K. J. (2019). The role of the plant antioxidant system in drought tolerance. Antioxidants, 8(4). https://doi.org/10.3390/antiox8040094

Lee, B. R., Huseby, S., Koprivova, A., Chételat, A., Wirtz, M., Mugford, S. T., Navid, E., Brearley, C., Saha, S., Mithen, R., Hell, R., Farmer, E. E., and Kopriva, S. (2012) Effects of fou8/fry1 mutation on sulfur metabolism: is decreased internal sulfate the trigger of sulfate starvation response

Li, Y., Di, Q., Luo, L., & Yu, L. (2024). Phytosulfokine peptides, their receptors, and functions. Frontiers in Plant Science, 14, 1326964.

Liere, K., Weihe, A., & Börner, T. (2011). The transcription machineries of plant mitochondria and chloroplasts: composition, function, and regulation. Journal of plant physiology, 168(12), 1345-1360.

Lin, G., Zhang, L., Han, Z., Yang, X., Liu, W., Li, E., Chang, J., Qi, Y., Shpak, E. D., & Chai, J. (2017). A receptor-like protein acts as a specificity switch for the regulation of stomatal development. Genes and Development, 31(9), 927–938. https://doi.org/10.1101/gad.297580.117

Lipmann, F. (1958) Biological sulfate activation and transfer. Science 128, 575-580

Litthauer, S., Chan, K. X., & Jones, M. A. (2018). 3′-phosphoadenosine 5′-phosphate accumulation delays the circadian system. Plant Physiology, 176(4), 3120-3135. May et al., 1998 PNAS

Liu, H., Wang, J., Liu, J., Liu, T., & Xue, S. (2021). Hydrogen sulfide (H2S) signaling in plant development and stress responses. ABIOTECH, 2(1), 32–63. https://doi.org/10.1007/s42994-021-00035-4

Locato, V., Cimini, S., & De Gara, L. (2017). Glutathione as a key player in plant abiotic stress responses

and tolerance. Glutathione in Plant Growth, Development, and Stress Tolerance, 127–145. https://doi.org/10.1007/978-3-319-66682-2_6

López-Coronado, J. M., Bellés, J. M., Lesage, F., Serrano, R., & Rodrıguez, P. L. (1999). A novel mammalian lithium-sensitive enzyme with a dual enzymatic activity, 3′-phosphoadenosine 5′-phosphate phosphatase and inositol-polyphosphate 1-phosphatase. Journal of Biological Chemistry, 274(23), 16034-16039.

Loudet, O., Saliba-Colombani, V., Camilleri, C., Calenge, F., Gaudon, V., Koprivova, A., North, K. A., Kopriva, S., & Daniel-Vedele, F. (2007). Natural variation for sulfate content in Arabidopsis thaliana is highly controlled by APR2. Nature Genetics, 39(7), 896–900. https://doi.org/10.1038/ng2050

Lu, B., Luo, X., Gong, C., & Bai, J. (2021). Overexpression of γ-glutamylcysteine synthetase gene from Caragana korshinskii decreases stomatal density and enhances drought tolerance. BMC Plant Biology, 21(1), 1–13. https://doi.org/10.1186/s12870-021-03226-9

Lu, S., & Xiao, F. (2024). Small Peptides: Orchestrators of Plant Growth and Developmental Processes. International Journal of Molecular Sciences, 25(14). https://doi.org/10.3390/ijms25147627

Matsubayashi, Y., & Sakagami, Y. (1996). Phytosulfokine, sulfated peptides that induce the proliferation of single mesophyll cells of Asparagus officinalis L. Proceedings of the National Academy of Sciences, 93(15), 7623–7627. https://doi.org/10.1073/pnas.93.15.7623

Matsuzaki, Y., Ogawa-Ohnishi, M., Mori, A., & Matsubayashi, Y. (2010). Secreted peptide signals required for maintenance of root stem cell niche in Arabidopsis. Science, 329(5995), 1065–1067. https://doi.org/10.1126/science.1191132

Mewis, I., Khan, M. A., Glawischnig, E., Schreiner, M., & Ulrichs, C. (2012). Water stress and aphid feeding differentially influence metabolite composition in Arabidopsis thaliana (L.). PLoS One, 7(11), e48661.Munemesa et al., 2013.

Monigatti, F., Gasteiger, E., Bairoch, A., & Jung, E. (2002). The Sulfinator: predicting tyrosine sulfation sites in protein sequences. Bioinformatics, 18(5), 769-770.

Mohamed, D., Vonapartis, E., Corcega, D. Y., & Gazzarrini, S. (2023). ABA guides stomatal proliferation and patterning through the EPF-SPCH signaling pathway in Arabidopsis thaliana. Development (Cambridge), 150(23), 1–13. https://doi.org/10.1242/dev.201258

Moolman, W. J., de Villiers, M., and Strauss, E. (2014) Recent advances in targeting coenzyme A biosynthesis and utilization for antimicrobial drug development. Biochemical Society transactions 42, 1080-1086

Moseler, A., Kruse, I., Maclean, A. E., Pedroletti, L., Franceschetti, M., Wagner, S., ... & Meyer, A. J. (2021). The function of glutaredoxin GRXS15 is required for lipoyl-dependent dehydrogenases in mitochondria. Plant Physiology, 186(3), 1507-1525.

Moseler, A., Wagner, S., & Meyer, A. J. (2024). Protein persulfidation in plants: Mechanisms and functions beyond a simple stress response. Biological Chemistry, 405, 547–566. https://doi.org/10.1515/hsz-2024-0038

Mueller, J. W., & Shafqat, N. (2013). Adenosine-5′-phosphosulfate – a multifaceted modulator of bifunctional 3′-phospho-adenosine-5′-phosphosulfate synthases and related enzymes. The FEBS Journal, 280(12), 3050–3057. https://doi.org/10.1111/febs.12252

Mueller, J. W., Gilligan, L. C., Idkowiak, J., Arlt, W., & Foster, P. A. (2015). The regulation of steroid action by sulfation and desulfation. Endocrine Reviews, 36(5), 526–563. https://doi.org/10.1210/er.2015-1036

Mugford, S. G., Yoshimoto, N., Reichelt, M., Wirtz, M., Hill, L., Mugford, S. T., Nakazato, Y., Noji, M., Takahashi, H., Kramell, R., Gigolashvili, T., Flügge, U. I., Wasternack, C., Gershenzon, J., Hell, R., Saito, K., & Kopriva, S. (2009). Disruption of adenosine-5′-phosphosulfate kinase in Arabidopsis reduces levels of sulfated secondary metabolites. Plant Cell, 21(3), 910–927. https://doi.org/10.1105/tpc.109.065581

Munemasa, S., Hauser, F., Park, J., Waadt, R., Brandt, B., & Schroeder, J. I. (2015). Mechanisms of abscisic acid-mediated control of stomatal aperture. Current Opinion in Plant Biology, 28, 154–162.

Nakayama, T., Shinohara, H., Tanaka, M., Baba, K., Ogawa-Ohnishi, M., & Matsubayashi, Y. (2017). A peptide hormone required for Casparian strip diffusion barrier formation in Arabidopsis roots. Science, 355(6322), 284–286. https://doi.org/10.1126/science.aai9057

Naumann, M., Hubberten, H., Watanabe, M., Hänsch, R., Schöttler, M. A., Hoefgen, R., & Bach, T. J. (2018). Sulfite Reductase Co-suppression in Tobacco Reveals Detoxification Mechanisms and Downstream Responses Comparable to Sulfate Starvation. 9(October), 1–18. https://doi.org/10.3389/fpls.2018.01423

Nowinski, S. M., Van Vranken, J. G., Dove, K. K., & Rutter, J. (2018). Impact of Mitochondrial Fatty Acid Synthesis on Mitochondrial Biogenesis. Current Biology, 28(20), R1212–R1219. https://doi.org/10.1016/j.cub.2018.08.022

Oguz, M. C., Aycan, M., Oguz, E., Poyraz, I., & Yildiz, M. (2022). Drought Stress Tolerance in Plants: Interplay of Molecular, Biochemical and Physiological Responses in Important Development Stages. Physiologia, 2(4), 180–197. https://doi.org/10.3390/physiologia2040015

Orf, G. S., Saer, R. G., Niedzwiedzki, D. M., Zhang, H., McIntosh, C. L., Schultz, J. W., Mirica, L. M., & Blankenship, R. E. (2016). Evidence for a cysteine-mediated mechanism of excitation energy regulation in a photosynthetic antenna complex. Proceedings of the National Academy of Sciences of the United States of America, 113(31), E4486–E4493. https://doi.org/10.1073/pnas.1603330113

Ormrod, D. P., Schmidt, A., & Livingston, N. J. (1997). Effect of UV-B radiation on the shoot dry matter production and stable carbon isotope composition of two Arabidopsis thaliana genotypes. Physiologia Plantarum, 101(3), 497–502. https://doi.org/https://doi.org/10.1111/j.1399-3054.1997.tb01029.x

Pantaleno, R., Scuffi, D., & García-Mata, C. (2021). Hydrogen sulphide as a guard cell network regulator. New Phytologist, 230(2), 451–456. https://doi.org/10.1111/nph.17113

Parisy, V., Poinssot, B., Owsianowski, L., Buchala, A., Glazebrook, J., & Mauch, F. (2007). Identification of PAD2 as a γ-glutamylcysteine synthetase highlights the importance of glutathione in disease resistance of Arabidopsis. The Plant Journal, 49(1), 159-172.Pasternak et al., 2008

Patron, N. J., Durnford, D. G., and Kopriva, S. (2008) Sulfate assimilation in eukaryotes: fusions, relocations and lateral transfers. BMC Evol. Biol. 8, 39

Peng, Z., & Verma, D. P. S. (1995). A rice HAL2-like gene encodes a Ca2+-sensitive 3′(2′), 5′-diphosphonucleoside 3′(2′)-phosphohydrolase and complements yeast met22 and Escherichia coli cysQ mutations. Journal of Biological Chemistry, 270(49), 29105-29110.Quintero et al., 1996;

Phua, S. Y., Yan, D., Chan, K. X., Estavillo, G. M., Nambara, E., & Pogson, B. J. (2018). The arabidopsis SAL1-PAP pathway: A case study for integrating chloroplast retrograde, light and hormonal signaling in modulating plant growth and development? Frontiers in Plant Science, 9(August), 1–8. https://doi.org/10.3389/fpls.2018.01171

Pinheiro, C., & Chaves, M. M. (2011). Photosynthesis and drought: Can we make metabolic connections

from available data? Journal of Experimental Botany, 62(3), 869–882. https://doi.org/10.1093/jxb/erq340

Pornsiriwong, W., Estavillo, G. M., Chan, K. X., Tee, E. E., Ganguly, D., Crisp, P. A., ... & Pogson, B. J. (2017). A chloroplast retrograde signal, 3′-phosphoadenosine 5′-phosphate, acts as a secondary messenger in abscisic acid signaling in stomatal closure and germination. eLife, 6, e23361. https://doi.org/10.7554/eLife.23361

Quintero, F. J., Garciadeblas, B., & Rodríguez-Navarro, A. (1996). The SAL1 gene of Arabidopsis, encoding an enzyme with 3'(2'), 5'-bisphosphate nucleotidase and inositol polyphosphate 1-phosphatase activities, increases salt tolerance in yeast. The Plant Cell, 8(3), 529-537.

Raghavendra, A. S., Gonugunta, V. K., Christmann, A., & Grill, E. (2010). ABA perception and signalling. Trends in Plant Science, 15(7), 395–401.

Rajab, H., Khan, M. S., Malagoli, M., Hell, R., & Wirtz, M. (2019). Sulfate-induced stomata closure requires the canonical ABA signal transduction machinery. Plants, 8(1), 1–13. https://doi.org/10.3390/plants8010021

Raudvere, U., Kolberg, L., Kuzmin, I., Arak, T., Adler, P., Peterson, H., & Vilo, J. (2019). g: Profiler: a web server for functional enrichment analysis and conversions of gene lists (2019 update). Nucleic acids research, 47(W1), W191-W198.

Ravilious, G. E., Nguyen, A., Francois, J. A., & Jez, J. M. (2012). Structural basis and evolution of redox regulation in plant adenosine-5′-phosphosulfate kinase. Proceedings of the National Academy of Sciences of the United States of America, 109(1), 309–314. https://doi.org/10.1073/pnas.1115772108

Ren, Z., Wang, R. Y., Huang, X. Y., & Wang, Y. (2022). Sulfur Compounds in Regulation of Stomatal Movement. Frontiers in Plant Science, 13(March), 2016–2023. https://doi.org/10.3389/fpls.2022.846518

Rens-Domiano, S. S., and Roth, J. A. (1987) Inhibition of M and P phenol sulfotransferase by analogues of 3'-phosphoadenosine-5'-phosphosulfate. Journal of neurochemistry 48, 1411-1415

Ristova, D., & Kopriva, S. (2022). Sulfur signaling and starvation response in Arabidopsis. IScience, 25(5), 104242. https://doi.org/10.1016/j.isci.2022.104242

Robe, K., Gao, F., Bonillo, P., Tissot, N., Gaymard, F., Fourcroy, P., Izquierdo, E., & Dubos, C. (2020).

Sulphur availability modulates Arabidopsis thaliana responses to iron deficiency. PLoS ONE, 15(8 August), 1–23. https://doi.org/10.1371/journal.pone.0237998

Robles, P., Fleury, D., Candela, H., Cnops, G., Alonso-Peral, M. M., Anami, S., ... & Ferrando, A. (2010). The RON1/FRY1/SAL1 gene is required for leaf morphogenesis and venation patterning in Arabidopsis. Plant Physiology, 152(3), 1357–1372. https://doi.org/10.1104/pp.109.149369

Rodríguez, V. M., Chételat, A., Majcherczyk, P., & Farmer, E. E. (2010). Chloroplastic phosphoadenosine phosphosulfate metabolism regulates basal levels of the prohormone jasmonic acid in Arabidopsis leaves. Plant Physiology, 152(3), 1335–1345. https://doi.org/10.1104/pp.109.150474

Romero, L. C., Aroca, M. Á., Laureano-Marín, A. M., Moreno, I., García, I., & Gotor, C. (2014). Cysteine and cysteine-related signaling pathways in arabidopsis thaliana. Molecular Plant, 7(2), 264–276. https://doi.org/10.1093/mp/sst168

Salehin, M., Li, B., Tang, M., Katz, E., Song, L., Ecker, J. R., Kliebenstein, D. J., & Estelle, M. (2019a). Auxin-sensitive Aux/IAA proteins mediate drought tolerance in Arabidopsis by regulating glucosinolate levels. Nature Communications, 10(1). https://doi.org/10.1038/s41467-019-12002-1

Scheerer, U., Haensch, R., Mendel, R. R., Bittner, F., & Kopriva, S. (2010). Sulphur flux through the sulphate assimilation pathway is differently controlled by adenosine 5′-phosphosulphate reductase under stress and in transgenic poplar plants overexpressing gamma-ECS, SO, or APR. Journal of Experimental Botany, 61(3), 609–622. https://doi.org/10.1093/jxb/erp327

Schröder, E., Gebel, L., Eremeev, A. A., Luippold, A. H., & Mueller, J. W. (2012). Human PAPS synthase isoforms are dynamically regulated enzymes with access to nucleus and cytoplasm. PLoS ONE, 7(1), e29559. https://doi.org/10.1371/journal.pone.0029559

Schwarz, G., & Mendel, R. R. (2006). Molybdenum cofactor biosynthesis and molybdenum enzymes. Annual Review of Plant Biology, 57, 623–647. https://doi.org/10.1146/annurev.arplant.57.032905.105437

Scuffi, D., Álvarez, C., Laspina, N., Gotor, C., Lamattina, L., & García-Mata, C. (2014). Hydrogen sulfide generated by L-cysteine desulfhydrase acts upstream of nitric oxide to modulate abscisic acid-dependent stomatal closure. Plant Physiology, 166(4), 2065–2076. https://doi.org/10.1104/pp.114.245373

Seleiman, M. F., Al-Suhaibani, N., Ali, N., Akmal, M., Alotaibi, M., Refay, Y., Dindaroglu, T., Abdul-Wajid, H. H., & Battaglia, M. L. (2021). Drought stress impacts on plants and different approaches to alleviate its adverse effects. Plants, 10(2), 1–25. https://doi.org/10.3390/plants10020259

Shen, J., Zhang, J., Zhou, M., Zhou, H., Cui, B., Gotor, C., Romero, L. C., Fu, L., Yang, J., Foyer, C. H., Pan, Q., Shen, W., & Xie, Y. (2020). Persulfidation-based modification of cysteine desulfhydrase and the NADPH oxidase RBOHD controls guard cell abscisic acid signaling. Plant Cell, 32(4), 1000–1017. https://doi.org/10.1105/tpc.19.00826

Shi, W., Wang, L., Yao, L., Hao, W., Han, C., Wang, W., & Bai, M. (2022). Spatially patterned hydrogen peroxide orchestrates stomatal development in Arabidopsis. Nature Communications, 1–12. https://doi.org/10.1038/s41467-022-32770-7

Shinohara, H., Mori, A., Yasue, N., Sumida, K., & Matsubayashi, Y. (2016). Identification of three LRR-RKs involved in perception of root meristem growth factor in Arabidopsis. Proceedings of the National Academy of Sciences, 113(14), 3897–3902. https://doi.org/10.1073/pnas.1522639113

Skirycz, A., & Inzé, D. More from less: plant growth under limited water, Current Opinion in Biotechnology, Volume 21, Issue 2, 2010, Pages 197-203,ISSN 0958-1669, https://doi.org/10.1016/j.copbio.2010.03.002.Vauclare et.al 2002

Sobrino-Plata, J., Meyssen, D., Cuypers, A., Escobar, C., & Hernández, L. E. (2014). Glutathione is a key antioxidant metabolite to cope with mercury and cadmium stress. Plant and Soil, 377(1–2), 369–381. https://doi.org/10.1007/s11104-013-2006-4

Solmonson, A., & DeBerardinis, R. J. (2018). Lipoic acid metabolism and mitochondrial redox regulation. Journal of Biological Chemistry, 293(20), 7522-7530.

Speiser, P. W., Arlt, W., Auchus, R. J., Baskin, L. S., Conway, G. S., Merke, D. P., ... & White, P. C. (2018). Congenital adrenal hyperplasia due to steroid 21-hydroxylase deficiency: an endocrine society clinical practice guideline. The Journal of Clinical Endocrinology & Metabolism, 103(11), 4043-4088.

Stuible, H. P., Meier, S., Wagner, C., Hannappel, E., & Schweizer, E. (1998). A novel phosphopantetheine: protein transferase activating yeast mitochondrial acyl carrier protein. Journal of Biological Chemistry, 273(35), 22334-22339.

Suliman, M. S. E., Elradi, S. B. M., Zhou, G., Meng, T., Zhu, G., Xu, Y., Nimir, N. E. A., Elsiddig, A. M.

I., Awdelseid, A. H. M., Ali, A. Y. A., Guo, X., & Ahmad, I. (2024). Exogenous glutathione protected wheat seedling from high temperature and water deficit damages. Scientific Reports, 14(1), 1–10. https://doi.org/10.1038/s41598-023-47868-1

Sun, M., & Leyh, T. S. (2006). Channeling in sulfate activating complexes. Biochemistry, 45(37), 11304–11311. https://doi.org/10.1021/bi060421e

Suzuki, N., Miller, G., Morales, J., Shulaev, V., Torres, M. A., & Mittler, R. (2011). Respiratory burst oxidases: the engines of ROS signaling. Current Opinion in Plant Biology, 14(6), 691–699.

Sønderby, I. E., Geu-Flores, F., & Halkier, B. A. (2010). Biosynthesis of glucosinolates - gene discovery and beyond. Trends in Plant Science, 15(5), 283–290. https://doi.org/10.1016/j.tplants.2010.02.005

Takahashi, H., Yamazaki, M., Sasakura, N., Watanabe, A., Leustek, T., Engler, J. D. A., ... & Saito, K. (1997). Regulation of sulfur assimilation in higher plants: a sulfate transporter induced in sulfate-starved roots plays a central role in Arabidopsis thaliana. Proceedings of the National Academy of Sciences, 94(20), 11102-11107.

Takahashi, H., Kopriva, S., Giordano, M., Saito, K., & Hell, R. (2011). Sulfur assimilation in photosynthetic organisms: molecular functions and regulations of transporters and assimilatory enzymes. Annual Review of Plant Biology, 62, 157–184. https://doi.org/10.1146/annurev-arplant-042110-103921

Takahashi, H., Marsolais, F., Cuypers, A., & Kopriva, S. (2023). Sulfur metabolism: actions for plant resilience and environmental adaptation. Journal of Experimental Botany, 74(11), 3271–3275. https://doi.org/10.1093/jxb/erad164

Tardieu, F., Simonneau, T., & Muller, B. (2018). The physiological basis of drought tolerance in crop plants: a scenario-dependent probabilistic approach. Annual review of plant biology, 69(1), 733-759.

Taylor, R. W., Schaefer, A. M., Barron, M. J., McFarland, R., & Turnbull, D. M. (2004). The diagnosis of mitochondrial muscle disease. Neuromuscular Disorders, 14(4), 237-245.

Telman, W., & Dietz, K. J. (2019). Thiol redox-regulation for efficient adjustment of sulfur metabolism in acclimation to abiotic stress. Journal of Experimental Botany, 70(16), 4223–4236. https://doi.org/10.1093/jxb/erz118

Toledano, E., Ogryzko, V., Danchin, A., Ladant, D., & Mechold, U. (2012). 3′-5′ Phosphoadenosine phosphate is an inhibitor of PARP-1 and a potential mediator of the lithium-dependent inhibition of

PARP-1 in vivo. Biochemical Journal, 443(2), 485–490. https://doi.org/10.1042/BJ20111057

Ullah, A., Sun, H., Yang, X., & Zhang, X. (2017). Drought coping strategies in cotton: increased crop per drop. Plant Biotechnology Journal, 15(3), 271–284. https://doi.org/10.1111/pbi.12688

Urano, K., Maruyama, K., Ogata, Y., Morishita, Y., Takeda, M., Sakurai, N., Suzuki, H., Saito, K., Shibata, D., Kobayashi, M., & others. (2009). Characterization of the ABA-regulated global responses to dehydration in Arabidopsis by metabolomics. The Plant Journal, 57(6), 1065–1078.

Van Hoewyk, D., Takahashi, H., Inoue, E., Hess, A., Tamaoki, M., & Pilon-Smits, E. A. (2008). Transcriptome analyses give insights into selenium-stress responses and selenium tolerance mechanisms in Arabidopsis. Physiologia plantarum, 132(2), 236-253.

Varin, L., DeLuca, V., Ibrahim, R. K., & Brisson, N. (1992). Molecular characterization of two plant flavonol sulfotransferases. Proceedings of the National Academy of Sciences, 89(4), 1286–1290. https://doi.org/10.1073/pnas.89.4.1286

Vauclare, P., Kopriva, S., Fell, D., Suter, M., Sticher, L., Von Ballmoos, P., Krähenbühl, U., Op Den Camp, R., & Brunold, C. (2002). Flux control of sulphate assimilation in Arabidopsis thaliana: Adenosine 5′-phosphosulphate reductase is more susceptible than ATP sulphurylase to negative control by thiols. Plant Journal, 31(6), 729–740. https://doi.org/10.1046/j.1365-313X.2002.01391.x

Voll, L. M., Jamai, A., Renné, P., Voll, H., McClung, C. R., & Weber, A. P. M. (2006). The photorespiratory arabidopsis shm1 mutant is deficient in SHM1. Plant Physiology, 140(1), 59–66. https://doi.org/10.1104/pp.105.071399

Von Caemmerer, S., Ghannoum, O., Pengelly, J. J. L., & Cousins, A. B. (2014). Carbon isotope discrimination as a tool to explore C4 photosynthesis. Journal of Experimental Botany, 65(13), 3459–3470. https://doi.org/10.1093/jxb/eru127

Wilson, P. B., Estavillo, G. M., Field, K. J., Pornsiriwong, W., Carroll, A. J., Howell, K. A., Woo, N. S., Lake, J. A., Smith, S. M., Harvey Millar, A., Von Caemmerer, S., & Pogson, B. J. (2009). The nucleotidase/phosphatase SAL1 is a negative regulator of drought tolerance in Arabidopsis. Plant Journal, 58(2), 299–317. https://doi.org/10.1111/j.1365-313X.2008.03780.x

Wirtz, M., & Hell, R. (2006). Functional analysis of the cysteine synthase protein complex from plants: structural, biochemical and regulatory properties. Journal of plant physiology, 163(3), 273-286.

Wolff, J. N., Ladoukakis, E. D., Enríquez, J. A., & Dowling, D. K. (2014). Mitonuclear interactions:

evolutionary consequences over multiple biological scales. Philosophical Transactions of the Royal Society B: Biological Sciences, 369(1646), 20130443.

Xia, Y., Jiang, S., Wu, W., Du, K., & Kang, X. (2024). MYC2 regulates stomatal density and water use efficiency via targeting EPF2/EPFL4/EPFL9 in poplar. New Phytologist, 241(6), 2506–2522. https://doi.org/10.1111/nph.19531

Yamaguchi-Shinozaki, K., & Shinozaki, K. (2006). Transcriptional regulatory networks in cellular responses and tolerance to dehydration and cold stresses. Annual Review of Plant Biology, 57, 781–803.

Yang, X., Lu, M., Wang, Y., Wang, Y., Liu, Z., & Chen, S. (2021). Response mechanism of plants to drought stress. Horticulturae, 7(3). https://doi.org/10.3390/horticulturae7030050

Yatusevich, R., Mugford, S. G., Matthewman, C. A., Gigolashvili, T., Frerigmann, H., Delaney, S., ... & Kopriva, S. (2010). Genes of primary sulfate assimilation are part of the glucosinolate biosynthetic network in Arabidopsis thaliana. The Plant Journal, 62(1), 1–11. https://doi.org/10.1111/j.1365-313X.2009.04118.x

Yoshida, T., & Fernie, A. R. (2023). Reactive oxygen species as key regulators of plant development and metabolism. Journal of Experimental Botany, 74(5), 1251–1261.

Yu, H., Du, X., Zhang, F., Zhang, F., Hu, Y., Liu, S., ... & Liu, D. (2012). A mutation in the E2 subunit of the mitochondrial pyruvate dehydrogenase complex in Arabidopsis reduces plant organ size and enhances the accumulation of amino acids and intermediate products of the TCA cycle. Planta, 236, 387-399.

Zallot, R., Agrimi, G., Lerma-Ortiz, C., Teresinski, H. J., Frelin, O., Ellens, K. W., ... & Hanson, A. D. (2013). Identification of mitochondrial coenzyme a transporters from maize and Arabidopsis. Plant physiology, 162(2), 581-588

Zhang, J., Aroca, A., Hervás, M., Navarro, J. A., Moreno, I., Xie, Y., Romero, L. C., & Gotor, C. (2024). Analysis of sulfide signaling in rice highlights specific drought responses. *Journal of Experimental Botany*, *75*(16), 5130–5145. https://doi.org/10.1093/jxb/erae249

Zhao, C., Wang, Y., Chan, K. X., Marchant, D. B., Franks, P. J., Randall, D., ... & Pogson, B. J. (2019). Evolution of chloroplast retrograde signaling facilitates green plant adaptation to land. Proceedings of the National Academy of Sciences, 116(11), 5015–5020.

https://doi.org/10.1073/pnas.1812092116

Zhu, J.-K. (2016). Abiotic stress signaling and responses in plants. Cell, 167(2), 313–324.

List of Figures:

List of Tables:

List of Supplementary Figures:

SUPPLEMENTARY FIGURES

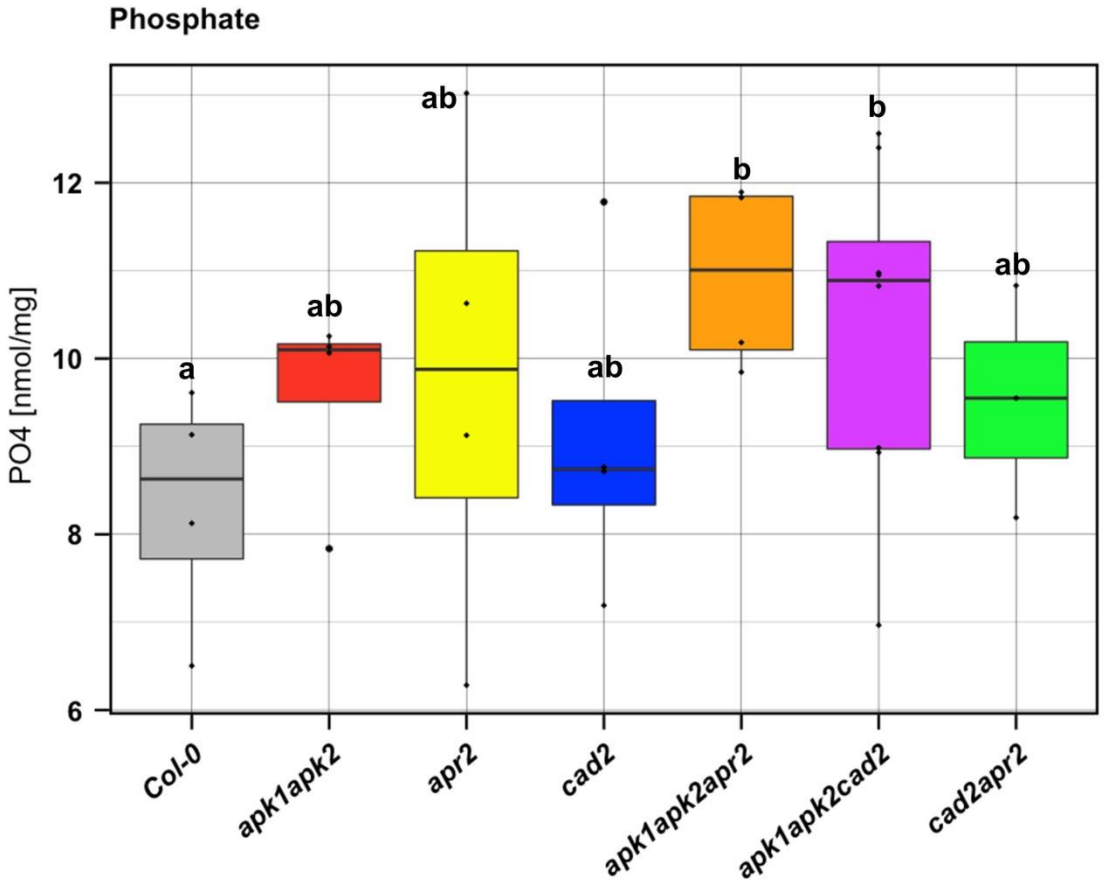

Supplementary Figure.1: Measurement of phosphate in the set of primary and secondary sulfur metabolism mutant seedlings.

Whole seedlings grown on ½ MS media for 2.5 weeks were analyzed**.** The collected data is fully shown as box plots, each point representing a sample. 4 biological replicate have been used. The significance analyses between each genotype were calculated with Student's t-test and different letters represent values that are significantly different ($P < 0.05$).

Supplementary Figure. 2: High light chamber drought experiment.
Col-0 *apk1apk2, cad2* and *apk1apk2cad2* 4-week-old greenhouse grown plants were placed in a high light chamber for 5 days under high temperatures (30°C) and high light (600 $\mu Em^{-2}s^{-1}$)

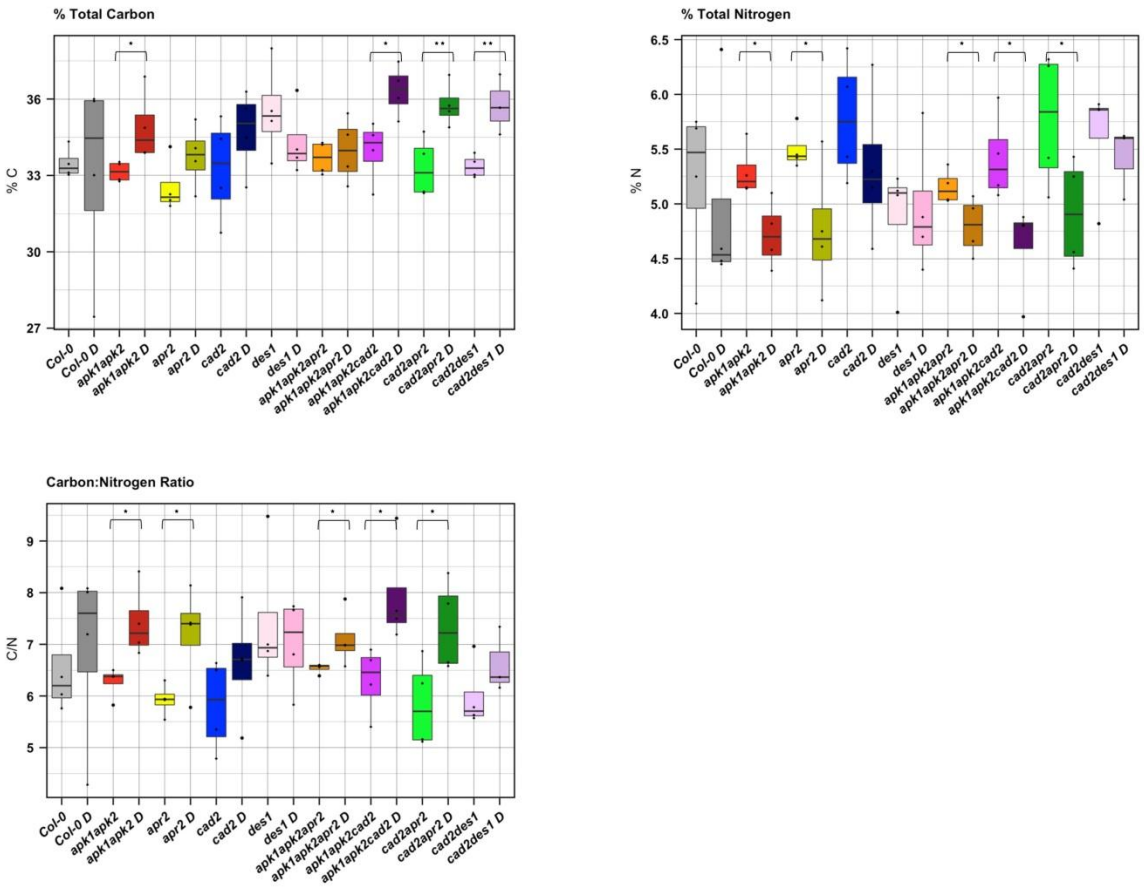

Supplementary Figure. 3: Carbon and Nitrogen values of sulfur metabolism mutants.
5 weeks old plants grown in growth chamber under short day conditions were subjected to water withdrawal for 3 weeks. Samples of fully expanded leaves were collected and fresh leaves were freeze dried and 1mg dry sample packed into tin foils send for the analysis. The samples were analyzed with EA-IRMS done by Philipp Westhoff. The data is shown as box plots, each point representing one of 4 biological replicates. Asterisks mark values significantly different from their respective control treatment (*:$P \leq 0.05$,**:$P \leq 0.01$,***:$P \leq 0.001$ Student t-test).

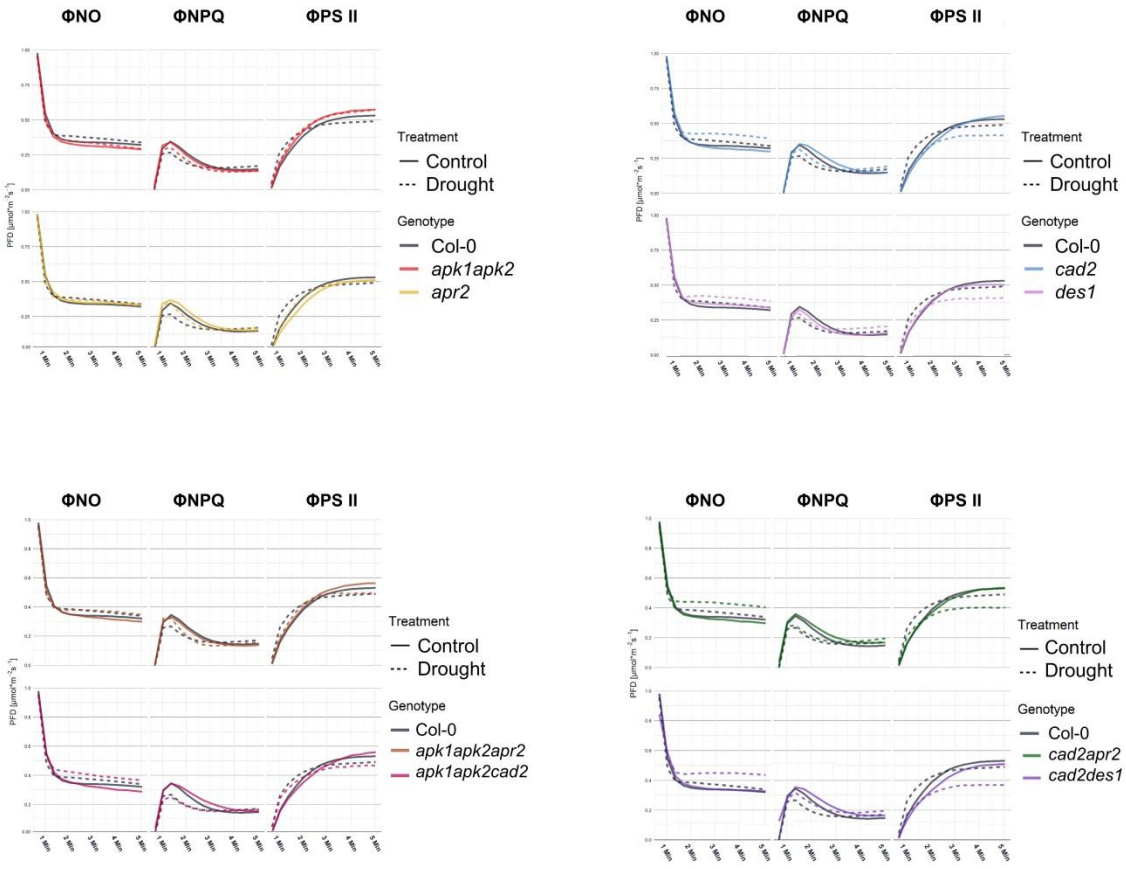

Supplementary Figure. 4 :PSII efficiency non photochemical quenching (NPQ) and other quenching(NO) measurement of sulfur metabolism mutants under control and drought conditions

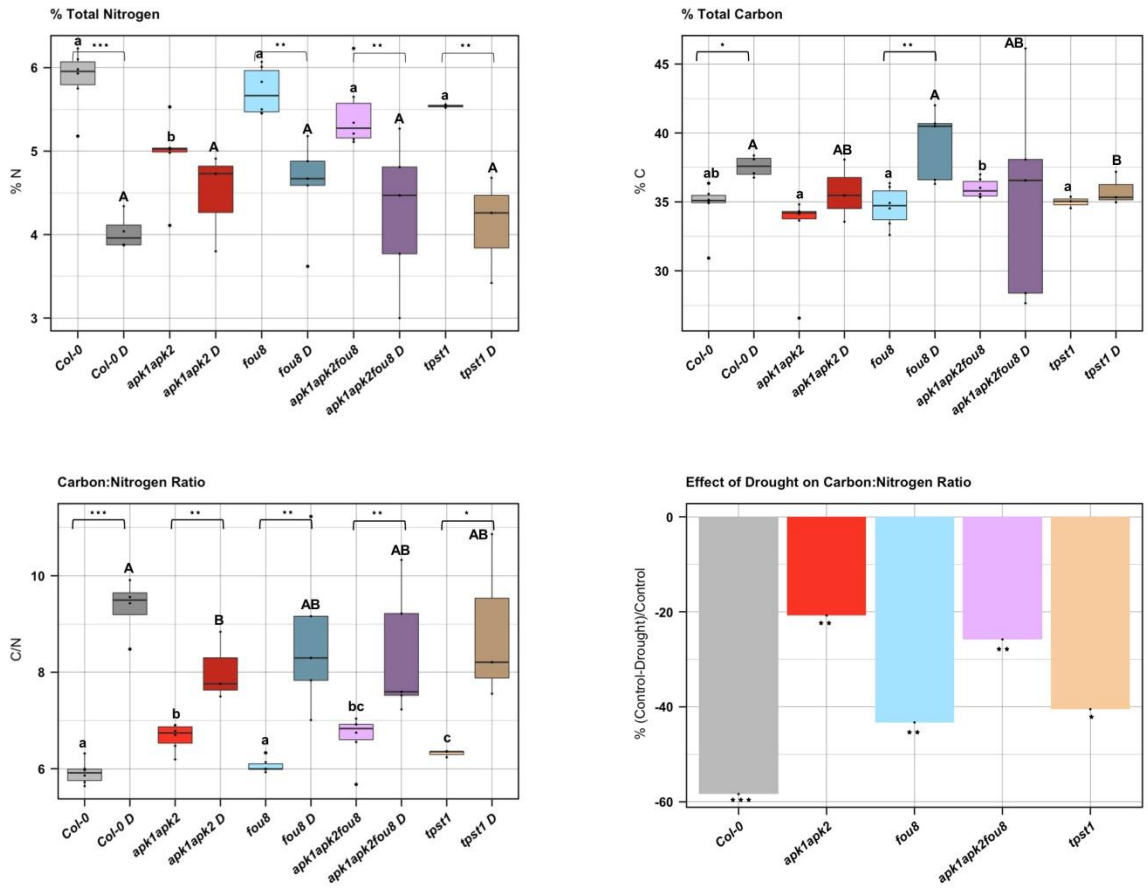

Supplementary Figure. 5:Carbon and Nitrogen measurements in sulfation pathway mutants

5 weeks old plants grown in growth chamber under short day conditions were subjected to water withdrawal for 2 weeks. Samples of fully expanded leaves were collected and fresh leaves were freeze dried and 1mg dry sample packed into tin foils send for the analysis. The samples were analyzed with EA-IRMS done by Philipp Westhoff. The data is shown as box plots, each point representing one of 4 biological replicates. Asterisks mark values significantly different from their respective control treatment (*:$P \leq 0.05$,**:$P \leq 0.01$,***:$P \leq 0.001$ Student t-test).

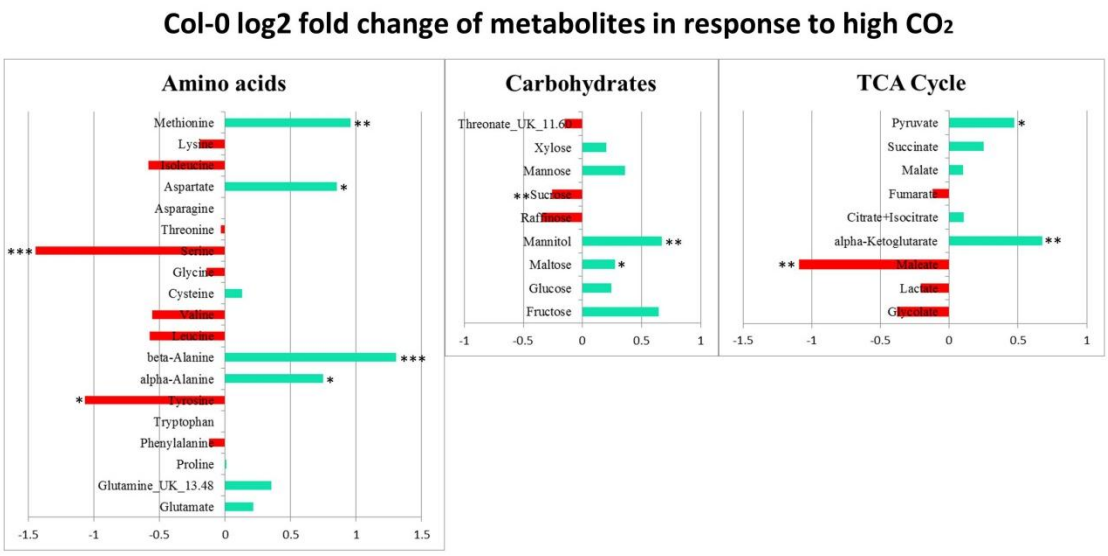

Supplementary Figure. 6: Change of metabolites in response to switch in high CO2 in wild type.

Plants were grown for 5 weeks in high CO_2 and either transferred to ambient air for 3 days or kept further in high CO_2. Metabolites in leaves were analyzed by GC-MS. Shown are fold change differences to WT at the given condition. Ambient air (AC):390 ppm CO_2 in air, High CO_2 (HC): 3,000 ppm CO_2 in air. Asterisks mark values significantly different from WT *:$P \leq 0.05$,**:$P \leq 0.01$,***:$P \leq 0.001$ t- test.

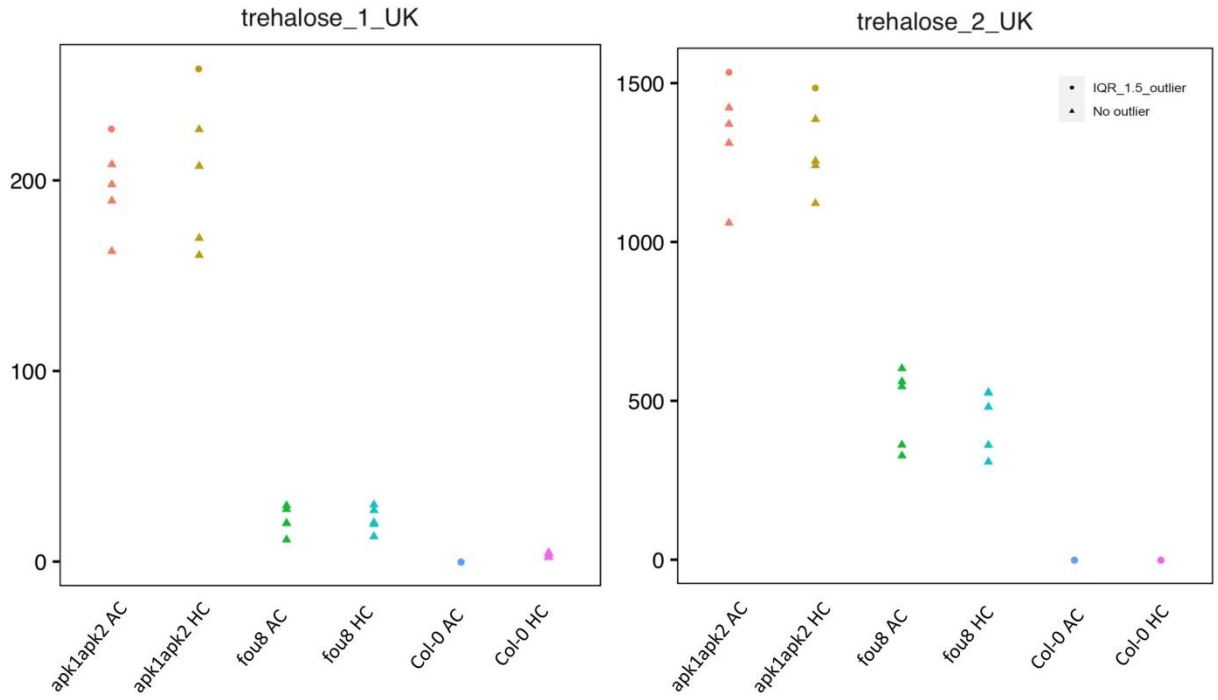

Supplementary Figure. 7: Change of Trehalose in response to high CO_2

Plants were grown for 5 weeks in high CO_2 and either transferred to ambient air for 3 days or kept further in high CO_2. Metabolites in leaves were analyzed by GC-MS. Response rates of the metabolites are shown on Y axis. Each sample taken into calculations indicated with triangles, while outliers (calculated 1.5.Interquartile Range (IQR_1.5)) are indicated with circles. Ambient air (AC):390 ppm CO_2 in air, High CO_2 (HC): 3,000 ppm CO_2 in air.

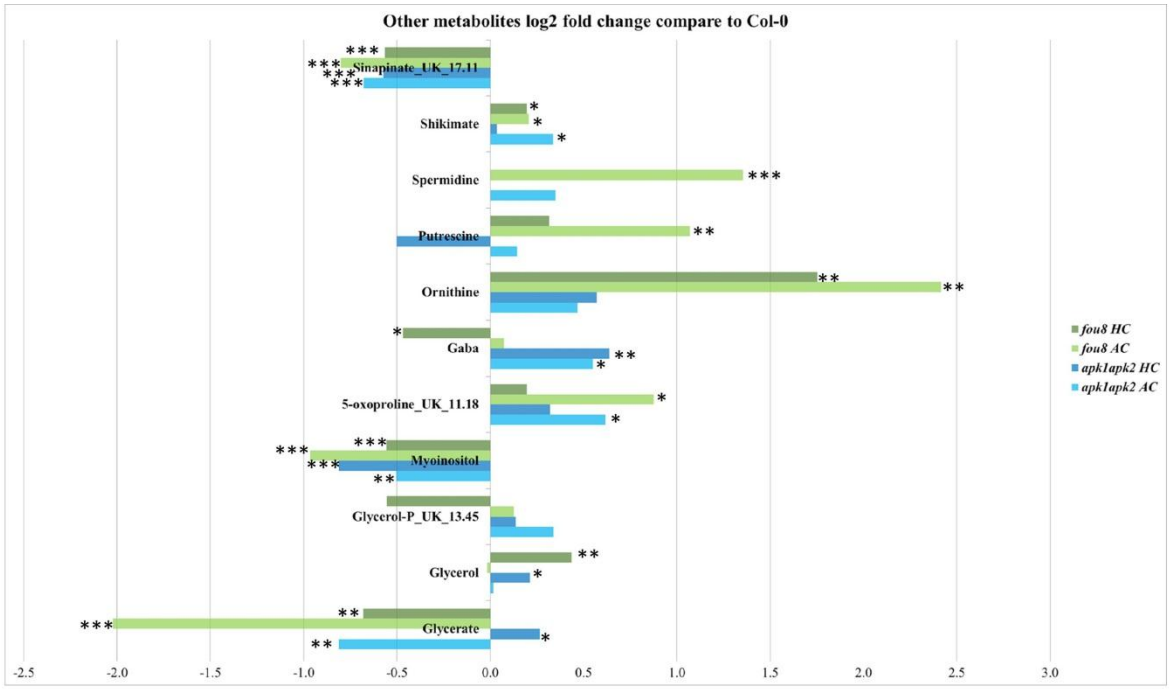

Supplementary Figure. 8: Response of rest of the metabolites measured in *fou8* and *apk1apk2* mutants.

Plants were grown for 5 weeks in high CO_2 and either transferred to ambient air for 3 days or kept further in high CO_2). Metabolites in leaves were analyzed by GC-MS. Shown are fold change differences to WT at the given condition. Ambient air (AC):390 ppm CO_2 in air, High CO_2 (HC): 3,000 ppm CO_2 in air. Asterisks mark values significantly different from WT *:$P \leq 0.05$,**:$P \leq 0.01$,***:$P \leq 0.001$ t- test.

Supplementary Figure. 9: Gene set enrichment analysis of chloroplast DEGs of sal1-8 mutant down regulated genes. A

Venn diagram of *sal1-8* DEG list with genes compared with complete list of genes located in chloroplast .RNA-Seq dataset (Crisp et al., 2017) B. Gene ontology analysis with g:profiler, analysis of down regulated genes in *sal1-8* mutant in chloroplast (GO: Gene Ontology BP: Biological Process, CC: Cellular component.)

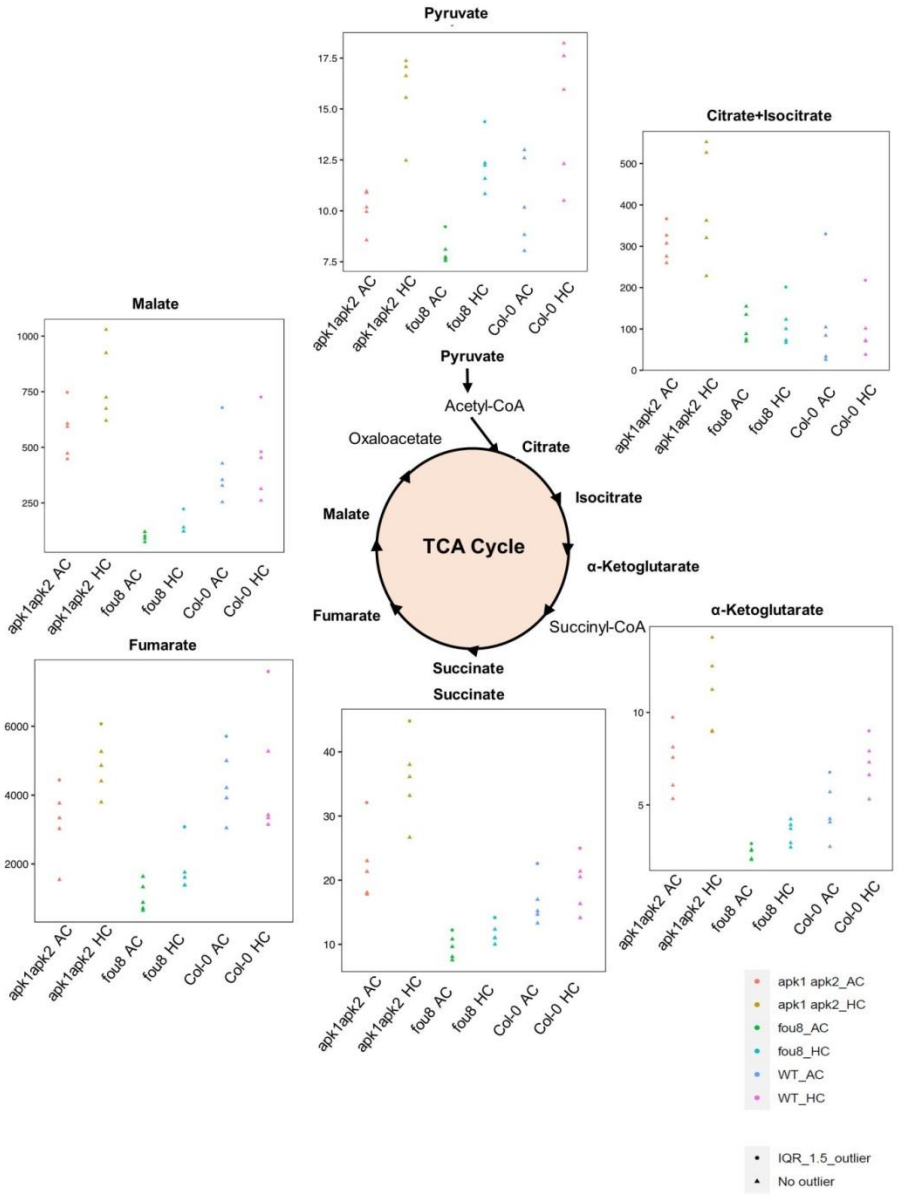

Supplementary Figure. 10: TCA cycle intermediates in wild type Col-0 and mutants *fou8* and *apk1apk2*.

Plants were grown for 5 weeks in high CO_2 and either transferred to ambient air for 3 days or kept further in high CO_2. Metabolites in leaves were analyzed by GC-MS. Response rates of the metabolites are shown on Y axis. Each sample taken into calculations indicated with triangles, while outliers (calculated 1.5.Interquartile Range (IQR_1.5)) are indicated with circles. Ambient air (AC):390 ppm CO_2 in air, High CO_2 (HC): 3,000 ppm CO_2 in air.

SUPPLEMENTARY TABLES

Supplementary Table.1: Statistical analysis of physiological and metabolomics results. Different letters indicate significant difference of $P \leq 0.05$. The effect of the treatment on each genotype indicated with asterisk *:$P \leq 0.05$,**:$P \leq 0.01$,***:$P \leq 0.001$ t- test.

Genotype	High light drought	Rosette area control	Water Content control	Water Content drought	Water Content treatment
Col-0	a	abc	a	abcd	*
apk1apk2	b	d	b	abc	n.s
apr2	cd	ae	bcde	d	n.s
cad2	c	b	acdf	ac	*
des1	d	c	af	ab	**
apk1apk2apr2	e	d	bc	cd	n.s
apk1apk2cad2	e	d	e	b	n.s
cad2apr2	ac	e	ad	abcd	n.s
cad2des1	c	e	bcf	abcd	n.s

Genotype	$\delta^{13}C$ control	$\delta^{13}C$ drought	$\delta^{13}C$ treatment	GSH control	GSH drought	GSH treatment
Col-0	abcde	abc	n.s	ab	a	*
apk1apk2	a	ab	n.s	a	a	**
apr2	abcd	a	**	ab	a	*
cad2	bde	abc	n.s	abc	a	n.s
des1	bc	bc	*	a	b	n.s
apk1apk2apr2	ac	bc	n.s	bc	a	n.s
apk1apk2cad2	a	ab	n.s	abc	ab	n.s
cad2apr2	e	bc	***	c	ab	n.s
cad2des1	de	c	n.s	c	ab	n.s

Genotype	Cysteine control	Cysteine drought	Cysteine Treatment	PAP control	PAP drought	PAP treatment
Col-0	a	abc	*	ab	a	n.s
apk1apk2	ab	abc	n.s	cd	ab	n.s
apr2	ac	a	**	e	ab	*
cad2	a	ab	*	cf	ab	n.s
des1	bd	de	**	acdf	ab	n.s
apk1apk2apr2	ab	cd	**	af	b	n.s
apk1apk2cad2	cd	e	*	b	ab	n.s
cad2apr2	ab	abc	*	cd	a	**
cad2des1	abcd	bc	*	d	ab	n.s

Genotype	Stomata density	PSII control	PSII drought	PSII treatment
Col-0	ab	bcd	a	n.s
apk1apk2	c	a	c	n.s
apr2	ade	bc	ac	n.s
cad2	d	abcd	bd	**
des1	de	c	bd	***
apk1apk2apr2	ce	ad	a	*
apk1apk2cad2	c	ad	ab	***
cad2apr2	b	abcd	bd	***
cad2des1	c	bc	d	***

Supplementary Table.2: Statistical analysis of physiological and metabolomics result in sulfation mutants. Different letters indicate significant difference of $P \leq 0.05$. The effect of the treatment on each genotype indicated with asterisk *:$P \leq 0.05$,**:$P \leq 0.01$,***:$P \leq 0.001$ t- test.

Genotype	Stomata density	PSII control	NPQ control
Col-0	a	a	ab
apk1apk2	b	a	a
fou8	b	a	b
apk1apk2fou8	a	a	ab
tpst1	b	a	ab

Supplemantary Table. 3: GC-MS metabolomics analysis of some of the metabolites. Average retention peak areas of all the genotypes under both conditions and standard deviation of the data is calculated for cysteine, glucose, trehalose_1 and trehalose_2.

Cysteine	Average		Stdev
WT AC	2.33	±	0.23
WT HC	2.64	±	0.90
apk1apk2 AC	23.75	±	6.44
apk1apk2 HC	27.46	±	5.90
fou8 AC	3.58	±	0.79
fou8 HC	2.21	±	0.49

Glucose	Average		Stdev
WT AC	1087.23	±	396.91
WT HC	1458.63	±	737.19
apk1apk2 AC	183.97	±	35.33
apk1apk2 HC	559.90	±	49.03
fou8 AC	44.70	±	8.25
fou8 HC	134.81	±	40.86

trehalose_1	Average		Stdev
WT AC	n.d	±	
WT HC	3.23	±	1.10
apk1apk2 AC	189.58	±	19.46
apk1apk2 HC	191.15	±	31.17
fou8 AC	21.71	±	7.10
fou8 HC	21.99	±	6.55

trehalose_2	Average		Stdev
WT AC	n.d	±	
WT HC	n.d	±	
apk1apk2 AC	1291.12	±	160.64
apk1apk2 HC	1250.85	±	108.18
fou8 AC	479.22	±	125.49
fou8 HC	440.29	±	100.18

Supplemantary Table.4: Statistical analysis of high CO_2 experiment metabolites with GC-MS. Blue indicates one* purple indicates two** red indicates*** asterisk for *:P ≤ 0.05,**:P ≤ 0.01,***:P ≤ 0.001 t- test .

5-oxoproline	***WT AC vs HC***		**WT AC**		**WT HC**
WT AC vs HC	0.010285799	***apk1apk2 AC***	0.013831489	***apk1apk2 HC***	0.077793877
		fou8 AC	0.017208267	***fou8 HC***	0.181047893
alpha-Alanine	**WT AC vs HC**		**WT AC**		**WT HC**
WT AC vs HC	0.027727593	***apk1apk2 AC***	0.462083583	***apk1apk2 HC***	0.022094231
		fou8 AC	0.015375483	***fou8 HC***	0.265361809
alpha-Ketoglutarate	**WT AC vs HC**		**WT AC**		**WT HC**
WT AC vs HC	0.00984109	***apk1apk2 AC***	0.013470253	***apk1apk2 HC***	0.004586327
		fou8 AC	0.011553271	***fou8 HC***	0.000429679
aminomalonate	**WT AC vs HC**		**WT AC**		**WT HC**
WT AC vs HC	0.485852922	***apk1apk2 AC***	0.255813244	***apk1apk2 HC***	0.283076364
		fou8 AC	-	***fou8 HC***	-
Asparagine	**WT AC vs HC**		**WT AC**		**WT HC**
WT AC vs HC	0.392713324	***apk1apk2 AC***	0.012826012	***apk1apk2 HC***	0.020642533
		fou8 AC	0.000607723	***fou8 HC***	0.048638051
Aspartate	**WT AC vs HC**		**WT AC**		**WT HC**
WT AC vs HC	0.028332584	***apk1apk2 AC***	0.013468294	***apk1apk2 HC***	0.340979205
		fou8 AC	0.034936686	***fou8 HC***	0.216032696
beta-Alanine	**WT AC vs HC**		**WT AC**		**WT HC**
WT AC vs HC	0.000860747	***apk1apk2 AC***	0.094953006	***apk1apk2 HC***	0.022282866
		fou8 AC	0.000472991	***fou8 HC***	0.140796284
Citrate+Isocitrate	**WT AC vs HC**		**WT AC**		**WT HC**
WT AC vs HC	0.360158402	***apk1apk2 AC***	3.98185E-05	***apk1apk2 HC***	0.001227731
		fou8 AC	0.0691715	***fou8 HC***	0.156165572

Cysteine	**WT AC vs HC**		**WT AC**		**WT HC**
WT AC vs HC	0.264309051	***apk1apk2 AC***	0.000158722	***apk1apk2 HC***	8.15648E-05
		fou8 AC	0.011561863	***fou8 HC***	0.217577657
DMPA	**WT AC vs HC**		**WT AC**		**WT HC**
WT AC vs HC	0.32822669	***apk1apk2 AC***	0.262761525	***apk1apk2 HC***	0.11452813
		fou8 AC	0.458760488	***fou8 HC***	0.136877093
Fructose	**WT AC vs HC**		**WT AC**		**WT HC**
WT AC vs HC	0.127290993	***apk1apk2 AC***	0.001242062	***apk1apk2 HC***	0.132817722
		fou8 AC	1.97139E-05	***fou8 HC***	0.025942667
Fumarate	**WT AC vs HC**		**WT AC**		**WT HC**
WT AC vs HC	0.356031871	***apk1apk2 AC***	0.061597026	***apk1apk2 HC***	0.114745582
		fou8 AC	8.58287E-05	***fou8 HC***	0.002085018
Gaba	**WT AC vs HC**		**WT AC**		**WT HC**
WT AC vs HC	0.023908774	***apk1apk2 AC***	0.013061265	***apk1apk2 HC***	0.003868493
		fou8 AC	0.298340402	***fou8 HC***	0.020447647
Glucose	**WT AC vs HC**		**WT AC**		**WT HC**
WT AC vs HC	0.204568772	***apk1apk2 AC***	0.001980177	***apk1apk2 HC***	0.025481186
		fou8 AC	0.00027679	***fou8 HC***	0.002342542
Glutamate	**WT AC vs HC**		**WT AC**		**WT HC**
WT AC vs HC	0.105221674	***apk1apk2 AC***	0.001637624	***apk1apk2 HC***	0.005885066
		fou8 AC	0.057683834	***fou8 HC***	0.43683139
Glutamine	**WT AC vs HC**		**WT AC**		**WT HC**
WT AC vs HC	0.122251973	***apk1apk2 AC***	0.0306007	***apk1apk2 HC***	0.0613814
		fou8 AC	0.014122597	***fou8 HC***	0.152051996
Glycerate	**WT AC vs HC**		**WT AC**		**WT HC**
WT AC vs HC	1.7776E-05	***apk1apk2 AC***	0.001248123	***apk1apk2 HC***	0.0247876
		fou8 AC	4.19981E-06	***fou8 HC***	0.001530576

Glycerol	**WT AC vs HC**		**WT AC**		**WT HC**
WT AC vs HC	0.069311391	***apk1apk2 AC***	0.378231626	***apk1apk2 HC***	0.018857756
		fou8 AC	0.445502646	***fou8 HC***	0.003919779
Glycerol-P	**WT AC vs HC**		**WT AC**		**WT HC**
WT AC vs HC	0.283014308	***apk1apk2 AC***	0.088841003	***apk1apk2 HC***	0.311510858
		fou8 AC	0.255535895	***fou8 HC***	0.108501652
Glycine	**WT AC vs HC**		**WT AC**		**WT HC**
WT AC vs HC	0.471175895	***apk1apk2 AC***	0.39915895	***apk1apk2 HC***	0.31224932
		fou8 AC	0.305895296	***fou8 HC***	0.285126808
Glycolate	**WT AC vs HC**		**WT AC**		**WT HC**
WT AC vs HC	0.076155377	***apk1apk2 AC***	0.43935099	***apk1apk2 HC***	0.325207754
		fou8 AC	0.026337264	***fou8 HC***	0.161457264
Isoleucine	**WT AC vs HC**		**WT AC**		**WT HC**
WT AC vs HC	0.09666693	***apk1apk2 AC***	0.120692265	***apk1apk2 HC***	0.120772018
		fou8 AC	0.053790313	***fou8 HC***	0.218314825
Lactate	**WT AC vs HC**		**WT AC**		**WT HC**
WT AC vs HC	0.176286332	***apk1apk2 AC***	0.215556105	***apk1apk2 HC***	0.347337877
		fou8 AC	0.48119621	***fou8 HC***	0.052915096
Leucine	**WT AC vs HC**		**WT AC**		**WT HC**
WT AC vs HC	0.114187468	***apk1apk2 AC***	0.192140104	***apk1apk2 HC***	0.017243153
		fou8 AC	0.003724495	***fou8 HC***	0.123887389
Lysine	**WT AC vs HC**		**WT AC**		**WT HC**
WT AC vs HC	0.124548537	***apk1apk2 AC***	0.052233098	***apk1apk2 HC***	0.47089766
		fou8 AC	0.001210358	***fou8 HC***	0.084736893
Malate	**WT AC vs HC**		**WT AC**		**WT HC**
WT AC vs HC	0.296541965	***apk1apk2 AC***	0.006526022	***apk1apk2 HC***	0.002085025
		fou8 AC	8.49338E-05	***fou8 HC***	0.001696936

Maleate	**WT AC vs HC**		**WT AC**		**WT HC**
WT AC vs HC	0.001795624	***apk1apk2 AC***	0.002692728	***apk1apk2 HC***	0.005797132
		fou8 AC	4.15388E-05	***fou8 HC***	0.078551777
Maltose	**WT AC vs HC**		**WT AC**		**WT HC**
WT AC vs HC	0.043698019	***apk1apk2 AC***	0.026435562	***apk1apk2 HC***	0.033923787
		fou8 AC	0.434140983	***fou8 HC***	0.10205262
Mannitol	**WT AC vs HC**		**WT AC**		**WT HC**
WT AC vs HC	0.00131055	***apk1apk2 AC***	4.99353E-05	***apk1apk2 HC***	0.00125663
		fou8 AC	0.027278825	***fou8 HC***	0.140607988
Mannose	**WT AC vs HC**		**WT AC**		**WT HC**
WT AC vs HC	0.117373049	***apk1apk2 AC***	0.034997397	***apk1apk2 HC***	0.039843316
		fou8 AC	0.000884737	***fou8 HC***	0.011564052
Methionine	**WT AC vs HC**		**WT AC**		**WT HC**
WT AC vs HC	0.003302643	***apk1apk2 AC***	0.004112359	***apk1apk2 HC***	0.072176313
		fou8 AC	0.002801754	***fou8 HC***	0.122109006
Myoinositol	**WT AC vs HC**		**WT AC**		**WT HC**
WT AC vs HC	0.004408982	***apk1apk2 AC***	0.007899721	***apk1apk2 HC***	2.16727E-05
		fou8 AC	1.11231E-05	***fou8 HC***	0.000847179
Ornithine	**WT AC vs HC**		**WT AC**		**WT HC**
WT AC vs HC	0.093630699	***apk1apk2 AC***	0.053709388	***apk1apk2 HC***	0.078407998
		fou8 AC	0.001745091	***fou8 HC***	0.005734199
Phenylalanine	**WT AC vs HC**		**WT AC**		**WT HC**
WT AC vs HC	0.259919648	***apk1apk2 AC***	0.023816512	***apk1apk2 HC***	0.15613859
		fou8 AC	0.03013975	***fou8 HC***	0.026710098
Proline	**WT AC vs HC**		**WT AC**		**WT HC**
WT AC vs HC	0.276889909	***apk1apk2 AC***	0.103956136	***apk1apk2 HC***	0.059256299
		fou8 AC	0.05644232	***fou8 HC***	0.076189011

Putrescine	**WT AC vs HC**		**WT AC**		**WT HC**
WT AC vs HC	0.013503662	***apk1apk2 AC***	0.197501129	***apk1apk2 HC***	0.067972437
		fou8 AC	0.0049328	***fou8 HC***	0.109649778
Pyruvate	**WT AC vs HC**		**WT AC**		**WT HC**
WT AC vs HC	0.020356876	***apk1apk2 AC***	0.355751985	***apk1apk2 HC***	0.310801234
		fou8 AC	0.021895069	***fou8 HC***	0.055440433
Raffinose	**WT AC vs HC**		**WT AC**		**WT HC**
WT AC vs HC	0.326756589	***apk1apk2 AC***	0.380809223	***apk1apk2 HC***	0.197618902
		fou8 AC	0.006572735	***fou8 HC***	0.026157405
Serine	**WT AC vs HC**		**WT AC**		**WT HC**
WT AC vs HC	0.000375674	***apk1apk2 AC***	0.039822626	***apk1apk2 HC***	0.181857836
		fou8 AC	0.214680758	***fou8 HC***	0.020299172
Shikimate	**WT AC vs HC**		**WT AC**		**WT HC**
WT AC vs HC	0.004558453	***apk1apk2 AC***	0.026880634	***apk1apk2 HC***	0.332021318
		fou8 AC	0.040077732	***fou8 HC***	0.041586631
Sinapinate	**WT AC vs HC**		**WT AC**		**WT HC**
WT AC vs HC	0.007894581	***apk1apk2 AC***	0.00074732	***apk1apk2 HC***	3.34794E-05
		fou8 AC	5.41629E-05	***fou8 HC***	8.77014E-05
Spermidine	**WT AC vs HC**		**WT AC**		**WT HC**
WT AC vs HC	-	***apk1apk2 AC***	0.059679	***apk1apk2 HC***	-
		fou8 AC	0.000233	***fou8 HC***	-
Succinate	**WT AC vs HC**		**WT AC**		**WT HC**
WT AC vs HC	0.07820471	***apk1apk2 AC***	0.007410565	***apk1apk2 HC***	0.001104613
		fou8 AC	0.000659745	***fou8 HC***	0.003925592
Sucrose	**WT AC vs HC**		**WT AC**		**WT HC**
WT AC vs HC	0.008452602	***apk1apk2 AC***	0.411136213	***apk1apk2 HC***	0.002560173
		fou8 AC	1.80427E-05	***fou8 HC***	6.25641E-05

Threonate	**WT AC vs HC**		**WT AC**		**WT HC**
WT AC vs HC	0.30240223	***apk1apk2 AC***	0.082657418	***apk1apk2 HC***	0.004705078
		fou8 AC	0.416385086	***fou8 HC***	0.01724108
Threonine	**WT AC vs HC**		**WT AC**		**WT HC**
WT AC vs HC	0.467382315	***apk1apk2 AC***	0.022556032	***apk1apk2 HC***	0.261657567
		fou8 AC	0.004476434	***fou8 HC***	0.33414727
trehalose_1	**WT AC vs HC**		**WT AC**		**WT HC**
WT AC vs HC	-	***apk1apk2 AC***	-	***apk1apk2 HC***	1.29056E-06
		fou8 AC	-	***fou8 HC***	0.000113806
trehalose_2	**WT AC vs HC**		**WT AC**		**WT HC**
WT AC vs HC	-	***apk1apk2 AC***	-	***apk1apk2 HC***	-
		fou8 AC	-	***fou8 HC***	-
Tryptophan	**WT AC vs HC**		**WT AC**		**WT HC**
WT AC vs HC	0.444062578	***apk1apk2 AC***	0.012813998	***apk1apk2 HC***	0.000571382
		fou8 AC	0.000850892	***fou8 HC***	2.53796E-05
Tyrosine	**WT AC vs HC**		**WT AC**		**WT HC**
WT AC vs HC	0.02222824	***apk1apk2 AC***	0.016406705	***apk1apk2 HC***	0.004877951
		fou8 AC	0.216330472	***fou8 HC***	0.070534378
Valine	**WT AC vs HC**		**WT AC**		**WT HC**
WT AC vs HC	0.114692077	***apk1apk2 AC***	0.452698321	***apk1apk2 HC***	0.006244009
		fou8 AC	0.26229707	***fou8 HC***	0.177241157
Xylose	**WT AC vs HC**		**WT AC**		**WT HC**
WT AC vs HC	0.064760211	***apk1apk2 AC***	0.043412186	***apk1apk2 HC***	0.233456127
		fou8 AC	8.76386E-05	***fou8 HC***	0.000347555

ERKLÄRUNG

Erklärung zur Dissertation

gemäß der Promotionsordnung vom 12. März 2020

Diese Erklärung muss in der Dissertation enthalten sein.

„Hiermit versichere ich an Eides statt, dass ich die vorliegende Dissertation selbstständig und ohne die Benutzung anderer als der angegebenen Hilfsmittel und Literatur angefertigt habe. Alle Stellen, die wörtlich oder sinngemäß aus veröffentlichten und nicht veröffentlichten Werken dem Wortlaut oder dem Sinn nach entnommen wurden, sind als solche kenntlich gemacht. Ich versichere an Eides statt, dass diese Dissertation noch keiner anderen Fakultät oder Universität zur Prüfung vorgelegen hat; dass sie - abgesehen von unten angegebenen Teilpublikationen und eingebundenen Artikeln und Manuskripten - noch nicht veröffentlicht worden ist sowie, dass ich eine Veröffentlichung der Dissertation vor Abschluss der Promotion nicht ohne Genehmigung des Promotionsausschusses vornehmen werde. Die Bestimmungen dieser Ordnung sind mir bekannt. Darüber hinaus erkläre ich hiermit, dass ich die Ordnung zur Sicherung guter wissenschaftlicher Praxis und zum Umgang mit wissenschaftlichem Fehlverhalten der Universität zu Köln gelesen und sie bei der Durchführung der Dissertation zugrundeliegenden Arbeiten und der schriftlich verfassten Dissertation beachtet habe und verpflichte mich hiermit, die dort genannten Vorgaben bei allen wissenschaftlichen Tätigkeiten zu beachten und umzusetzen. Ich versichere, dass die eingereichte elektronische Fassung der eingereichten Druckfassung vollständig entspricht."

Teilpublikationen:

• **Günal, S**., Hardman, R., Kopriva, S., & Mueller, J. W. (2019). Sulfation pathways from red to green. The Journal of biological chemistry, 294(33), 12293–12312.

• **Günal, S**., & Kopriva, S. (2022). Measurement of flux through sulfate assimilation using [^{35}S]sulfate. Methods in enzymology, 676, 197–209.

Datum,	Name	Unterschrift
24.03.2025	Süleyman Günal	

ACKNOWLEDGEMENTS

I would like start with thanking my supervisor **Prof.Dr. Stanislav Kopriva** for giving me this opportunity and for the encouragement to finalize my work. I also would like to thank all the members of the **AG Kopriva** over the years for making this research possible.

Big thanks to **Prof.Dr. Tatjana Hildebrandt** for accepting to be my second advisor and **Prof.Dr. Günter Schwarz** for accepting being the chair of this thesis.

I am sending my gratidues to our CEPLAS collabrators **Dr. Philipp Westhoff** and **Dr. Marion Eisenhut** for their help and expertise. Thanks, as well to **Dr. Rainer Häusler** and **Dr. Hannes Dittberner** from University of Cologne for their technical help.

Two great students contributed to this work, **Dilara Nemli** and **Peter Wolf**, thank you very much for bringing energy and curiousty to lab everyday.

Special thanks to **Richard Jacoby** for his friendship and guidance inside and outside of the office. I am also grateful for our talks with **Parisa Rahimzadeh Karvansara** and **Tim Jobe** and their support and friendship. I also would like to thank **Daniela Ristova** for her help with the official process.

Of course I can not forget to thank **Ivan Zenzen** for being there for up and down times and being a true friend. Also I must thank fellow PhD students **Christopf Dietzen** and **Melina Schwier** for their great support.

Even though there were huge distances, my close friends who believed in me and encouraged me all these years, thank you; **Sabri Can Çelik, Enes Durgut, Fulya Akçimen, Salvatore Chierenza**, and **Sam Sturgis-Seabrook**.

I would like to express my heartfelt gratitude to **Luise Waldow** for always being there for me, supporting me, and never stopping to believe in me.

I would like to express my deepest gratitude to my parents, my sister **Hamide Atak** and my brother **Tunahan Günal** who have always loved and supported me and have never lost faith in me.